This is to certify that the

thesis entitled

Material Functions from Large-Amplitude Oscillatory Shearing of Polyisobutylene in Cetane by a Modified R-16 Weissenberg Rheogoniometer

presented by

David James Henry Cross

has been accepted towards fulfillment
of the requirements for

M.S. degree in ChE

Major professor

Date 1/28/83

MATERIAL FUNCTIONS FROM LARGE-AMPLITUDE OSCILLATORY SHEARING OF POLYISOBUTYLENE IN CETANE BY A MODIFIED R-16 WEISSENBERG RHEOGONIOMETER

By

David James Henry Cross

A THESIS

Submitted to
Michigan State University
in partial fulfillment of the requirements
for a degree of

MASTER OF SCIENCE

Department of Chemical Engineering

ABSTRACT

MATERIAL FUNCTIONS FROM LARGE-AMPLITUDE OSCILLATORY SHEARING OF POLYISOBUTYLENE IN CETANE BY A MODIFIED R-16 WEISSENBERG RHEOGONIOMETER

By

David James Henry Cross

Early investigators who used the unmodified Weissenberg Rheogoniometer (WRG) encountered some inadequacies in the machine design which permits the cone-plate gap to open. The enhancements are the replacement of the bending cantilever beam by a stationary piezotron load cell and the use of weights to prevent the dove-tail slide and torsion-head assembly from moving. The objective is to collect material functions from oscillatory shearing in the nonlinear region of polyisobutylene in cetane by using a modified R-16 WRG. There is a considerable amount of scatter in the data presumably due to variations in room temperature; nevertheless, the following trends are apparent. For nonlinear behavior the dynamic storage moduli and loss moduli are related to the odd components of the Fourier series for shear stress. The frequency response over a range of strain amplitudes shows that the storage modulus increases with the increase in frequency. At each test frequency, the strain response curve shows that the storage modulus decreases linearly with the increase in shear strain. The loss modulus is a function of frequency only.

ACKNOWLEDGEMENTS

It is a pleasure to acknowledge with gratitude the assistance and cooperation of several people associated with this project directly or indirectly:

Dr. K. Jayaraman for proposing this topic, his guidance as thesis advisor, and equally importantly, for his ready accessibility for suggestions and discussions during this research. His personal enthusiasm and interest have been most inspiring.

Dr. R.F. Blanks as academic advisor for most of my graduate studies.

Dr. B.W. Wilkinson as academic advisor for much of my undergraduate studies.

Dr. C.M. Cooper for his many helpful comments and discussions during my stay in the department.

Messrs. R. Rose and D. Childs for performing the necessary electronic and mechanical repairs.

Mrs. D. Breuss and Ms. Jean Cobb for typing the final draft.

The many graduate students, faculty and staff who made my stay at Michigan State a very pleasant experience.

Michigan State University and the Macromolecule Research Group for providing a graduate assistantship and research funds, and finally,

My parents for their encouragement and support.

TABLE OF CONTENTS

LIST OF FIGURES v

LIST OF TABLES x

LIST OF NOTATION xiii

CHAPTER I - INTRODUCTION
1.1 Background on Materials 1
1.2 Rheometry 6
1.3 Basic Equations & Assumptions 8
1.4 Motivations 16
1.5 Objective 20

CHAPTER II - METHOD OF APPROACH
2.1 Material Functions for the Unmodified WRG . . . 23
2.2 Enhancements to the R-16 WRG 28
2.3 Material Functions for the Modified WRG 32

CHAPTER III - DESCRIPTION OF APPARATUS AND EXPERIMENTS
3.1 Unmodified R-16 Weissenberg Rheogoniometer . . . 37
3.2 Modified R-16 Weissenberg Rheogoniometer 44
3.3 Laboratory Techniques 49
3.4 Experiments for the Unmodified WRG 52
3.5 Experiment for the Modified WRG 54

CHAPTER IV - ANALYSIS OF DATA PROCESSING
4.1 Dynamic Material Functions and Formulas 56
4.2 Visicorder Calculation Methods and Problems . . 62
4.3 Computer Program and Fourier Analysis 66

CHAPTER V - RESULTS OF THE INVESTIGATION
5.1 Material Function from the Unmodified WRG . . . 68
5.2 Material Functions from the Modified WRG 72

CHAPTER VI - SUMMARY AND CONCLUSION
6.1 Highlights 85
6.2 Inferences 86

CHAPTER VII - RECOMMENDATIONS
7.1 Temperature Control 88
7.2 Graphics Terminal 90

LIST OF REFERENCES 92

Appendices

A. Listing of the Program

B. Collection of Data

LIST OF FIGURES

Figure 1a	Simple Shear Strain	2
Figure 1b	Simple Shear Stress	2
Figure 2a	Ideal Cone & Plate Gometry	7
Figure 2b	Truncated Cone	7
Figure 3a	Cantiliver Beam and Clamp	29
Figure 3b	Cross-section Area of Beam	29
Figure 4	Sketch of C-Ring	31
Figure 5	Weissenberg Rheogoniometer Internals	38
Figure 6	Normal Force Measuring Assembly	40
Figure 7	Harmonic Motion Mechanism	42
Figure 8	Measurement Paths	45
Figure 9	Sketch of Modified Normal Force Measuring System	46
Figure 10	Piezotron Calibration	48
Figure 11	Pair of Cosine Waves Forms	57
Figure 12	Visicorder Output Measurement	63
Figure 13	Oscilloscope Measurements	65
Figure 14a	Shear Stress Growth	69
Figure 14b	Normal Stress Growth	69
Figure 15	Frequency Response of Dynamic Viscosity and and Storage Modulus for 1490 Polyisobutylene in Cetane	70
Figure 16	Shear Stress and Normal Stress Growth of 1490 Polyisobutylene in Cetane from a Modified WRG..	71
Figure 17	Frequency Response of the Dynamic Storage Modulus for 1490 Polyisobutylene in Cetane at 0.5 Strain Amplude from a Modified WRG	73

Figure 18 Frequency Response of the Dynamic Storage Modulus for 1490 Polyisobutylene in Cetane at 1.3 Strain Amplitude from a Modified WRG 74

Figure 19 Frequency Response of the Dynamic Storage Modulus for 1490 Polyisobutylene in Cetane at 2.1 Strain Amplitude from a Modified WRG 75

Figure 20 Frequency Response of the Dynamic Storage Modulus for 1490 Polyisobutylene in Cetane at 3.3 Strain Amplitude from a Modified WRG 76

Figure 21 Strain Amplitude Response of the Dynamic Storage Modulus for 1490 Polyisobutylene in Cetane at the Frequency of 0.6 and 3.77/ second from a Modified WRG 78

Figure 22 Strain Amplitude Response of the Loss Storage Modulus for 1490 Polyisobutylene in Cetane at the Frequency of 0.6 and 3.77/ second from a Modified WRG 80

Figure 23 Calcomp Plot of the Large-Amplitude Oscillatory Shearing of Polyisobutylene in Cetane at the Frequency of 0.0952 c/s and Strain Amplitude of 3.3 81

Figure 24 Calcomp Plot of the Large-Amplitude Oscillatory Shearing of Polyisobutylene in Cetane at the Frequency of 0.0952 c/s and Strain Amplitude of 2.17 ..... B1

Figure 25 Calcomp Plot of the Large-Amplitude Oscillatory Shearing of Polyisobutylene in Cetane at the Frequency of 0.0952 c/s and Strain Amplitude of 1.31. ..... B3

Figure 26 Calcomp Plot of the Large-Amplitude Oscillatory Shearing of Polyisobutylene in Cetane at the Frequency of 0.0952 c/s Strain Amplitude of 1.31 ..... B5

Figure 27 Calcomp Plot of the Large-Amplitude Oscillatory Shearing of Polyisobutylene in Cetane at the Frequency of 0.0952 c/s and Strain Amplitude of 1.31 ..... B7

Figure 28 Calcomp Plot of the Small-Amplitude Oscillatory Shearing of Polyisobutylene in Cetane at the Frequency of 0.0952 c/s and Strain Amplitude of 0.5515 ..... B9

Figure 29 Calcomp Plot of the Small-Amplitude Oscillatory Shearing of Polyisobutylene in Cetane at the Frequency of 0.0952 c/s and Strain Amplitude of 0.53613 ..... B11

Figure 30 Calcomp Plot of the Small-Amplitude Oscillatory Shearing of Polyisobutylene in Cetane at the Frequency of 0.0952 c/s and Strain Amplitude of 0.5340 ..... B13

Figure 31 Calcomp Plot of the Small-Amplitude Oscillatory Shearing of Polyisobutylene in Cetane at the Frequency of 0.0952 c/s and Strain Amplitude of 0.5309 ..... B15

Figure 32 Calcomp Plot of the Small-Amplitude Oscillatory Shearing of Polyisobutylene in Cetane at the Frequency of 0.0952 c/s and Strain Amplitude of 0.5097 ..... B17

Figure 33 Calcomp Plot of the Small-Amplitude Oscillatory Shearing of Polyisobutylene in Cetane at the Frequency of 0.0952 c/s and Strain Amplitude of 0.5035 ..... B19

Figure 34 Calcomp Plot of the Oscillatory Shearing of Polyisobutylene in Cetane at the Frequency of 0.38 c/s and Strain Amplitude of 0.5488 ..... B21

Figure 35 Calcomp Plot of the Oscillatory Shearing of Polyisobutylene in Cetane at the Frequency of 0.38 c/s and Strain Amplitude of 0.5390 ..... B23

Figure 36 Calcomp Plot of the Oscillatory Shearing of Polyisobutylene in Cetane at the Frequency of 0.38 c/s and Strain Amplitude of 0.5200 ..... B25

Figure 37 Calcomp Plot of the Oscillatory Shearing of Polyisobutylene in Cetane at the Frequency of 0.38 c/s and Strain Amplitude of 0.5090 ..... B27

Figure 38 Calcomp Plot of the Large-Amplitude Oscillatory Shearing of Polyisobutylene in Cetane at the Frequency of 0.6 c/s and Strain Amplitude of 3.4123 ..... B29

Figure 39 Calcomp Plot of the Large-Amplitude Oscillatory Shearing of Polyisobutylene in Cetane at the Frequency of 0.6 c/s and Strain Amplitude of 3.3088 ..... B31

Figure 40 Calcomp Plot of the Large-Amplitude Oscillatory Shearing of Polyisobutylene in Cetane at the Frequency of 0.6 c/s and Strain Amplitude of 3.3048 ..... B33

Figure 41 Calcomp Plot of the Large-Amplitude Oscillatory Shearing of Polyisobutylene in Cetane at the Frequency of 0.6 c/s and Strain Amplitude of 2.160 ..... B35

Figure 42 Calcomp Plot of the Large-Amplitude Oscillatory Shearing of Polyisobutylene in Cetane at the Frequency of 0.6 c/s and Strain Amplitude of 2.1363 ..... B37

Figure 43 Calcomp Plot of the Large-Amplitude Oscillatory Shearing of Polyisobutylene in Cetane at the Frequency of 0.6 c/s and Strain Amplitude of 1.3168 ..... B39

Figure 44 Calcomp Plot of the Large-Amplitude Oscillatory Shearing of Polyisobutylene in Cetane at the Frequency of 0.6 c/s and Strain Amplitude of 1.2982 ..... B42

Figure 45 Calcomp Plot of the Large-Amplitude Oscillatory Shearing of Polyisobutylene in Cetane at the Frequency of 0.6 c/s and Strain Amplitude of 1.2973 ..... B44

Figure 46 Calcomp Plot of the Large-Amplitude Oscillatory Shearing of Polyisobutylene in Cetane at the Frequency of 0.6 c/s and Strain Amplitude of 1.2678 ..... B46

Figure 47 Calcomp Plot of Oscillatory Shearing of Polyisobutylene in Cetane at the Frequency of 0.6 c/s and Strain Amplitude of 0.5194 ..... B49

Figure 48a Calcomp Plot of Oscillatory Shearing of Polyisobutylene in Cetane at the Frequency of 0.6 c/s and Strain Amplitude of 0.5139 for Shear Stress Response B52

Figure 48b Calcomp Plot of Oscillatory Shearing of Polyisobutylene in Cetane at the Frequency of 0.6 c/s and Strain Amplitude of 0.5139 for Normal Stress Response B54

Figure 49 Calcomp Plot of Oscillatory Shearing of Polyisobutylene in Cetane at the Frequency of 0.6 c/s and Strain Amplitude of 0.5128 ..... B56

LIST OF TABLES

Table 1 Fourier Components and Material Functions at the Frequency of 0.0952 c/s and the Strain Amplitude of 3.3. 82

Table 2 Fourier Components and Material Functions at the Frequency of 0.0952 c/s and the Strain Amplitude of 2.17 ..... B2

Table 3 Fourier Components and Material Functions at the Frequency of 0.0952 c/s and the Strain Amplitude of 1.31 ..... B4

Table 4 Fourier Components and Material Functions at the Frequency of 0.0952 c/s and the Strain Amplitude of 1.31. ..... B6

Table 5 Fourier Components and Material Functions at the Frequency of 0.0952 c/s and the Strain Amplitude of 1.31 ..... B8

Table 6 Fourier Components and Material Functions at the Frequency of 0.0952 c/s and the Strain Amplitude of 0.5515 ..... B10

Table 7 Fourier Components and Material Functions at the Frequency of 0.0952 c/s and the Strain Amplitude of 0.53613 ..... B12

Table 8 Fourier Components and Material Functions at the Frequency of 0.0952 c/s and the Strain Amplitude of 0.5340 ..... B14

Table 9 Fourier Components and Material Functions at the Frequency of 0.0952 c/s and the Strain Amplitude of 0.5309 ..... B16

Table 10 Fourier Components and Material Functions at the Frequency of 0.0952 c/s and the Strain Amplitude of 0.5097 ..... B18

Table 11 Fourier Components and Material Functions at the Frequency of 0.0952 c/s and the Strain Amplitude of 0.5097 ..... B20

Table 12 Fourier Components and Material Functions at the Frequency of 0.38 c/s and the Strain Amplitude of 0.5488 ..... B22

Table 13 Fourier Components and Material Functions at the Frequency of 0.38 c.s and the Strain Amplitude of 0.5390 ..... B24

Table 14 Fourier Components and Material Functions at the Frequency of 0.38 c/s and the Strain Amplitude of 0.5200 ..... B26

Table 15 Fourier Components and Material Functions at the Frequency of 0.38 c/s and the Strain Amplitude of 0.5090 ..... B28

Table 16 Fourier Components and Material Functions at the Frequency of 0.6 c/s and the Strain Amplitude of 3.4123 ..... B30

Table 17 Fourier Components and Material Functions at the Frequency of 0.6 c/s and the Strain Amplitude of 3.3088 ..... B32

Table 18 Fourier Components and Material Functions at the Frequency of 0.6 c/s and the Strain Amplitude of 3.3048 ..... B34

Table 19 Fourier Components and Material Functions at the Frequency of 0.6 c/s and the Strain Amplitude of 2.160 ..... B36

Table 20 Fourier Components and Material Functions at the Frequency of 0.6 c/s and the Strain Amplitude of 2.1363 ..... B38

Table 21 Fourier Components and Material Functions at the Frequency of 0.6 c/s and the Strain Amplitude of 1.3168 ..... B40

Table 22 Fourier Components and Material Functions at the Frequency of 0.6 c/s and the Strain Amplitude of 1.2982 ..... B43

Table 23 Fourier Components and Material Functions at the Frequency of 0.6 c/s and the Strain Amplitude of 1.2973 ..... B45

Table 24 Fourier Components and Material Functions at the Frequency of 0.6 c/s and the Strain Amplitude of 1.2678 ..... B47

Table 25 Fourier Components and Material Functions at the Frequency of 0.6 c/s and the Strain Amplitude of 0.5194 ..... B50

Table 26 Fourier Components and Material Functions at the Frequency of 0.6 c/s and the Strain Amplitude of 0.5139 ..... B57

Table 27 Fourier Components and Material Functions at the Frequency of 0.6 c/s and the Strain Amplitude of 0.5128 ..... B59

LIST OF NOTATION

$\eta(\dot{\gamma})$ - apparent viscosity

η_o - limiting viscosity as rate of shear approaches zero

$\eta^*(\omega)$ - complex dynamic viscosity

$\eta'(\omega)$ - dynamic viscosity

$\eta''(\omega)$ - imaginary part of complex dynamic viscosity

G' - dynamic rigidity

G'' - loss modulus

γ - strain

$\dot{\gamma}$ - rate of strain, shear rate

τ - shear stress

$\underline{\dot{\gamma}}$ - shear rate matrix

$\dot{\gamma}_{re}$ - $\underline{r}$th, θ $\underline{th}$ element of shear rate matrix

$\underline{\tau}$ - shear stress matrix

τ_{re} - $\underline{r}$th, θ $\underline{th}$ element of shear stress matrix

ω - angular velocity, angular frequency in oscillatory shear flow

v - linear velocity

ρ - density

W - torque

F - total normal force

r - spherical coordinate - radius

θ - spherical coordinate - polar angle

ϕ - spherical coordinate - azimuthal angle

δ - phase lag

K - restoring constant of torsion bar

I - moment of inertial

p - isentropic pressure

i - imaginary number

A_o - Fourier component for displacement

A_n - Fourier series

B_n - Fourier series

t - time

T - Temperature

ω_o - resonant frequency

π - pii = 3.14159

f - frequency in cycles/sec

τ_o - shear stress magnitude

k - thermal conductivity

θ_o - gap angle of cone and plate

N_1 - first normal stress coefficient

N_2 - second normal stress coefficient

R - radius of cone or plate

Ω - amplitude of oscillation

ν_1 - first normal stress difference

ν_2 - second normal stress differences

ζ^* - complex normal stress coefficient gram/cm

ζ' - real part of $\zeta\dot{\gamma}$ gram/cm

ζ'' - imaginary part of $\zeta\dot{\gamma}$ gram/cm

ζ^d - normal stress displacement function gm/cm

CHAPTER I

INTRODUCTION

1.1 Background on Materials

Two extreme laws for the behavior of materials are Newton's law of constant viscosity and Hooke's law of constant elasticity. For example, water at constant temperature and pressure obeys Newton's law, while rubber obeys Hooke's law quite accurately to large deformations. Yet, materials which obey one of these two laws are regarded as common everyday materials, and they pose no problem to the engineer. Modern engineering is increasingly involved in the processing of non-Newtonian fluids such as suspensions, polymer solutions and melts which behave much differently than water or rubber does. Latexes, polymer solutions and melts are examples of pseudoplastic behavior. A contrasting behavior is dilatant fluids which are particulate dispersion such as concentrated suspensions, slurries, and resins in plasticizer. Pseudoplastic behavior shows a decrease in viscosity with shear rate, while dilatant behavior shows an increase in viscosity with shear rate.

The shear rate is the instantaneous rate of strain. A simple shear strain, shown in Figure 1a, is similar to a pack of playing cards. This deformation causes successive layers of the volume element to move in their planes relative to the reference plane in such a way that the displacement of a layer is proportional to its distance from the reference plane. The dimension perpendicular to the plane of shear,

SHEAR STRAIN AND STRESS

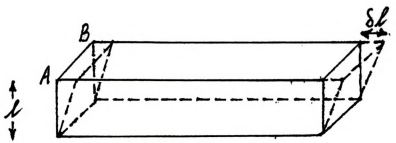

Figure 1a. Simple Shear Strain

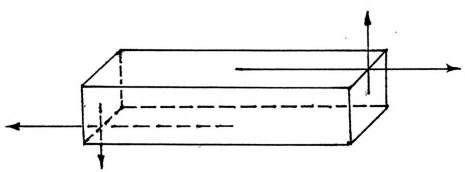

Figure 1b. Simple Shear Stress

such as length AB in Figure 1a remains constant. The relative displacement of the top and bottom layer divided by their separation, $\gamma\ell/\gamma$, is called simple shear strain. This term may be abbreviated to 'shear strain', 'strain', or 'shear' for the deformation in Figure 1a. The angle of shear, γ, is related to $\gamma\ell / \ell$ by $\tan \gamma = \delta\ell / \ell$. If the deformation is small, γ, expressed in radians, equals the shear strain.

The force providing a shear stress is shown acting on the top surface of the volume element of material in Figure 1b. An equal opposite force must be applied to the bottom surface if the element is to remain at rest or steady motion. Also, equal opposite forces must be applied to the other two surfaces, as shown in Figure 1b, if the element is not to experience angular acceleration. The forces that are parallel to the surfaces are known as shear stress, while forces that are normal to the surfaces are known as normal stresses. The term stress implies a force per unit area and has units of pressure.

If the stress is removed for the deformation shown in Figure 1b, the strain may or may not return to zero. Flow occurs when the strain does not eventually return to zero. If flow occurs for an infinitesimal stress the material is a liquid, otherwise it is considered a solid. Many seemingly solids, such as clay, will flow above a certain "yield" stress. The flow in Figure 1 is a particular example of streamline flow. The fluid elements at that point follow the

same path which need not be a straight line. Inelastic materials show no recovery of strain or energy. Some liquids such as many adhesives demonstrate partial recovery of strain and energy; these liquids are called elastic liquids. If the deformation and recovery of the material is instantaneous, then it is ideally elastic. Some responses can be quite slow as with many polymers which are referred to as viscoelastic. Walters[1] strictly uses this term as viscoelastic solid, but most researchers use it for liquids.

Viscoelastic liquids that are sheared in their linear region obey Hooke's law. Williams[2] gave the concise definition of linearity, that "the ratio of stress to strain for any history is a function of time only." The strain, whether constant or not, imposed on this liquid at all times before time zero had been increased by a factor, the stress at earlier time would have increased by the same factor. Likewise, if the stresses had been applied to the earlier times the strains would have been proportional to the stresses. Linearity implies the principle of superposition, which can be interrupted in two ways. The first way is that when simultaneous small strains are imposed on the viscoelastic liquid, the resultant stress is proportional to the sum of the individual strains acting separately. The second way is successive strains imposed on the viscoelastic liquid, which may cause certain types of nonlinear behavior to also appear as discussed by Williams. Normally, non-linear behavior appears by imposing a large strain on a

viscoelastic liquid.

When a strain rate is imposed suddenly on a fluid, the initial stress may not be maintained for two reasons, besides inertial effect. The first reason is the linear versus non-linear region, because part of the mechanical energy supplied to the material may be stored as elastic energy. The stored energy appears as elastic strain recovery when the stress reduces to zero. The second reason for a change in stress is that the structure changes. Perhaps weak bonds between suspended particles are broken, or long chain molecules become aligned. No elastic strain recovery is observed when stress reduces to zero. The stress usually decreases, but may increase with time. An irreversible loss of viscosity indicates a permanent degradation of the fluid. If the viscosity returns to its original value after the material has relaxed long enough with no strains imposed, the behavior is either rheopexy or thixotropy. Rheopexy behavior is the increase in viscosity with time of shearing, while thixotropy behavior is the decrease in viscosity with time of shearing. Bauer and Collins[3] have given the history of the use of thixotropy.

Thixotropic and viscoelastic behaviors could be confused if changes in stress are caused by changes in temperature. Or, viscoelasticity could be confused with rheopexy if the recovery of the material was not observed when strain is removed. Other differences between elastic and thixotropic material are the initial stress of a viscoelastic material is

controlled by the inertia of the fluid, whereas the initial stress of a time dependent material depends on initial viscosity. Most polymers exhibit both elastic and time dependent behavior.

1.2 Rheometry

Rheometry is the science of measuring the deformation and flow of fluids, and a rheometer such as the Weissenberg Rheogoniometer, is a measuring instrument. Measurements of fluids exhibiting both elastic and time dependent behavior are best made on a rotational rheometer where shearing can be done as long as desired. Figure 2a show the ideal cone and plate geometry that is often used on a Weissenberg Rheogoniometer. A cone with a radius R has its axis perpendicular to a plate, the vertex of the cone being in the surface of the plate. The cone rotates or oscillates with a relative angular velocity of ω. The angle θo between the cone and the plate is usually less than 5° and may be as small as 0.3°. Large angles are not normally used because the analysis of the results for non-Newtonian fluids is complex. Some theoreticians, such as Cheng,[4] have derived explicit formula for the shear rate at the cone in time-independent non-Newtonian fluids for large cone angles, but the assumption that the free fluid surface forms part of a sphere may not be justified. Small gap causes the shear rate to be uniform, the inertia of the sample to be less, the temperature rise to be minimized, and a small sample to be sufficient. For streamline flow the shear rate at any point

CONE AND PLATE GEOMETRY

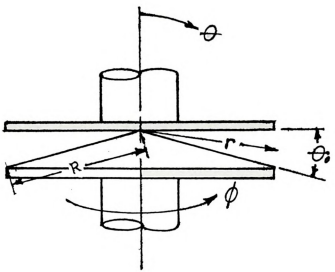

Figure 2a. Ideal Cone and Plate Geometry

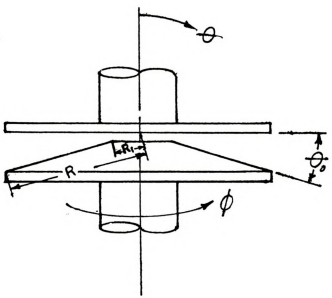

Figure 2b. Truncated Cone

is approximately given by:

$$\dot{\gamma} = \frac{r\,\omega}{r \sin \theta_o} = \frac{\omega}{\theta_o}$$

where for small cone angle $\sin \theta_o = \theta_o$. Shear rate is independent of position in the gap. This property gives the cone and plate an enormous advantage when studying time dependent behavior because all elements of a sample have the same shear history. For uniform shear rate the shear stress, τ, is a constant throughout the small gap. The torque, W, on the plate is the summation of narrow rings between radius r and $r + \delta r$ which gives

$$\delta W = \tau 2\pi r^2 \delta r$$

The total torque is

$$W = \int_o^R 2\pi r^2 \tau dr = 2\pi R^3 \tau/3$$

In most practices the tip of the cone is ground flat as shown in Figure 2b to a radius R_1, which gives

$$W = \int_{R_1}^{R} 2\pi r^2 \tau dr = 2\pi (R^3 - R_1^3)\tau/3.$$

If R_1 equals 0.1 R the torque is reduced by 0.1%. The total torque is reduced by less than 0.1% because the parallel section of the cone contributes to the torque on the plate.

1.3 Basic Equations and Assumptions

The cone and plate rheometer is a popular apparatus, because experiments with this geometry measures forces generated by known velocity profiles that have only material functions as unknowns. Velocity profiles and torque-stress relationship can be derived from the equation of motion,

which is Newton's second law of motion, and from the equation of continuity, which is the 'conservation of mass' principle.

For a geometric volume element, V, fixed in space and bounded by a surface S, the rate of change of momentum with V and across S are controlled by the body forces throughout V and the surface forces over S. The relevant momentum balance can be expressed as:

rate of momentum accumulated	=	rate of momentum in	-	rate of momentum out	+	sum of forces of system	(1.3.1)

Bird, Stewart, and Lightfoot[5] consider the rates of flow of the component direction of momentum into and out of the volume element. Momentum flows into and out of the volume by convection and by molecular transfer. There are nine components of the convective momentum flux ρvv which is the "dyadic product" of the mass velocity vector ρv and the velocity v. Similarly, there are nine stress components to the stress tensor $\underline{\tau}$. The single vector-tensor equation for the momentum balance equation (1.31) is

$$\frac{\partial}{\partial t}\rho v = -\nabla\cdot\rho vv - \nabla\cdot\underline{\tau} - \nabla p + \rho g \qquad (1.3.2)$$

rate of increase of mom.per unit volume	rate of mom. gain by convection per unit vol.	rate of mom. gain by viscous transfer per unit volume	sum of other forces on sys.

The rate of momentum gain by convection term can be combined with the rate of accumulation term by means of the substantial time derivative, D/Dt. The substantial time

derivative is the derivative following the streamline flow of velocity vector $\mathbf{v}$. The equivalent equation to (1.3.2) is

$$\rho \frac{D\mathbf{v}}{Dt} = -\nabla \cdot \tau - \nabla p + \rho g \tag{1.3.3}$$

This form of the equation of motion is a statement in the form of mass times acceleration equals the sum of forces; Newton's second law of motion. The arbitrary volume element moving with the fluid is accelerated because of the forces acting on it.

The equation of continuity is developed by writing a mass balance over the geometric volume element. By a similar method, the conservation of mass is as follows:

$$\frac{D\rho}{Dt} = -\rho(\nabla \cdot \mathbf{v}). \tag{1.3.4}$$

The term, $D\rho/Dt$ is the substantial derivative of density.

The corresponding equations of (1.3.3) and (1.3.4) for spherical polar coordinates are given in Bird, Steward, and Lightfoot.[6] In the analysis of spherical flow the use of spherical coordinates allows the description of velocity in terms of fewer velocity components and results in a simplification of the boundary conditions. The equations in are general for all problems of spherical flow and for Newtonian or non-Newtonian fluids. For the cone and plate geometry the assumptions are as follows:

(1) Flow is strictly tangential, so $v_\phi = f(r,\theta)$ and $v_r = v_\theta = 0$,

(2) No bulk flow occurs,

(3) "Inertia" effects are negligible,

(4) Gap angle between cone and plate is less than 5°,

(5) Cone and plate are of radius R,

(6) Free surface of the liquid is part of a sphere of radius R with its center at the cone vertex,

(7) Surface-tension forces are negligible.

After applying these assumptions to the generalized equations, the three components of the equation of motion for steady state reduce to

$$\text{r-comp.} \quad -\rho\frac{v_\phi^2}{r} = -\frac{1}{r^2}\frac{\partial}{\partial r}(r^2\tau_{rr}) + \frac{(\tau_{\theta\theta}-\tau_{\phi\phi})}{r} \tag{1.3.5}$$

$$\theta\text{-comp.} \quad -\rho\frac{v^2\phi\cot\theta}{r} = -\frac{1}{r\sin\theta}\frac{\partial}{\partial\theta}(\tau_{\theta\theta}\sin\theta)+\frac{\tau_{\phi\phi}\cot\theta}{r} \tag{1.3.6}$$

$$\phi\text{-comp.} \quad 0 = -\frac{1}{r^2}\frac{\partial}{\partial r}(r^2\tau_{r\phi})-\frac{1}{r}\frac{\partial\tau_{\theta\phi}}{\partial\theta}-\frac{\tau_{r\phi}}{r}-\frac{2\cot\theta}{r} \tag{1.3.7}$$

with the following boundary conditions:

$$\text{at} \quad \theta = \pi/2 \quad , \quad v_\phi = 0 \tag{1.3.8}$$

$$\text{at} \quad \theta = \pi/2 + \theta_1 \quad , \quad v_\phi = r\omega \sin\theta_1 \tag{1.3.9}$$

$$\text{at} \quad r = 0 \quad , \quad v_\phi = 0 \tag{1.3.10}$$

Equation (1.3.9) is the condition for steady rotational shearing. For oscillatory shearing, (1.3.9) would be

$$\text{at} \quad \theta = \pi/2 + \theta_1 \quad , \quad v_\phi = r\omega \sin\theta_1 \sin\omega t \tag{1.3.11}$$

The equations (1.3.5) through (1.3.11) are still general for Newtonian and non-Newtonian fluids. In order to use these equations to derive velocity profiles, however, the various stresses must be substituted with expressions for velocity gradients and fluid properties. Nally[7] derives the velocity profile in steady location shear as an infinite series involving Bessel and associated Legendre functions for Newtonian fluids. For non-Newtonian fluids, the derivation of the velocity profile would require a rheological model such as the Power-law model.[8]

The equation of energy is developed by an energy balance over geometric volume element. The relevant balance can be expressed as:

rate of internal and kinetic energy accumulated	=	net rate of internal and kinetic energy in by convection	+	net rate of heat addition by conduction	-	net rate of work done by system on surroundings	(1.3.12)

Although this first law balance does not include all forms of energy, it generalizes the work and kinetic energy effects. The kinetic energy is the $\rho v^2/2$ on a per unit-volume basis for the fluid in motion. The internal energy is the random translational, rotational, and interaction energy of the molecules which depends on the local temperature and density of the fluid. The single vector-tensor equation for the energy balance equation (1.3.12) is[9]

$$\frac{\partial}{\partial t}\rho\,(U + v^2/2) = -\,(\nabla\cdot\rho v(U + v^2/2)) \;-\; (\nabla\cdot q)$$

rate of energy gained	rate of energy in by convection	rate of energy in by conduction
$+\rho\,(v\cdot g)$	$-\,(\nabla\cdot\rho v)$	$-\,(\nabla\cdot(\underline{\tau}\cdot v))$
rate of work done on fluid by gravity	rate of work done of fluid by pressure	rate of work done on fluid by viscous forces

(1.3.13)

Each of the terms in equation (1.3.13) is on a per unit volume basis. By mathematical manipulation of equation (1.3.13) and use of the equation of continuity and motion, the rate of energy gained by convection can be combined with the rate of accumulation term by means of the substantial time derivative, D/Dt. The substantial time derivative is the derivative that follows the streamline flow. The equivalent equation to (1.3.13) is

$$\rho\,\frac{DU}{Dt} = -\,(\nabla\cdot q) \;-\; \rho(\nabla\cdot v) \;-\; (\underline{\tau}:\nabla v) \qquad (1.3.14)$$

where the double dot product $(\underline{\tau}:\nabla v) = (\nabla\cdot(\underline{\tau}\cdot v)) - (v\cdot(\nabla\cdot\underline{\tau}))$. The $(\underline{\tau}:\nabla v)$ is the viscous dissipation term which is left when $\rho D(v^2/2)$ is substituted by the equation of mechanical energy. The equation of mechanical energy is written as

$$\rho\,\frac{D(v^2/2)}{Dt} = -\,(v\cdot\nabla\rho) \;-\; (v\cdot(\nabla\cdot\underline{\tau})) + \rho(v\cdot g)$$

The terms, such as $(v\cdot\nabla\rho)$ and $\rho(v\cdot g)$, cancel out of equation (1.3.13) after the substitution.

For the calculation of temperature rise, the equation (1.3.14) for thermal energy is more useful in terms of heat capacity and fluid temperature than in terms of internal energy. Again by mathematical manipulation and the use of the equation of continuity, the total derivative of internal energy U, and the fact that the substantial derivative is linear operator, the equation of energy becomes

$$\rho C_v = \frac{DT}{Dt} = -(\nabla \cdot q) - T\left(\frac{\partial \rho}{\partial T}\right)_v (\nabla \cdot v) - (\underline{\tau} : \nabla v) \qquad (1.3.15)$$

The corresponding equation of (1.3.15) in spherical polar coordinates are given in Bird, Steward, and Lightfoot.[10]

In a rheogoniometer, the same sample of material can be sheared indefinitely, the temperature rise due to viscous shear heating is frequently a problem at low shear rates. Bird and Turian[11] made very good approximations of the temperature rise distribution for both Newtonian and non-Newtonian fluids in a cone-plate instruments.

The energy equation describing the temperature profile in the fluid region between the cone and plate is obtained from the general energy equation by the appropriate simplification. For small gap angles the equation of motion has an approximate solution in which it is assumed the components of the velocity have the form $v_\phi = rf(\theta)$, $v_r = 0$, $v_\theta = 0$. The energy equation for constant thermal conductivity k reduces to

$$k\left[\frac{1}{r^2}\frac{\partial}{\partial r}\left(r^2\frac{\partial T}{\partial r}\right) + \frac{1}{r^2 \sin\Theta}\frac{\partial}{\partial \Theta}\left(\sin\Theta \frac{\partial T}{\partial \Theta}\right)\right] - \tau_{\theta\phi}\left(\frac{1}{r}\frac{\partial v}{\partial \theta} - \frac{\cot\theta v_\phi}{r}\right) = 0 \qquad (1.3.16)$$

The term $\tau_{\theta\phi}$ in equation (1.3.16) is the heat generated by irreversible mechanical energy degradation which is the $(-\underline{\tau}:\nabla v)$ term in equation (1.3.14). The normal stress components $\tau_{rr}, \tau_{\theta\theta}, \tau_{\phi\phi}$, which are generally not zero, do not contribute to the $(-\underline{\tau}:\nabla v)$, because the associated components of the dyadic ∇v are identically zero for the assumed velocity profile. For the torque W that is applied to rotate the cone at an angular velocity ω, the $\theta\phi$ - component of the viscous portion of the stress tensor $\underline{\tau}$ and the ϕ - component of the velocity v are approximately given by

$$\tau_{\theta\phi} \cong 3W/2\pi R^3 \qquad (1.3.17)$$

$$v_\phi \cong \omega r(\pi/2-\theta)/\theta_o \qquad (1.3.18)$$

A further approximation is $\sin\theta \cong 1$ and $\cot\theta \cong 0$, since θ is nearly equal to $\pi/2$. Equation (1.3.16) has the following boundary conditions:

at $\theta = \pi/2$ $T = T_o$ (1.3.19)

at $\theta = \pi/2 + \theta_o$ $T = T_o$ (1.3.20)

at $r = 0$ $T = T_o$ (1.3.21)

at $r = R$ $\partial T/\partial r = o$ (1.3.22)

The boundary conditions (1.3.19), (1.3.20) and (1.3.21) state that the metallic surfaces of the cone and plate stay at temperature To where as the last boundary condition (1.3.22)

indicates that no heat loss occurs at the liquid-air interface.

Although the geometry is such that an exact solution of the equation of motion and heat conduction is fairly difficult, Bird and Turian satisfactorily estimated the temperature rise by use of calculus of variations. In the derivation they did not need to use any specific rheological model to obtain the following formula:

$$(T - To)max \cong 3W\omega\Theta o/16\ \pi\ k\ R \qquad (1.3.19)$$

This equation estimates the maximum temperature rise from experimental conditions even for non-Newtonian fluid with normal stresses. A rheogoniometer typically has a maximum speed of 1000 r.p.m. and maximum torque bar of 1200 g (force) cm. A cone and plate may have a radius R = 1 cm and gap angle $\Theta o = \pi/180$ radian. Most organic fluids have a thermoconductivity on the order of 0.001 cal/cm/sec/C. For these values and using the conversion factors 980 erg/g-cm and 4.186×10^7 erg/cal, the equation (1.3.19) gives (T-To) max = 3C.

1.4 Motivations

Data on materials showing linear viscoelastic behavior with experimental error under small shear is well documented since the advent of Dr. Weissenberg's[12] first design of a rheogoniometer in 1948. Many authors such as Ferry[13] and Lodge[14] have written on linear viscoelastic theory. Although

the linear region gives useful information, manufacturers apply large shear rates during processing, so mathematical models for large deformation is a necessity which makes nonlinear models more practical than linear models. Until a decade ago there was little attempt at theoretical analysis of the nonlinear behavior in a form suitable for practical application. More recently proposed nonlinear theories, such as Acierno's,[22] involve parameters which must be evaluated from experiments at large deformations.

An obvious way to increase the rate of shear for oscillatory or rotational shearing in a rheogoniometer is to decrease the cone-plate gap angle Θ_0 , or to increase the angular velocity ω. In oscillatory shearing an increase in the amplitude of the oscillation increases the angle of shear or the shear strain γ_0. Large-amplitude oscillatory shearing is a way to increase the shear rate without increasing the angular velocity which can throw the test fluid out of the cone-plate gap by centrifugal force. Another way of testing the dynamic behavior of a material under nonlinear conditions is to shear it steadily and to super-impose a low-amplitude oscillatory shear so that linear methods can be used to relate the shear strain to the stress variations. Various superpositions will produce different waveforms for measuring the primary and secondary stresses which depends on the type of polymers under test. Walters[15] has summarized this type of test and its theory.

In 1969 MacDonald[16], Marsh, and Ashare made large-amplitude oscillatory tests using a Weissenberg rheogoniometer, but it was necessary to watch for waveform distortion caused by instrument defects. The waveform distortions prompted many investigators to modify their rheogoniometer. In 1970, Lee[17] , et. al. published a paper on modifications on their R-16 Weissenberg rheogoniometer. They installed a versatile oscillatory mechanism that allowed both amplitude and frequency variation. Also, they replaced the solenoids for torque and normal force measuring with piezoelectric load cells. Their modifications were not completely satisfactory, so new designs were being developed at the time of their publication. In 1972 Higman[18] introduced a new torque and normal thrust measuring system for both the R-16 and R-18 Weissenberg rheogoniometers. The modifications by Higman consisted of a torque and normal thrust piezoelectric transducer which replaced the air bearing displacement transducer for the torque measurement and the servo-cantilever displacement transducer for the normal thrust measurement in the standard rheogoniometer. Also in 1972, Meissner[19] published a new machine design of a cross-beam support to increase axial rigidity in the rheogoniometer. In 1973, MacDonald[20] used the rheogoniometer with the cone-plate geometry for superimposing a low-amplitude harmonic strain during steady shearing. MacDonald discussed in his paper some problems in the test, such as, those associated with the slackness in the gears. In 1977,

Crawley and Greassley[21] incorporated both the piezoelectric load cells and the cross-beam support for an enhanced axial and torque measuring system.

The industrial need for nonlinear models has led many investigators to collect data by a variety of high shear rate experiments. The Weissenberg rheogoniometer is a versatile machine which allows the testing of nonlinear models by such experiments. Unfortunately, the recent venture into the nonlinear region has shown the need for mechanical enhancements to the Weissenberg rheogoniometer. The original or unmodified R-16 Weissenberg rheogoniometer had measuring devices called linear variable differential transducer or LVDT, that requires a movement for recording forces. The opening of the cone-plate gap and the twisting of the stationary plate violates the spherical geometry and the no "slip" boundary condition of the basic equations and assumptions. The movement of rigid machine members is a design flaw that became only noticeable because the recent testing of polymers in the nonlinear region produced much larger forces than earlier tests in the linear region. Data that were collected by unmodified rheogoniometer in the nonlinear region of viscoelastic fluids are questionable. Before models such as the set of differential equations proposed by Acierno et. al.[22] can be used to predict the stresses in materials subjected to large deformation, the models need to be evaluated against data collected from modified rheogoniometers.

1.5 Objectives

Walters [23] distinguishes between two objectives which are related for rheological measurements.

Objective 1 -

> ...involves a straightforward attempt to determine the behavior of non-Newtonian liquids in a number of simple rheometrical flow situations using suitably defined material functions. The simple desire here is to seek a correlation between molecular structure and material behavior or alternatively between material properties and observed behavior in practical situations.

Objective 2 -

> ...is more sophisticated and decidely more difficult. It involves the prediction of behavior in non-simple flow situations from the results of simple rheometrical experiments.

Fortunately, many industrial process involve simple flow geometrics and the material functions that are determined can be used for similar applications. The progress that has been made on Objective 2 is for certain types of materials such as viscoelastic liquids. The most reliable data has been collected from the linear region. This data has been used to develop constitutive equations for use in the stress equation of motion and continuity to predict behavior for practical flows. Contrarily, the data from the nonlinear region is questionable because the measuring machines such as rheogoniometer will bend some stationary parts because large forces are exerted by some polymers that are undergoing large shearing. The R-16 Weissenberg Rheogoniometer needs to be modified so that the data collected can be used to develop constitutive equations for the nonlinear region for shearing.

With respect to the collection of data from the nonlinear region, the state of the art is closer to Objective 1.

Consequently, the objective of this thesis is to collect material functions from oscillatory shearing in the nonlinear region of polyisobutylene in centane by using a modified R-16 Weissenberg Rheogoniometer.

Polyisobutylene in cetane was chosen because it is available from the National Bureau of Standards (NBS) as a viscoelastic fluid. Also, a number of rheologist have reported the data on it. A comparison with reported data would verify our modifications as a bonafide approach for measuring nonlinear behavior.

Our R-16 Weissenberg Rheogoniometer is a gracious gift from Dow Chemical Company of Midland, Michigan. Unfortunately, the rheogoniometer had received a thorough usage at Dow Chemical and many electronic parts need replacing. Since we had limited funds, we decided to do as much of the repairs and modifications ourselves. Our research funds were spent on a piezoelectric load cell and a torsion bar assembly. The piezoelectric cell was used for the normal stress measuring, because the normal force servo mechanism was completely inadequate. The materials of interest in our work are polymer solution of high concentration, and these have time constants of a few seconds. Spriggs, et. al.[24] have shown that the unmodified normal force servo mechanism can be used only on materials with a time constant of a minute or more. The new torsion bar assembly allows us to change the torsion

bar to a stiffer bar without changing the sample fluid and resetting the cone-plate gap. The torsion bar assembly was bought because there was not enough funds to buy both the piezoelectric load cell and a temperature controller. The money that was spent on the torsion bar assembly was well spent, because the experiments can always be conducted by only allowing the minimum movement of the plate to measure the shear stress.

The temperature controller was not working because the heating element was burnt out. If the on-off temperature controller was working, it would not benefit the experiment because previous data on polyisobutylene in the literature were collected at 25 to 30C which is ambient. Also, the controller had a very course temperature scale which could not indicate the temperature better than plus or minus 5C. By necessity, the experiments were conducted at room temperature during the Winter. Since the electronic tube equipment dissipated heat, sufficient time was given before shearing to allow the room temperature to become stable. During the summer months the experiments were conducted after sundown, because the room temperature would go down and the heat dissipated from the electronic equipment would compensate to help keep the temperature leveled. This method for room temperature control is not a substitute for a room thermostat which the old laboratory does not have.

Consequently, this thesis is more of a feasibility study to determine the quality of the data collected from the nonlinear region.

CHAPTER II

METHOD OF APPROACH

2.1 Material Functions from an Unmodified WRG

The viscosity, η , defined by the canonical equation

$$\eta(\dot{\gamma}) = \tau_{r\theta}(\dot{\gamma})/\dot{\gamma} \qquad 2.1$$

is a material function. Material functions are physical properties which may depend on strain, strain rates, or shear stress, etc. Also, for steady shear flow of non-Newtonian fluids the remaining stress distribution is

$$\tau_{r\phi} = \tau_{\theta\phi} = 0 \qquad 2.2$$

$$\tau_{rr} - \tau_{\theta\theta} = \nu_1(\dot{\gamma}) = \dot{\gamma}^2 N_1(\dot{\gamma}) \qquad 2.3$$

$$\tau_{\theta\theta} - \tau_{\phi\phi} = \nu_2(\dot{\gamma}) = \dot{\gamma}^2 N_2(\dot{\gamma}) \qquad 2.4$$

The flow in the cone-plate gap is described by three material functions η , ν_1 , ν_2 . The variable η is best called the shear-dependent viscosity or "apparent viscosity"; ν_1, ν_2 are called the first and second normal stress difference, and N_1, N_2 are by definition called the first and second normal stress coefficients. For Newtonian liquids the apparent viscosity η is a constant and the normal stress differences ν_1, and ν_2 are zero at all shear rates. The elastic liquids will behave as Newtonian liquids if shear rate is small enough, because the normal stress difference tends to zero faster than the apparent viscosity goes to a constant or "zero shear" viscosity. For most viscoelastic fluids, the

apparent viscosity is a monotonic decreasing function which decreases from a zero-shear value to a lower value at higher shear rates. The lower value may not be observed, since it can be several orders of magnitude lower than the zero-shear viscosity.

In a preliminary investigation, the steady state shearing offers little information on needed enhancements for dynamic measurements. Stress growth or stress relaxation curves give "diagnostic" information on the machine's capability to respond to a sudden change of shear rate such as a step input. The time constant is the time for the shear stress to reach 67% of its steady state value, and the shorter the time constant the better. The unmodified Weissenberg Rheogoniometer or WRG appears at first to be well suited for this test. The cone or lower platen can be rotated for as long as necessary to achieve steady conditions, and the clutch and brake mechanism should stop the rotation in 10 milliseconds (ms.) The rotation of the plate or upper platen should be negligible for most materials or very small as relaxation proceeds. However, Batchelor, Berry and Horsfall[25] have found three potential flaws during studies on stress buildup and decay in polyisobutylene. Firstly, the impact of the clutch striking the driving plate may introduce a small spurious torque. Secondly, a fast switch must be used to switch off the clutch current and switch on the brake current otherwise the lower plate may "free wheel" for a time. And lastly, the motion of the upper

platen as the torque falls rapidly may introduce a strain rate which is comparable to the initial shear rate.

The best way to check this last flaw is to repeat the measurement using a stiffer torsion bar to detect any differences. During start-ups the normal force causes a slight separation of the cone and plate, and radial flow of the sample does occur. Part of the normal force generated by the fluid goes to overcome the shear stresses of the radial flow so a fraction of the force is not measured. The normal force will build up slower than the real rate of increase should be. Meissner[26] increased the response of the unmodified WRS by increasing the cone-plate gap angle. The 8 degree cone-plate angle preferred by Meissner reduces the time for peak stress to be reached, but the edge of the fluid breaks apart at much lower shear rates. Also, Galvin and Whorlow[27] have studied the change of the cone-plate angle and normal force buildup in polyethylene. Chang, Yoo, and Hartnett[28] studied a series of normal stress measurements with several cantilevers to obtain data which show that the normal force in transient experiment approach asymptotic values as the cantilever rigidity increases. These asymptotic values were taken as representing the material response. Kearsley and Zapas[29] have concluded that even when mathematical correction to all known errors are taken into account, the transient normal stress measurement are not reliable on the unmodified WRG.

Another dynamic test besides transient stress growth is

small-amplitude oscillatory shearing. The input shear rate by the cone with the motion given by equation (1.3.11) is approximately described by the following equation

$$\dot{\gamma} = -\omega\gamma_o \sin\omega t \qquad (2.5)$$

$$= -\dot{\gamma}_o \sin\omega t \qquad (2.6)$$

where $\dot{\gamma}_o$ is the strain rate amplitude. The corresponding stress distribution for viscoelastic materials is

$$\tau_{r\theta} = \dot{\gamma}\left(-\eta' \sin\omega t + \frac{G'}{\omega}\cos\omega t\right) \qquad (2.7)$$

$$\tau_{r\phi} = \tau_{\theta\phi} = \tau_{rr} - \tau_{\theta\theta} = \tau_{\theta\theta} - \tau_{\phi\phi} = 0 \qquad (2.8)$$

where η' is the 'dynamic viscosity' and G' is the 'dynamic rigidity'. For a Newtonian fluid, equation (2.7) implies that the stress is proportional to the shear rate so G' = 0 and η' is the constant viscosity. For Hookean solid the converse is suggested by equation (2.7). Generally, most of the literature shows the mathematics with complex variables. The equation (2.7) is now given by

$$\tau_{r\theta} = \dot{\gamma}\eta^* \exp(i\omega t) \qquad (2.9)$$

where $\eta^* = \eta' - i\,\frac{G'}{\omega} = \eta' - i\,\eta''$ (2.10)

which η^* is called "complex dynamic viscosity" and η'' is the "loss viscosity'. Similarly, the literature uses the definition

$$G^* = G' + iG'' \qquad (2.11)$$

as the 'complex modulus' and

$$G'' = \omega\eta' \qquad (2.12)$$

where G" is called the 'loss modulus'. The assumption of small-amplitude oscillatory-shear experiment is that the material deforms linearly. Equation (2.5) and (2.7) indicate that the harmonic strain results in a harmonic stress of amplitude proportional to the strain amplitude with a phase lag which is independent of amplitude. This assumption is tested by varying the strain amplitude on the amplitude ratio, τ_0/γ_0 , while shearing at a common frequency.

For all viscoelastic liquids in the linear region the complex viscosity η^* goes to the zero shear viscosity η_o as the frequency of oscillation goes to zero. The amplitude ratio goes to zero and the phase lag goes to $\pi/2$ as the frequency of the oscillation goes to zero. Some experiments are conducted to identify the system's natural frequency, ω_o, because machine's resonance at the natural frequency voids all measurements. The machine's resonance causes the amplitude ratio to go to one and the phase lag to go to zero, hence, the machine is insensitive to the material properties of the test fluid. Fortunately, the natural frequency can be changed by using a different torsion bar. The most common practice is to collect data above and below the natural frequency and to draw a smooth curve through the discontinuity.

Although there is a "natural frequency" in the normal force direction, it seems to be at a high enough frequency to unaffect the stress measurement, regardless, whether a cantilever beam or a piezoelectric load cell is used.

2.2 Enhancements to the R-16 WRG

Normal stress growths in simple rotational shear and first normal stress difference in oscillatory shear are impractical experiments with the unmodified WRG, because the normal force measurement uses the cantilever beam. In the nonlinear region the normal stress differences oscillates with the frequency 2ω at a displacement level which independent of time. A peak force during oscillatory shearing of polyisobutylene might be 10 N(Newtons). Such a produced force may move the upper platen (plate) upward about 1 μm (micron) and may move the lower platen (cone) and cantilever beam downward about 10 μ m. Figure 3a shows a force, F, acting downward on the cantilever beam. The depression due to its own weight at any point on a uniform beam which is rigidly clamped horizontally at one end is

$$y_1 = Wx^2(x^2 - 4Lx + 6L^2) \; / \; (24\ EI) \qquad (2.14)$$

where E is Young's modulus, W is the weight per unit length, and I is the second moment of area of the cross section. Figure 3b shows a rectangular cross section bar, which is bent in a plane perpendicular to the edge of length b. The second moment is given by

$$I = bd^3/12 \qquad (2.15)$$

The load, F, at the end increases the depression by

$$y_2 = Fx^2\ (3L - x) \; / \; (6\ EI) \qquad (2.16)$$

UNMODIFIED WRG

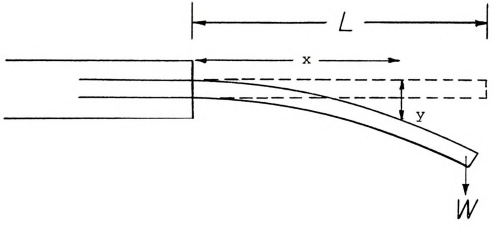

Figure 3a. Cantilever Beam and Clamp

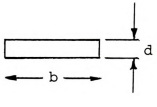

Figure 3b. Cross-Section Area of Beam

F at x = L, becomes

$$y_1 + y_2 = L^3 \ (F/3 + WL/8) \ / \ (EI) \qquad (2.17)$$

The cantilever beam is replaced as an enhancement by a piezoelectric load cell, which has a movement of about 0.1 μm. Naturally, the upper platen does move upward by more than 1 μ m. A force greater than or equal to 10N is required to restrict the upper platen to 1 μ m. This enhancement is simply accomplished by standard weights that are usually used for a balancing scales. The most benefit from added weights is placing the weights as close as possible to the upper platen. Figure 4 shows a C-ring which can be placed on the upper platen. Depending on the gage of metal, the C-rings are cut to a diameter for a specific weight. A pair of C-rings affords more symmetry, but the C-rings do increase the moment of inertia. The increased moment of inertia affects the acceleration term in the equation of motion of the upper platen. The equation of motion is approximately given by,

$$W_o \cos\omega t = I\frac{d^2\phi}{dt^2} + \frac{2\pi R^3}{3\text{Oo}} \frac{G''}{\omega} \frac{d\phi}{dt} + \left(\frac{2\pi R^3}{3\text{Oo}} G' + C\right)\phi \qquad (2.18)$$

where W_o cos wt is the harmonic torque, I is the moment of inertia, ϕ is the angle the platen rotates through, and C is the spring constant for the torsion bar. The C-rings are temporary and inexpensive device, which minimizes the upward movement of the upper platen.

Usually a Honeywell Visicorder is used to trace the harmonic stresses and strain on ultraviolet sensitive paper.

MODIFIED WRG

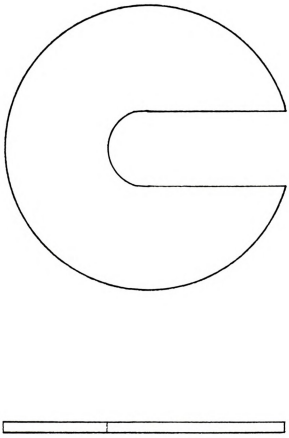

Figure 4. Sketch of C-ring

The analysis of the galvaniometer recording is tedious and not very accurate. Although the galvaniometer gives qualitative information, a computer gives the means to analysis the signals from the transducers. The IBM 1800 is an analog/digital computer which uses a digital voltmeter, DVM, to convert the electrical signals between -10 volts to +10 volts into discrete numerical values for the computer program. The Fourier method, which is programmed for tabular data gives the equations for the shear stress and normal stress in terms of a series of sines and cosines. These equations are used to compute the material functions. The IBM 1800 computer is interfaced with a Calcomp plotter, which provides a trace of the signal for qualitative purposes.

2.3 Material Function from a Modified WRG

The modified WRG is best evaluated by varying only one enhancement at a time. All stress growth and relaxation experiments use the IBM 1800 computer and the Calcomp plotter which offer more consistency during comparisons. With the piezoelectric load cell installed, the tests are conducted with and without C-Rings. If the stress growth curve is shaped more similar to the step increase function with the C-ring, then the modification is an enhancement. Naturally, the stress relaxation curve is shaped as a step decrease function.

The modified WRG does not offer any advantage for small amplitude oscillatory shearing, but an experiment that was done by the unmodified WRG needs to be repeated by the

modified WRG for comparison. The computer interface does permit the calculation of more difficult material functions. Williams and Bird[30] discussed the time-dependent behavior of normal stresses exhibited by fluids is small-amplitude oscillation. They solved the equation of motion for the cone-plate geometry to relate the amplitude and phase relationship of the oscillating stresses to experimental measurements. The results are expressed in terms of a "complex normal stress coefficient," ζ^*, and a "normal stress displacement function," ζ^d, which are given by definition,

$$\zeta^* = - \frac{\overset{\circ}{\tau}_{\phi\phi} - \overset{\circ}{\tau}_{\theta\theta}}{\Omega^2 \left(\frac{\partial}{\partial \Psi} \frac{\nu \phi^{\circ}}{r\Omega} \right)^2} \tag{2.19}$$

$$\zeta^d = - \frac{\mathrm{Re}\{ d_{\phi} - d_{\theta} \}}{\Omega^2 \left| \frac{\partial}{\partial \Psi} \frac{\nu \phi^{\circ}}{r\Omega} \right|^2} \tag{2.20}$$

where (2.21)

$$\zeta^* = \zeta' - i \ \zeta'',$$

ζ' and ζ'' are the real and imaginary parts (2.22)

$$\psi = \pi / 2 + \Theta, \tag{2.23}$$

$$\tau_{jj} = \mathrm{Re}\{ d_j + \overset{\circ}{\tau}_{jj} \exp(2i \ wt) \} \text{ for } j = r, \theta, \phi \tag{2.24}$$

$\overset{\circ}{\tau}_{jj}$ is the complex amplitude of the stress, and Ω is the amplitude of the angular velocity of the cone, radian/sec.

The equation of motion for oscillatory shearing are the same as the equations for steady rotation except the equation

(1.3.7) for the ϕ - component is

$$\rho \frac{\partial v\phi}{\partial t} = - \frac{1}{r^2} \frac{\partial}{\partial r} (r^2 \tau r\phi) - \frac{1}{r} \frac{\partial \tau\theta\phi}{\partial \theta} - \frac{\tau r\phi}{r} - \frac{2 \cot \theta \, \tau\theta\phi}{r} \qquad (2.25)$$

since $v_\phi = v_\phi (r, \theta, t)$. For small amplitude oscillatory shearing, the $\tau_{r\phi}$ terms are assumed to be small when compared to other terms in equation (2.25). Another assumption is that the normal components of stress which are perpendicular to the flow direction are equal. When these two assumptions are made, the equation of motion becomes:

$$- \rho \frac{v^2\phi}{r} = - \frac{\partial \tau\theta\theta}{\partial r} + \frac{\tau\phi\phi - \tau\theta\theta}{r} \quad , \qquad (2.26)$$

$$- \rho \frac{v\phi^2}{r} \cot \theta = - \frac{1}{r} \frac{\partial \tau\theta\theta}{\partial \theta} + \frac{\cot\theta}{r} (\tau\phi\phi - \tau\theta\theta) \quad , \qquad (2.27)$$

$$\rho \frac{\partial v\phi}{\partial t} = - \frac{1}{r} \frac{\partial \tau\theta\phi}{\partial \theta} - \frac{2\cot\theta}{r} \tau\theta\phi \quad . \qquad (2.28)$$

The boundary conditions are:

At $\theta = \pi / 2$ $\quad v\phi = 0$, (2.29)

At $\theta = \pi /2 + \theta o$ $\quad v\phi = r \Omega \sin \omega t$, (2.30)

At $r = 0$ $\quad \phi = 0$. (2.31)

The modified WRG is best suited for large-amplitude oscillatory shearing. MacDonald, Marsh, and Ashare[31] studied the rheological behavior for large-amplitude motion. Since shear stress is a continuous function of time, the Fourier

expansion is

$$\tau_{\theta\phi} = \sum_{n=o}^{\infty} A_{2n+1} \cos^{2n+1} (\omega t + \phi) \tag{2.32}$$

where ϕ is the phase shift occurring between the input strain and the output stress. The assumption of a linear velocity profile in the fluid has been shown valid for small cone angles of less than 4 degrees and angular velocity less than 119 sec^{-1}. The large-amplitude complex viscosity is defined by

$$\eta^* (\omega, \gamma^0) = - \frac{\tau_O}{\gamma_O} \eta'(\omega,\gamma_O) - i\eta'' (\omega,\gamma_O) \tag{2.33}$$

With large strain amplitudes or high frequency, shear stress measured on the plate shows higher odd harmonics. Equations (2.32) and (2.33) reduce to small-amplitude shear stress and complex viscosity in the limit of small strain amplitudes. If the higher harmonics can be determined, then experiments may be used to fit fluid models to experimental results.

Walters and Jones[32] have concluded that the amplitude of the third harmonic could be very small because the spring constant and the moment of inertia can be large. The exception is near one-third of the natural frequency, which may resonant similar to the natural frequency for the first harmonic. Their experiments on Newtonian fluid and a viscoelastic liquid clearly indicate a third harmonic content at the one-third of the natural frequency. A similar

resonance occurs near one-fifth of the natural frequency which is caused by the fifth harmonic. If the nonlinear effects are not noticeable, the oscillatory experiment could be performed at frequency close to $\omega o/(2M + 1)$, M = 1, 2, 3...

The normal stresses have nonlinear effects that are caused from large-amplitude shearing. Akers and Williams[33] used the total force method to determine the first normal stress difference, which was complicated by machine-compliance problems. Christiansen and Leppard[34] used flushed-mounted transducers to investigate the first and second normal stress differences. Tanner[35] correlated the normal stress data for polyisobutylene solutions from 28 papers. The first normal stress data are correlated as a function of concentration, molecular weight, and shear stress.

CHAPTER III

DESCRIPTION OF APPARATUS AND EXPERIMENTS

3.1 Unmodified R-16 Weissenberg Rheogoniometer

The Weissenberg Rheogoniometer to be described in Figure 5 is the model R-16 manufactured by Sangamo Controls Ltd.[36] It is an intermediate successor to a series of machines, developed from the original ideas of Weissenberg, which were intended to measure not only shear stress in steady rotation but also oscillatory stresses and normal stresses.

A 1 hp, 1800 rpm, synchronous motor drives a 60-speed gearbox covering about six decades of angular velocity in approximately logarithmic index so that the period of oscillation of the platen can be varied from 0.016s. to 1.325 x 10^4 s. It is necessary to stop the motor to change gears. The output shaft of the gearbox is connected to a drive box containing an electromagnetic brake-clutch unit which allows the stopping and starting of the platen within 10 ms while the gearbox is still running. Also the drivebox comprises a variable sinewave generator for oscillatory tests. The horizontal output shaft of the drive box has a worm gear engaging with a worm wheel on the main vertical drive shaft of the machine. The test fluid is held between the platen attached to the top of the drive shaft and a platen attached to the bottom of the air bearing rotor in the torsion head. Normally the upper platen is a flat plate and the lower platen is the cone, but they may be interchanged for thinner fluids.

WEISSENBERG RHEOGONIOMETER

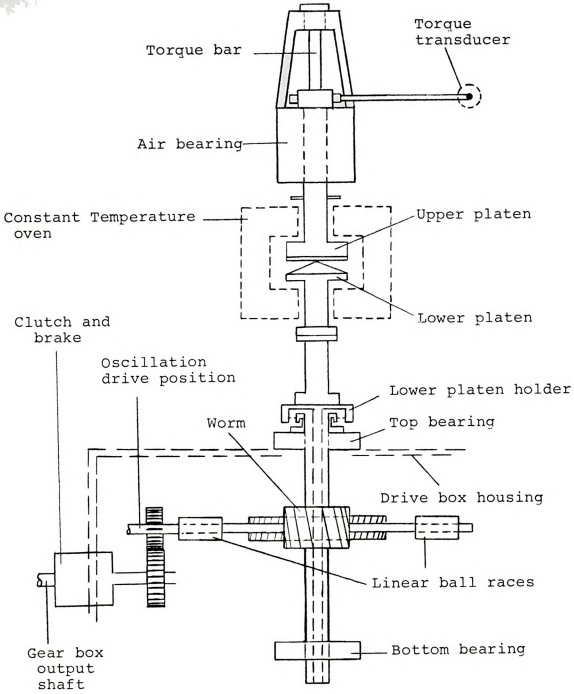

Figure 5. Weissenberg Rheogoniometer Internal
(from Sangamo Controls Ltd.)

The torsion head consists of a torque bar, which is available in a wide range of stiffnesses, that is clamped at the top and attached at the bottom to the rotor of an air bearing which holds the upper platen. The twist in the torque bar is measured with a linear variable inductance transducer. The armature is connected to a radius arm 100 mm long clamped to the bottom of the torque bar. With the Farol electronic equipment the range of measurable torques ranges from about 2×10^{-8} Nm to 20 Nm. the entire torsion head assembly including the air bearing and torque transducer can be moved vertically along a dove-tail slide, its movement near the lower platen is measured by a second transducer so the platens may be separated for cleaning and returned back to the same cone-plate gap. The tip of the cone is usually grounded away by a known amount. The location of the cone relative to the plate is critical for the best operation of WRG.

For many years the only normal force measuring system for the WRG was the servo arrangement shown in Figure 6.[37] The lower platen is driven through a beryllium copper diaphram which has a high torsional rigidity but allows free vertical movement. A rod connected to the lower platen holder passes down through a hollow drive shaft and ends in a ball. This ball is kept centered in a conical bearing mounted on the cantilever. When a downward force is exerted to the lower platen, the movement is detected by a null-detecting transducer below the cantilever and the original position of

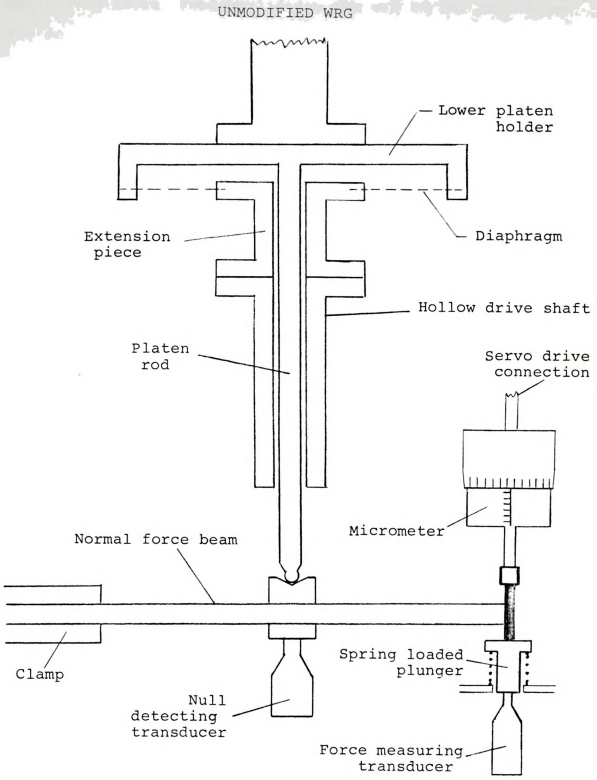

Figure 6. Normal Force Measuring Assembly
(from Sangamo Controls Ltd.)

the platen is returned by lifting the end of the cantilever. The end is moved by a plunger that is loaded by a strong spring below the cantilever and is controlled by a micrometer above the cantilever. The movement of the micrometer is proportional to the force on the platen. The micrometer can be adjusted by hand. In practice a servomotor which is controlled by the null-sensing transducer makes the necessary adjustment. The movement of the end of the cantilever is measured by another transducer. The servo-system returns the middle of the cantilever spring back to its original position within 0.1 mm is a couple seconds, but the cone-plate gap may not return back to 0.1 m.

The WRG uses a variable amplitude, variable frequency, harmonic rotation which can be superimposed on a steady rotation. Figure 7[38] shows a circular cam eccentrically mounted on a shaft driven through bevel gears and a gearbox to give oscillation frequencies up to 60 Hz. The oscillation thimble rotates a lever arm, which by a transfer slide, rotates the actuator. The lever pivot can be moved from the indicated position until it is line with the transfer slide, which reduces the oscillation to zero. The platen shaft is driven via a worm gear which oscillates by the actuator or rotates by a separate motor and gearbox. The details that are not shown include spring to keep the worm shaft in contact with the actuator and to keep the worm in firm contact with the worm wheel. The spring prevents backlash. Also, the axial cam on the end of the camshaft which contacts

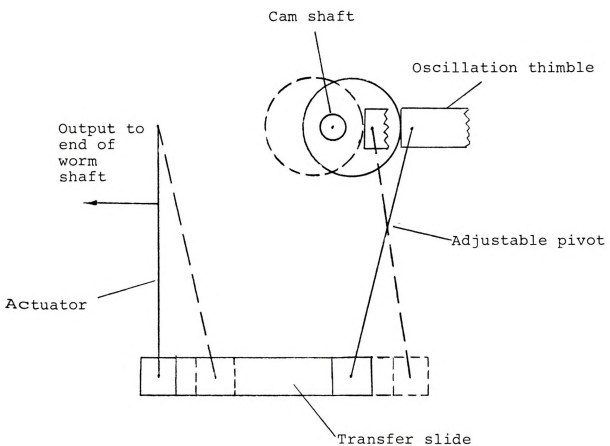

Figure 7. Harmonic Motion Mechanism
(from Sangamo Controls Ltd.)

a spring loaded follower is not shown in Figure 7. The cam provides an opposing load on the oscillatory drive motor and gearbox to the load which is produced by the main cam. Hence, backlash in the gears is avoided which would be caused by cyclic bad variations. The sinewave that are produced for worm shaft amplitudes between 0.025 and 1.0 mm are free of distortions.

For temperature control the platens may be surrounded by an electric oven. At lower temperature the oven may be cooled or heated by circulating silicone fluid through the double walled chamber from a thermostat. The enclosure may be filled with an inert gas. Although a thermocouple may be attached to the upper platen, it is doubtful that the actual fluid temperature is being measured at the extreme temperatures of -50°C to 400°C, which the machine was designed. The temperature controller and pen recorder were inoperable, so experiments were conducted at room temperature during the entire research.

The R-16 WRG is a second hand machine that was graciously donated from Dow Chemical. After the WRG was installed and running, some peculiar waveforms occurred during oscillatory shearing of an NBS calibration oil. A spike appeared on the shear stress waveform at large strain amplitude and at all frequencies. While using the Honeywell visicorder, the set screw that is located on the front side of the WRG was turned counterclockwise to adjust the worm gear and the helical bevel gear until the spike on the

waveform was eliminated. The gears can introduce vibrations if they are not meshing properly.

During the moving of the WRG from Dow Chemical, the torsion head became misaligned from the centerline of the hollow drive shaft. Using a precision indicator that can measure to 0.0001 of an inch, the air-bear rotor of the torsion head was centered for trueness at the top and bottom of the rotor to within 0.0002 inches.

3.2 Modified R-16 Weissenberg Rheogoniometer

An overall simplification of the measuring system is given in Figure 8. Each block represents a possible electronic fault in the system. The new system has fewer blocks, hence, the number of possible sources of errors and the time required for searching is reduced. Low-pass filters are often used in oscillatory work; Van Rijn[39] pointed out that they should be carefully matched.

The piezoelectric crystal system that was used to replace the LVDT transducer is a Solartron Corporation model piezotron and a charge amplifier. The piezotron, which is a fast response transducer is shown in Figure 9. The electric charge is proportional to the applied force on the cell. The piezotron is very rigid with an operating range from 1000 gm of compression to 500 gm of tension. The operating range for temperature environment is from below -50°C to 250°C. However, the piezotron is very sensitive to temperature variations. When the ambient temperature changes by 5-10°C the electrostatic output from the cell becomes unstable, but

BLOCK DIAGRAM

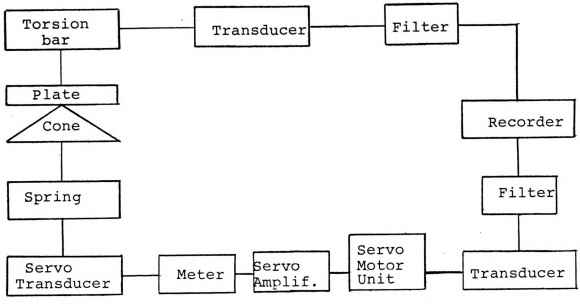

a.) For the Unmodified System

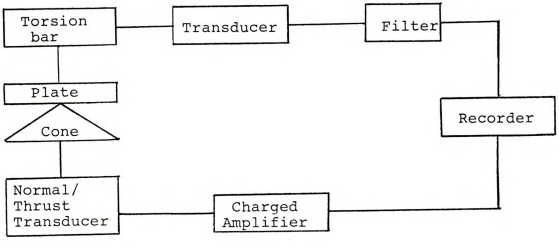

b.) For the Modified System

Figure 8. Measurement Paths

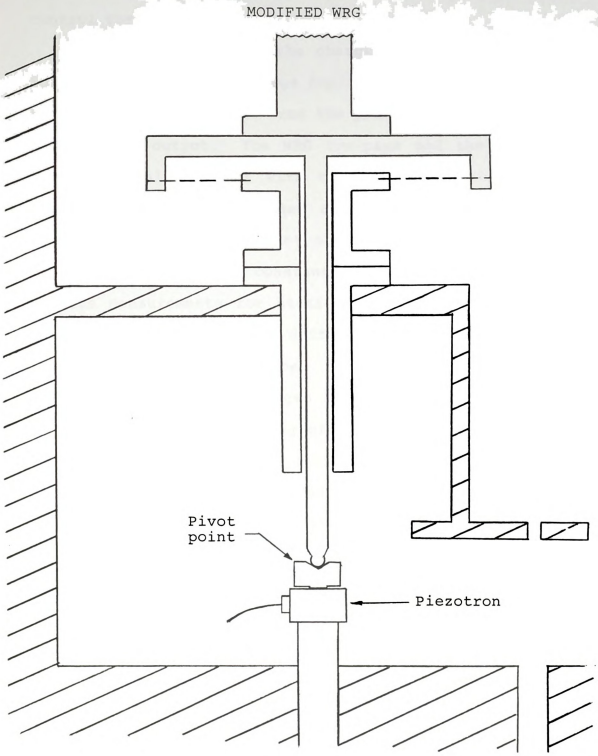

Figure 9. Sketch of Modified Normal Force Measuring System

it has been proposed to install temperature and humidity control for the room.

In order to amplify the charge from the piezotron, a Solartron Calibration Charge Amplifier is used. It converts the electrostatic output from the piezotron cell to a current and voltage output. The WRG low-pass and the IBM 1800 Analog/Digital computer with the Calcomp plotter or the Honeywell visicorder is used to display the output. The amplifier has five different scales for operating purposes and a short-long time constant positions. The selection permits measurements for static response by using a high input resistance, and for drift-free dynamic operation by using a low input resistance. When the GND button switch is pressed, the residual charges from the measuring system is removed. During the loading of the test polymer an unwanted charge can build up. The calibration which is shown in Figure 10 is linear and was made on the four scales.

As discussed in Chapter II the C-ring which is shown in Figure 4 provide the counterweight to oppose the normal force exerted by the viscoelastic fluid. The C-rings that are used in our research are made from aluminum with a diameters from 3 to 5 inches. The slots are cut wide enough to accommodate the diameter of the air rotor. The C-rings are not used with the oven, because the weight of oven changes the cone-plate gap.

The IBM 1800 Analog/Digital computer has about a 60 K memory, which doesn't allow for a very sophisticated program.

MODIFIED WRG

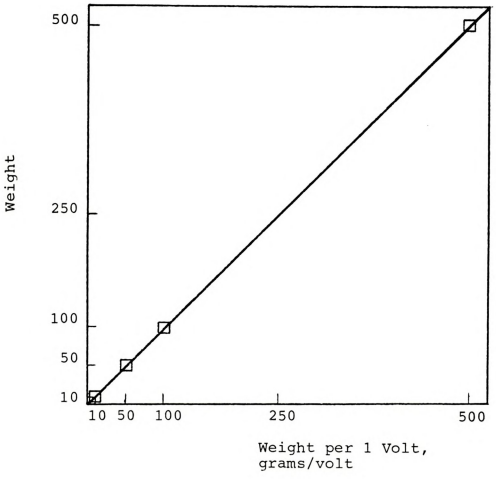

Figure 10. Piezotron Calibration

The programs which are given in Appendix A reads the voltages from the analog input and converts these voltages into physical parameters. Only the digital voltmeter DVM is used from the analog portion of the computer system. This voltage reading is accomplished by a "canned" subroutine which is accessed by CALL HFAI. The trunk number, which is the terminal connection, and the number of lines is indicated in the call statement. The pause between voltage readings is accomplished by another canned subroutine which is accessed by CALL HYDLY in terms of milliseconds. The other support equipment is the card reader, the 1443 line printer, and the typewriter which are on-line terminals that are accessed by the file numbers in the Fortran read and write statements. The Calcomp plotter is wired through teh analog output and the program accesses the plotter by CALL HYPLT. The plotter inherently draws straight lines between successive points. The sinusoidal waves obtain a "curvature" by using many points. The plotted signals give a qualitative description. A better plot of transient data is recorded by the Honeywell 1508 Visicorder. The recorder has a maximum recording speed of 80 inches per second, and it gives time lines in intervals of 10, 1, 0.1, or 0.01 seconds. The M100-120A galvanometer, which has a response time of 0.01 seconds, is used during the recording of transient experiments.

3.3 Laboratory Procedures and Techniques

The platens were cleaned after every experiment. Whenever the next run within an experiment was at a reduced

shear rate from the previous run, the platens were cleaned and reloaded with a new test sample. Most of the bulk used sample was removed by paper towel, and any film on the surfaces and edges of the platens are cleaned by Kimwipes with acetone. The lower platens were checked for concentricity and tilt before sample loading, while the upper platen was checked only between experiments. Whenever the platens were changed, the platen holder was checked for concentricity. The lower platen extension piece was centered at the bottom first then at the top to ensure squareness.

Transducer Calibration. In order to ensure the accuracy of the data it was necessary to perform calibration checks periodically for the proper function of the rheometer. The following calibration procedure was generally adopted for all transducer, transducer meter and amplifier on a monthly basis or immediately after repairs. The oscillation input, torsion head, and gap set transducer and transducer meter unit were calibrated with the help of a micrometer jig for known linear movements of the transducer armature.

1. The mechanical set zero of the transducer meter is described in the rheogoniometer operating manual by Sangamo Controls.

2. Set the transducer meter/amplifier range switch to "cal" position and adjust to full scale deflection on the meter by means of "set cal."

3. Adjust the position of the transducer body and amplifier zero-offset to obtain a null reading on the

transducer meter.

4. Next adjust the transducer meter unit of the amplifier so that ± 100, ± 35, and ± 10 micron movement of the armature results in a corresponding identical reading on the amplifier meter with the meter range switch set on "100 " range.

5. Repeat the above procedure for each of the other meter range setting 100, 25, 10, 2.5 and 0.25.

By this method the calibrations were verified to be linear and to be within a maximum error bound of 5 percent on the most sensitive range 0.25, and generally better on the other ranges.

Gap Setting. The piegotron cell is an expensive enhancement, so the gap setting must be done carefully. A white piece of paper provides a good contrasting background. The alligator leads of a voltmeter are connected to the adjusting screw of the top and bottom platen. The torsion head is lowered as close as possible to the bottom platen, then the voltmeter is watched while slowly turning the torsion-head handle in clockwise rotation. If a "hard" contact is made, then the torsion head should be raised high enough to eliminate any backlash in the lead screw of the torsion-head slide. When the voltmeter indicates an electrical circuit is made, the platens have made contact. The thumb setting screw for the gap setting transducer is turned to depress the transducer armature by the required cone-plate gap beyond the null or zero micron point on the

gap setting meter. The torsion head is then raised high enough to load the sample.

Sample Loading. Although only 1- to 2- c.c. of the test sample is required, care must be exercised during loading. When the sample, such as polyisobutylene in cetane, is poured on the bottom platen, air bubbles tend to become trapped in the liquid. A chemist's spatula can be used to burst the bubbles from the sample. After all the bubbles have been removed, the top platen or plate is lowered to just kiss the convexed puddle of sample. If the sample puddle is concaved, then an air bubble will be trapped and a new sample must be loaded. To detect the air bubble a pen flashlight can shine light through a translucient sample against a contrasting background of a white piece of paper. As the top platen is being lowered to the null point of the gap meter, the polymer sample is squeezed out to the edge of the platens, and it will start to drip from the cone-plate gap. The spatula can be used to trim the excess sample during the gap setting. The polymer sample needs to relax for about 30-minutes to relieve any stresses that have been induced.

3.4 Experiments for an Unmodified WRG

The stress growth experiments used a 7.5 cm diameter plate with a 1.533 degree cone-plate angle. The tests with the unmodified WRG used a cantilever of 403 gm/micron, torsion bar of 0.943 dynes-cm/micron and a gearbox setting of 1.6 or 11.3 rpm. During the shear stress growth the visicorder is

set at a chart speed of 8 inches/second with a timer at 0.1 second. Since the normal stress growth is much slower, the visicorder is operated at 1/2 inch/second with the timer on 1.0 second.

The small-amplitude oscillatory shearing comprises the frequency response and the strain amplitude response experiments. During the frequency response experiments the strain amplitude is held constant and the frequency is varied. The strain amplitude dial is set at a low enough indication such that operating at the highest frequency permits shearing in the linear viscoelastic region. Shearing of the polymer is begun at the lowest frequency and is increased in steps to the highest frequency. The machine must be stopped to change the gearbox index for the new frequency. At a strain amplitude of 1.0 the literature indicates a frequency of about 0.6 cycle/second as an upper limit for linear viscoelastic region. Since the upper limit is an a posteriori fact, the frequency is usually increased beyond the upper limit to also collect data in the nonlinear region.

Similarly for strain-amplitude response experiments, the strain amplitude dial is changed from zero to the upper limit for the linear viscoelastic region while the frequency is held constant. The strain amplitude dial can be moved slowly while the machine is running. Likewise the strain amplitude is increased above the upper limit for the linear region. The cone can be changed from 1.533 degree gap angle to 0.5533 degrees to increase the strain amplitude if necessary.

3.5 Experiments for a Modified WRG

The stress growth experiments used a 7.5 cm diameter plate with a 0.5533 degree cone-plate angle. These experiments test the benefit of using C-rings. The modified WRG uses the piezotron load cell, torsion bar of 0,943 dyne-cm/micron and a gearbox setting of 3.0 or 0.45 rpm. To convert the computer time into the real time corresponding to 0.45 rpm, a delay factor of 37 is used in the TESTY program. The TESTY program simply reads and prints the voltages for the torsion, oscillatory, and piezotron tranducers. For these tests the shear rate is 9.8/second.

For oscillatory shearing experiments the following input data is required for the WEISS program,

1.) Number of cycles for averaging (eg 1-5)
2.) Number of the highest harmonic (eg 1-6)
3.) JMAX for the Rhomberg integration (eg 6-7)
4.) Cone angle in degrees (eg 0.5522)
5.) Platen diameter in centimeters (eg 7.5)
6.) Delay/point (eg 9, 37, 109)
7.) Torsion bar constant in dynes-cm/thousandth (eg 2.395E04)
8.) Strain amplitude dial indication (eg 16.4)
9.) Frequency in cycles/second (eg 0.0952)
10.) Range on torsion meter (eg 2.5)
11.) Range on oscillatory meter (eg 100)
12.) Transfer function for piezotron in volts/gm (eg 0.02).

The program asks for the above information in this order, and the format for the entries is printed by the program before the input is required.

The number of cycles for averaging depends on how well the signal reading is synchronized to the number of points read per cycle. A typical range for cycle averaging is from 1 to 5. The number of points for the cycle is determined by JMAX which is used in the Rhomberg integration. JMAX is equal to 1 plus 2 raised to the JMAX + 1 power, so JMAX of 7 equals 257 points for the cycle. For a given frequency, the delay/point is chosen from experience to read the 257 points in the period. For example, at a frequency of 0.0952 c/s a delay/point of 109 will cause the digital voltmeter on the IBM 1800 analog/digital computer to read 257 voltages in about 10.5 seconds.

CHAPTER IV

ANALYSIS OF DATA PROCESSING

4.1 Dynamic Material Functions

As mentioned in section 2.1 for small-amplitude oscillatory shearing, the input shear rate is approximately described by equation (2.6),

$$\dot{\gamma} = -\dot{\gamma}_o \sin \omega t \tag{4.1}$$

where $\dot{\gamma}_o = \omega \gamma_o$. Figure 11 shows a pair of sinusoidal waves for stress and strain. Point 0 is the point of origin for the strain waveform, which is given by

$$\gamma = \gamma_o \cos \omega t \tag{4.2}$$

It is assumed the strain produces a shear stress

$$\tau = \tau_o \cos (\omega t + \delta) \tag{4.3}$$

where is the phase shift, so

$$\tau = \tau_o \cos \delta \cos \omega t - \tau_o \sin \delta \sin \omega t \tag{4.4}$$

$$= \gamma_o (G' \cos \omega t - G'' \sin \omega t) \tag{4.5}$$

$$= G' \gamma + \frac{G''}{\omega} \dot{\gamma} \tag{4.6}$$

The dynamic storage modulus

$$G' = (\tau_o \cos \delta)/\gamma_o \tag{4.7}$$

gives the phase stress amplitude and loss modulus,

$$G'' = (\tau_o \sin \delta)/ \gamma_o \tag{4.8}$$

gives the quadrature stress amplitude.

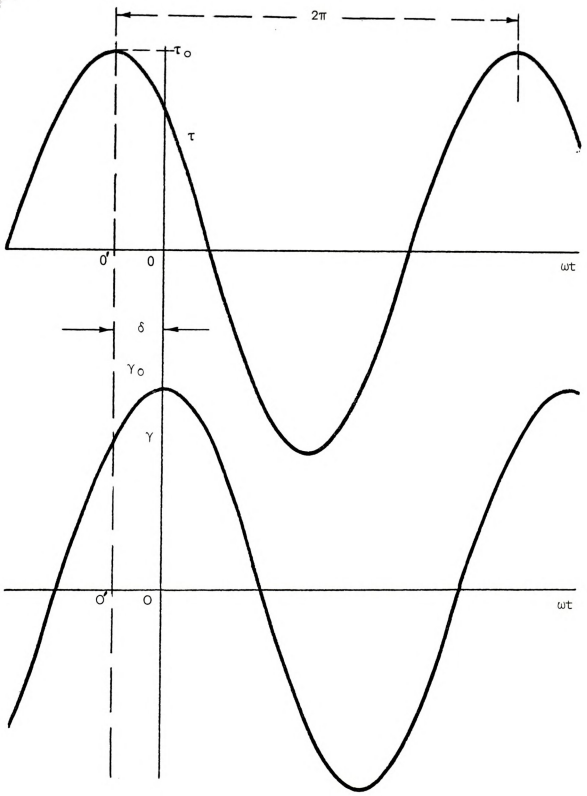

Figure 11. Pair of Cosine Waveforms

The dynamic viscosity and loss viscosity arises if the shear rate is considered, as is usually done for essentially fluid systems. Equation (4.4) becomes in terms of the strain rate amplitude γ_o,

$$\tau = \gamma_o (-\eta' \sin\omega t + \eta'' \cos \omega t) \tag{4.9}$$

where $\eta' = (\tau_o \sin \delta)/\gamma_o$ and $\eta'' = (\tau_o \cos \delta)/\gamma_o$ (4.10)

The factor $\gamma_o \eta'$ gives a measure of the component of stress in phrase with the strain rate.

In the above discussion for Figure 11, point O is an arbitrary origin for the measurement of time. Point O' could be taken as the origin with respect to shear stress waveform, so that the strain

$$\gamma = \gamma_o \cos (\omega t - \delta) \tag{4.11}$$

produces a shear stress

$$\tau = \tau_o \cos \omega t \tag{4.12}$$

The phase lag δ and the strain amplitude ratio τ_o/γ_o are a function of the material, and can be regarded as material properties for linear viscoelasticity, but these quantities generally will vary with frequency. Only two frequency-dependent quantities are required to determine the stress for a harmonic strain, so a variety of different pairs of such quantities are commonly used depending on the particular situation.

Equation (4.11) may be rewritten as

$$\gamma = \gamma_o \cos\delta \cos\omega t + \gamma_o \sin\delta \sin\omega t , \qquad (4.13)$$

where $\gamma_o \cos\delta$ is the amplitude of the strain component which is in phase with the stress, and $\gamma_o \sin\delta$ is the amplitude of the strain component which is out of phase with the stress. For stored and dissipated energy the following quantities are defined,

$$J' = (\gamma_o \cos\delta)/\tau_o \text{ and } J'' = (\gamma_o \sin\delta)/\tau_o \qquad (4.14)$$

so that $$\gamma = \tau_o (J' \cos\omega t + J'' \sin\omega t) \qquad (4.15)$$

and $$\tan\delta = J''/J' \qquad (4.16)$$

The J' is sometime called the dynamic storage compliance and J" is called the loss compliance. For ideally elastic solid, the stress and strain are in phase, $\delta = 0$, $J'' = 0$ and J' is related to the elastic energy stored in the material with no energy lost. Similarly for a Newtonian fluid, the stress and strain rate are out of phase, so $\delta = 90$ degrees, $J' = 0$ and J" is the rate of energy dissipated. Generally for viscoelastic fluid both J' and J" are nonzero for measuring the degree of stored and dissipated energy.

By differentiating and using equation (4.12) equation (4.15) becomes

$$\gamma = J'\tau - \frac{J''}{\omega} \tau \qquad (4.17)$$

and also differentiating equation (4.15)

$$\gamma = J'\tau + \omega J''\tau .$$

The Euler's equation, which is $\cos\omega t + i \sin \omega t = \exp(i \omega t)$ where $i = \sqrt{-1}$, is used for relationship based on the previous expressions for stress, strain, and shear rate because $\sin \omega t$ and $\cos \omega t$ are tedious to manipulate. Equations (4.11) and (4.12) are written as

$$\tau = \mathrm{Re}\ (\tau_o \exp (i \omega t)) \tag{4.18}$$

and

$$\gamma = \mathrm{Re}\ (\gamma_o \exp (i(\omega t - \delta))$$

$$= \mathrm{Re}\ (\gamma_o \exp (-i\delta) \exp (i\omega t)) \tag{4.19}$$

The complex strain amplitude is $\gamma_o \exp(-i\delta)$, which is sufficient to establish both the physical amplitude and the phase lag of the strain. If the complex compliance J* of the material is known, where

$$J^* = \gamma_o \exp (-i\delta) / \tau_o \tag{4.20}$$

then the stress can be calculated for any strain amplitude. Also,

$$J^* = \frac{\gamma_o}{\tau_o} (\cos \delta - i \sin\delta) \tag{4.21}$$

$$= J' - i J'' \tag{4.22}$$

so that J* may be found from the previously defined compliances. J' is the real part of the complex compliance, but J" is not the imaginary part of the complex compliance. Although -iJ" is called the imaginary part, J" is real and positive. In equation (4.20) the complex stress amplitude is real because the stress was used as the phase reference.

The complex modulus, G* is sometime defined as

$$G^* = 1/J^* \tag{4.23}$$

So $G^* = \frac{\tau_o \exp(i\delta)}{\gamma_o} = G' + iG''$, (4.24)

$$G' = J'/(J'^2 + J''^2) \quad (4.25)$$

$$G'' = J''/(J'^2 + J''^2) \quad (4.26)$$

$$J' = G'/(G'^2 + G''^2) \quad (4.27)$$

$$J'' = G''/(G'^2 + G''^2) \quad (4.28)$$

and $$\tan\delta = J''/J' = G''/G' \quad (4.29)$$

The shear rate is obtained by differentiating the complex strain in equation (4.19) to give

$$\dot{\gamma} = \mathrm{Re}\,(i\omega\gamma_o \exp(i\delta)\exp(i\omega t))$$
$$= -\omega\gamma_o \sin(\omega t - \delta) \quad (4.30)$$

The complex dynamic viscosity is sometimes defined by

$$= \eta^* = \frac{\tau_o}{i\omega\gamma_o \exp(-i\delta)}, \quad (4.31)$$

and using equation (4.10), it follows

$$\eta^* = \eta' - i\eta'' \quad (4.32)$$

The advantage of using complex variables is that time appears in the equation in the form $\exp(i\omega t)$, so such terms cancel out when stress-strain ratios are taken. At any point in the calculation in which the complex amplitude of stress and strain occurs, the physical amplitude and phase shift may be determined by multiplying the complex amplitude by $\exp(i\omega t)$ and taking the real part of the expression.

By analogy to the mechanical equivalent of the "Q-factor", this may be defined as

$$Q = 2\pi \quad \frac{\text{Maximum stored elastic energy}}{\text{Energy dissipated per cycle}}$$

For an initially undeformed ideally elastic solid that is sheared by a strain γ_o, the work done is

$$\int_o^{\gamma_o} \tau \, d\gamma = G'\gamma_0^2/2. \tag{4.33}$$

Apparently, the stored energy is recovered if the strain is slowly reduced to zero. For viscoelastic fluid, the $G'\gamma_0^2/2$ is a measure of stored energy, but the work done in the deformation and the energy recovered does depend on how the strain varies with time. For harmonic motion the total work done on a unit volume per cycle is,

$$\int_o^{2\pi/\omega} \tau\dot{\gamma} \, dt = \int_o^{2\pi/\omega} -\omega \gamma^2 o(G'\cos \omega t - G'' \sin \omega t)\sin \omega t \, dt \tag{4.34}$$

$$= \pi \gamma^2_o G''.$$

From previous definitions, it follows

$$Q = G'/G'' = 1/\tan\delta \tag{4.35}$$

4.2 Visicorder Calculation Methods and Problems

Figure 12 shows a typical visicorder record for strain and stress waveforms which should have their centerlines parallel but not necessarily coincident. The distances corresponding to a complete cycle and to the phase shift can be measured from the curves respective centerlines. Alternatively, Walters[40] shows that the measurements can be

UNMODIFIED WRG

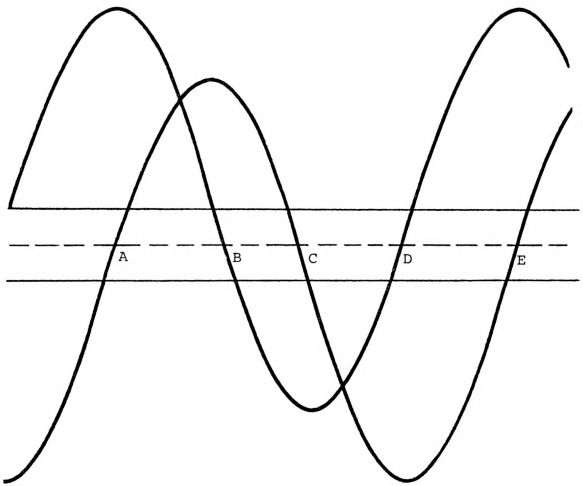

Figure 12. Visicorder Output Measurement

made along any line parallel to the centerlines such as ABCDE. The phase difference would be calculated as

$$\delta = \pi\ (AB + CD)/AE \qquad (4.36)$$

Obviously, the ABCDE line must intersect both curves, and it should be well away from the peaks for reasonable accuracy.

The accuracy is somewhat affected when the peaks for the wave form are small and the frequency is low. The reason is the curves become more horizontal so the intersection becomes ambiguous. The lengths for AB, CD and AE can be measured a little longer or shorter than the actual length such that a ±10% error will be introduced into the phase lag calculation. This method tends to be tedious and time consuming; it is more practical to have the signal interfaced with a computer.

Smith et. al.[41] used an accurate method on an oscilloscope to measure the plase shift. Figure 13a shows elliptical traces that are analyzed by measuring the distances corresponding to $2x_o$, $2F_o$ and $2\ x_o \sin\delta$. The force and displacement voltages are analyzed on separate axes. If the phase shift is small, then Figure 13b shows the major and minor axis of the ellipse are measured rather than $2\ x_o \sin\delta$. Two expressions for the area of the ellipse are equated as

$$\S F dx = \int F_o \cos(\omega t+\delta')\,\omega x_o \sin\omega t\ dt = F_o x_o \sin\delta = \pi ab$$

so that $\sin\delta = ab\pi/F_o x_o$

Some oscilloscopes include a calibrated phase shift network in the circuits which is adjusted instead of an ellipse.

UNMODIFIED WRG

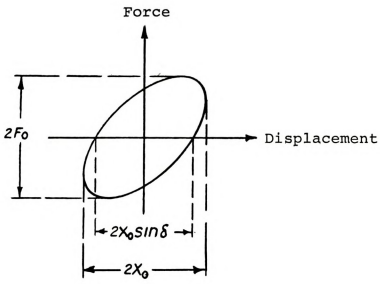

a.) Large phase shift

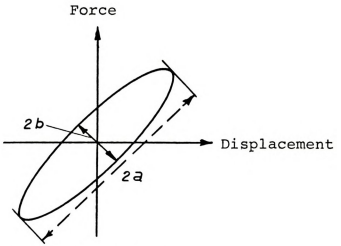

b.) Small phase shift

Figure 13. Oscilloscope Measurements

If a distorted line appears then higher harmonics exist in the stress wafeform.

4.3 Computer Programs and Fourier Analysis

The theory of Fourier analysis and formulaes for computing the Fourier coefficients are given in a text by Churchhill.[42] For shear stress and strain the phase shift with respect to the origin is computed as

$$\text{phase shift} = \arctan(-A_1/B_1)$$

and the amplitude is computed as

$$\text{amplitude} = (A_1^2 + B_1^2)^{\frac{1}{2}}$$

where A_1 and B_1 are the first Fourier coefficients of the sine and cosine series.

Since the normal stress has a displacement and has twice the frequency of the shear stress waveforms the phase shift with respect to the origin is calculated as

$$\text{phase shift} = \arctan(-A_2/B_2)$$

and the amplitude is calculated as

$$\text{amplitude} = (A_2^2 + B_2^2)^{\frac{1}{2}}$$

where A_2 and B_2 are the second Fourier coefficients of the sine and cosine series for the normal stress waveform. The displacement or total normal force is equal to A_0 which is the integral average of the tabulated normal stress signal. The phase lag for shear stress or normal stress is simply the phase shift for the input strain oscillation minus the phase shift of the output oscillation for the shear stress or normal stress.

The necessary integration of the tabulated function is computed by the Rhomberg extrapolation method which is program-

med in a text by Carnahan and Wilkes.[43] IBM also provides a utility program that calculates the Fourier coefficients based on a recursion formula. Unfortunately, for the same accuracy on recovery of the Fourier coefficients the IBM program required 10 times the number of points as required by the Rhomberg integration. An accuracy of 98% for the recovery was achieved by numerical simulation of an analytical sine and cosine series which was not generated with the use of the digital voltmeter and the WRG. The fewer number of points is particularly important for oscillations with short periods, because the digital volt meter may not be able to read the analog voltage signal at a fast enough speed. Consequently, experiments must be limited to shearing frequency of less than 1 c/s.

CHAPTER V

RESULTS OF THE INVESTIGATION

5.1 Material Functions from an Unmodified WRG

Figure 14a shows a typical shear stress growth from the unmodified WRG, which employed the cantilever spring but not the C-rings. The shear stress growths always showed overshooting with vibrations superimposed. The vibrations are suspected to be caused by the separating movement of the the torsion-head assembly and dove-tail slide. The lack of a brace or added weight permits the tosion-head assembly and the dove-tail slide to bend in an arc, hence, increasing the cone-plate gap. The response time for the shear stress growth is 0.01 seconds. Figure 14b shows a typical normal stress growth. The normal stress growth has a response time of 0.6 seconds. The response time for normal stress relaxation is 5.2 seconds.

Figure 15 is a frequency response plot of the dynamic viscosity and the storage modulus that summarizes one of the oscillatory shearing experiments by the unmodified WRG. The test conditions can be found in section 3.4. The original purpose was to find the natural or resonance frequency. Although the phase lag did not become zero, the resonance frequency is estimated to be 42 cycles/second. A plot of phase lag versus frequency, which is not shown, has inflections at 14 and 8 cycles/second. Figure 15 uses 8 out of 15 data points because the use of anymore points would be too close to the natural frequency.

UNMODIFIED WRG

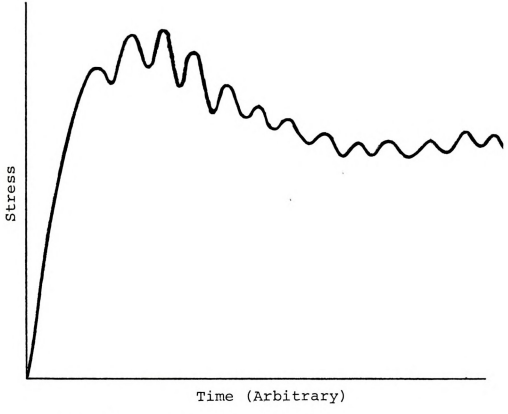

Figure 14a. Shear Stress Growth

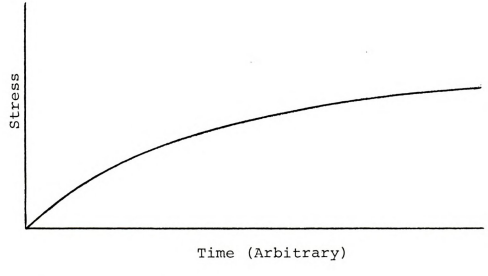

Figure 14b. Normal Stress Growth

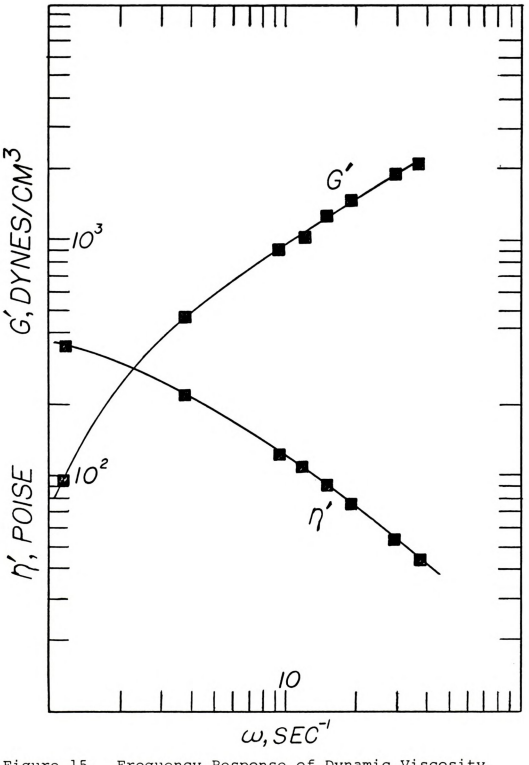

Figure 15. Frequency Response of Dynamic Viscosity and Storage Modulus for 1490 Polysobutylene in Cetane

MODIFIED WRG

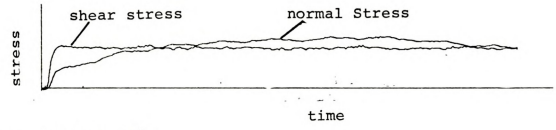

a.) Plot at 26°C

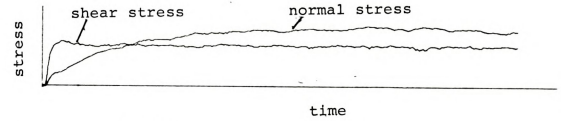

b.) Plot at 26.5°C

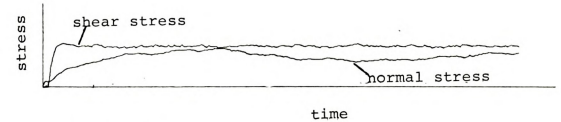

c.) Plot at 27°C

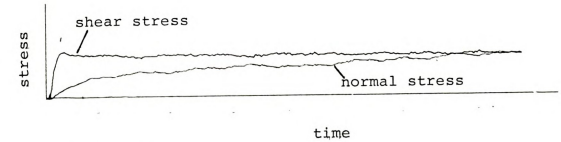

d.) Plot at 28°C

Figure 16. Shear Stress and Normal Stress Growths of 1490 Polyisobutylene in Cetane from a Modified WRG.

5.2 Material Functions from a Modified WRG

Under the test conditions that are given in section 3.5, there was not a significant enhancement in the response time for the stress growth experiments. The differences in the test conditions are the C-rings with weights and the room temperatures. The test without the use of C-rings was conducted first from a temperature of 23° to 25° C, while the test with the use of C-rings with weights was conducted second from 26° to 28° C. Figure 16 shows the plots of the four runs from the second test. The temperature increases approximately a 0.5°C per plot from plots "a" to "d". Although the response time from plot "a" did not change from the first test, it did become longer as the room temperature increased during the second test. Much of the noticeable differences is in the normal stress growth since the piezotron as mentioned earlier is sensitive to temperature changes. For the shear stress growths, there are small differences which may be attributed to the temperature effects on polyisobutylene.

Figures 17, 18, 19, and 20 are frequency response plots of the storage modulus that summarizes the oscillatory experiment done on a modified WRG. Figure 17 has a strain amplitude from 0.5 to 0.53. Since there is a large amount of scatter on the semilog plot, the curve through the points is not a statistical curve fit. The large deviation of some points is caused by room temperature effects. The experiments were conducted on different evenings, so the room temperature varied from 23°

MODIFIED WRG

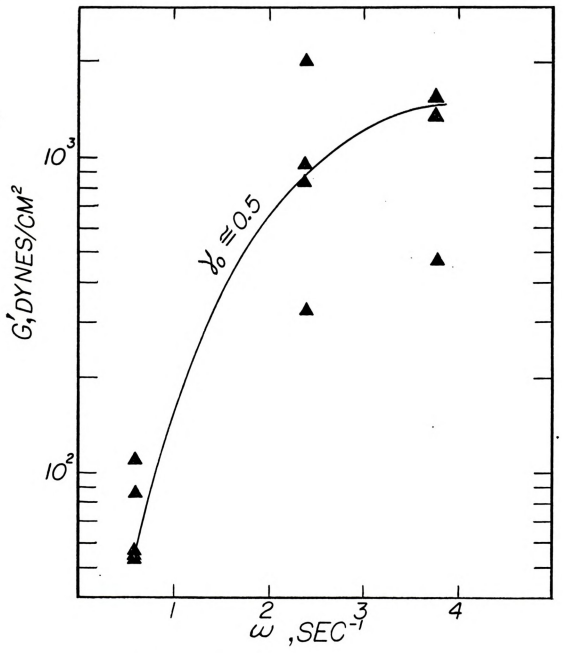

Figure 17. Frequency Response of the Dynamic Storage Modulus for 1490 Polyisobutylene in Cetane at 0.5 Strain Amplitude from a Modified WRG.

MODIFIED WRG

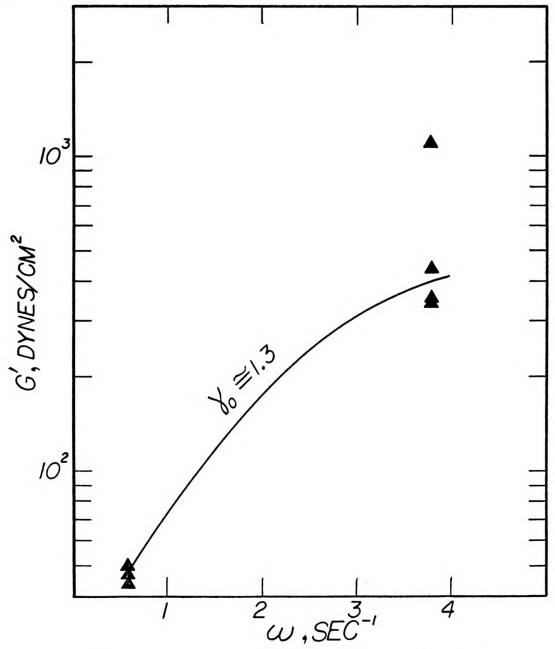

Figure 18. Frequency Response of the Dynamic Storage Modulus for 1490 Polyisobutylene in Cetane at 1.3 Strain Amplitude from a Modified WRG.

MODIFIED WRG

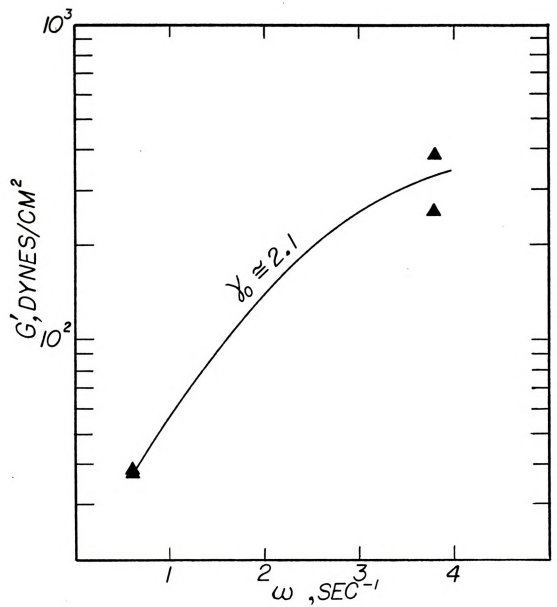

Figure 19. Frequency Response of the Dynamic Storage Modulus for 1490 Polyisobutylene in Cetane at 2.1 Strain Amplitude from a Modified WRG.

MODIFIED WRG

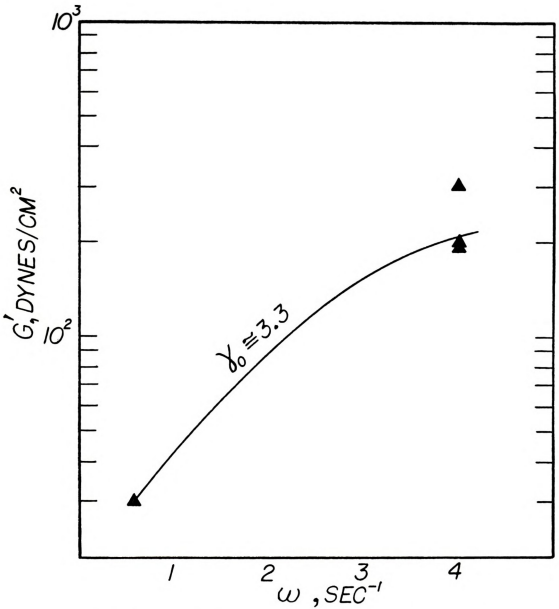

Figure 20. Frequency Response of the Dynamic Storage Modulus for 1490 Polyisobutylene in Cetane at 3.3 Strain Amplitude from a Modified WRG.

to 35° C. Any experiment that was conducted above 37°C is not included because of obvious electronic failures that had occurred. The shearing was conducted at only three frequencies because the input parameter for the delay per point was obtained by trial and error. Although more frequencies are needed for a better curve fit, the data does suggest the drawn curve.

Figure 18 is a frequency response plot of the storage modulus at a strain amplitude from 1.29 to 1.32. Although there are points at only two frequencies, a line with a small curvature is drawn through the two sets of points because the previous figure suggested a curve. Experiments at a frequency of 2.38/second had failed because the room temperature was too high. Similarly, Figures 19 and 20 are frequency response plots of the storage modulus at the strain amplitude of approximately 2.1 and 3.3 respectively.

If the curves of Figure 17 through 20 were plotted on one figure, there would be a family of curves such that the position of each of the curves becomes lower with the increase in the strain amplitude. This is quantified better in the following figure.

Figure 21 is a strain amplitude response plot of the storage modulus at the frequencies of 0.6/second and 3.77/second. Since there is information at only one strain amplitude for the frequency of 2.38/second, a line is not drawn for it. The data for the frequency of 0,6/second suggest a straight

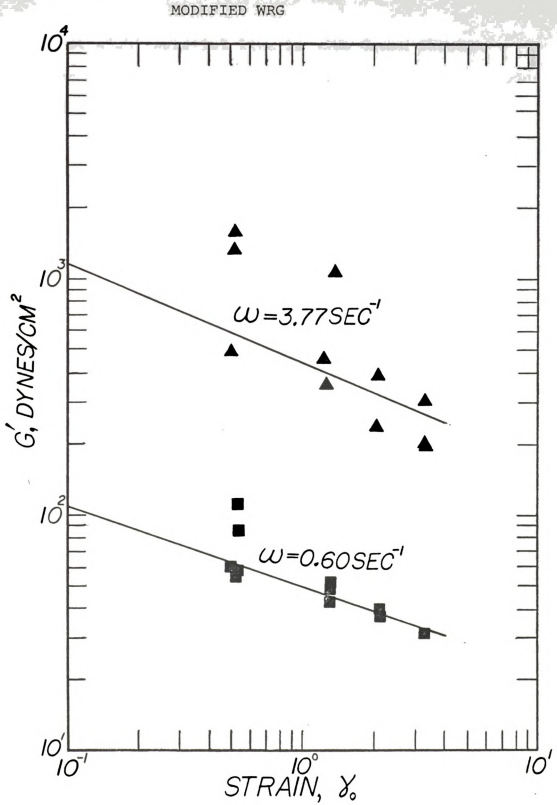

Figure 21. Strain Amplitude Response of the Dynamic Storage Modulus for 1490 Polyisobutylene in Cetane at the Frequency of 0.6 and 3.77/ second from a Modified WRG

line, so a straight parallel line is also drawn through the data for the frequency of 3.77/second. The storage modulus decreases with the increase of strain amplitude. An extrapolation of the straight lines indicates a "zero shear" storage modulus of 100 dynes/sq cm and 1000 dynes/sq cm for the frequencies of 0.6/second and 3.77/second respectively.

Figure 22 is a plot of the loss modulus versus strain amplitude. The data for the frequency of 0.6/second suggest a straight horizontal line, so a similar line is drawn for the other frequency. This figure indicates that the loss modulus is a function of frequency only and not a function of strain amplitude.

Appendix B contains the data that was used in the previous figures. Each table which comprises the Fourier components, material functions, and computer input is preceded by its Calcomp figure which is a plot of the raw data. The Calcomp plots show electrical noise that the low-frequency pass filters did not remove and the electrical noise that is induced by long shielded wire from the WRG electronics to the computer. The computer is located 60 feet away from the WRG. All the Calcomp plots have a labeled strain curve which is a single-cycle waveform that goes through the origin.

Shear Stress. Figure 23 is a Calcomp plot of a large-amplitude oscillatory shear experiment at 0.0952 cycle/second and a strain amplitude of 3.3. The shear stress waveform is similar to the strain waveform, but the stress waveform has a slight phase shift with respect to the origin. The Fourier

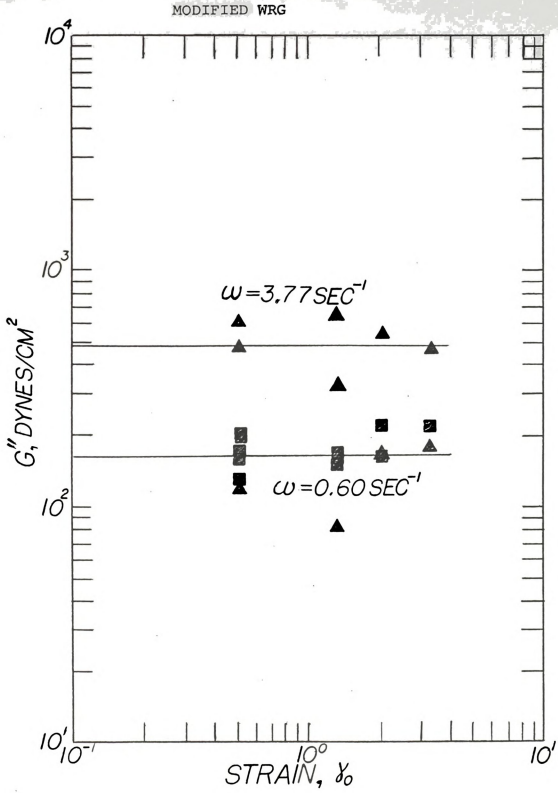

Figure 22. Strain Amplitude Response of the Loss Storage Modulus for 1490 Polyisobutylene in Cetane at the Frequency of 0.6 and 3.77/second from a Modified WRG.

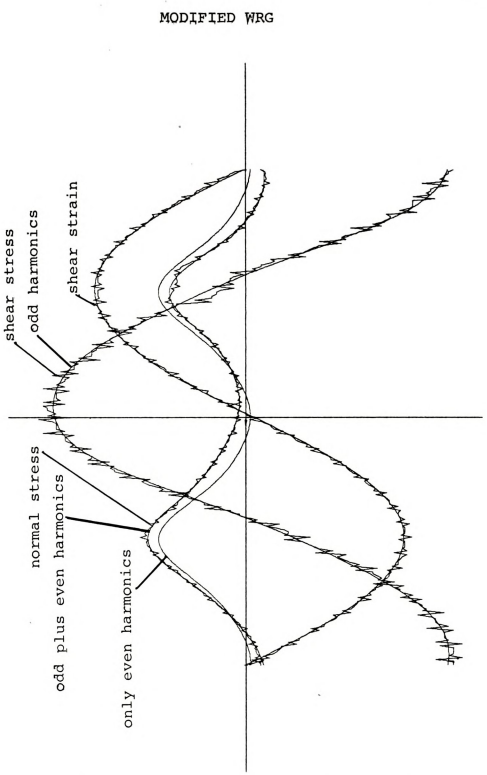

Figure 23. Calcomp Plot of the Large-Amplitude Oscillatory Shearing of Polyisobutylene in Cetane at the Frequency of 0.0952 c/s and Strain Amplitude of 3.3.

Table 1. Fourier Components and Material Functions

harmonic		1	2	3	4	5	6
stress	An	516.04	4.3158	7.8768	-2.7144	5.5888	3.7059
	Bn	120.02	-7.0896	-16.338	0.4610	-3.1261	-1.0911
strain	An	-0.1188	0.0285	0.0081	-0.0014	-0.0050	0.0095
	Bn	3.2871	-0.0369	0.0318	-0.0203	0.0064	-0.0080
normal	An	118.75	-466.02	21.578	76.512	-3.9225	-20.175
	Bn	-133.17	-13.384	-21.425	9.4735	-2.2631	-5.1019

shear stress Ao = -13.811 dynes/sq cm
shear strain Ao = -0.0768
normal stress Ao = 360.05 dynes/sq cm

Strain Amplitude = 3.2892

Shear Stress

stress amplitude	= 529.81	dynes/sq cm
amplitude ratio	= 161.08	dynes/sq cm
phase shift	= 1.3784	radians
dynamic viscosity	= 264.32	poise
imaginary part	= 51.492	poise
dynamic rigidity	= 30.798	dynes/sq cm
loss modulus	= 222.03	dynes/sq cm

Normal Stress

normal stress displacement	= 360.05	dynes/sq cm
normal stress amplitude	= 466.21	dynes/sq cm
phase shift	= 0.8072	radians
normal stress displacement function	=	gm/cm
normal stress coefficient: real part of	=	gm/cm
imaginary part of	=	gm/cm

Computer Program Input

interval spacing number	= 257	torsion head range	= 25.0
rhomberg jmax	= 7	oscillatory range	= 100.0
maximum harmonic	= 6	peak voltage	= 0.25
cycle averaging number	= 1	cone angle	= 0.5522°
delay/point	= 109	frequency	= 0.0952 c/s

series is plotted as a superimposed waveform on the raw data signal. Usually only the odd harmonics are used to evaluate the Fourier series for the shear stress curve, because the data substantiates the theory. Table 1 contains both the odd and even harmonics of the Fourier components. The magnitude of the first component is larger than the magnitude of the second component and the third is larger than the fourth, and so on.

By starting with equation (4.3) for only the odd harmonics a similar derivation for equation (4.5) gives the following,

$$\tau = \sum_{0}^{\infty} \gamma_0 \{G'_{2n+1} \cos(2n+1)\omega t - G''_{2n+1} \sin(2n+1)\omega t\}$$

where

$$G'_{2n+1} = A_{2n+1}/\gamma_0$$

$$G'_{2n+1} = -B_{2n+1}/\gamma_0$$

are related to the Fourier A_n and B_n series for the odd harmonics. For n=0 , we obtain the equation (4.5) for linear viscoelastic theory.

Normal Stress. Figure 23 also shows the normal stress waveform which is a plot of the data signal. Unlike the shear stress waveform, the normal stress is a two cycle waveform. A normal force is produced for each directional movement of the bottom platen. Unfortunately, the even harmonics do not curve fit the raw data as well as they should. There is a labeled superimposed curve for the even harmonics and a labeled superimposed curve for both odd plus even harmonics. The superimposed curve of odd plus even harmonics always goes through the normal stress signal by staying within the bounds of the elec-

trical noise. The closer the match between the superimposed curves, the better the experimental technique. The unlevel heights of the peaks are mostly due to the lower platen not being in the null position before loading the polyisobutylene sample. With the exception of B_2 Table 1 indicates the relative domance of the even harmonics over the odd harmonics for the normal stress signal.

Generally, the normal stress displacement increases with the increase of strain amplitude. For the linear region, the effects are almost null because the diaphram may not be flexiable enough. For the nonlinear region, the effects of increasing strain amplitude is very pronounced.

Earlier normal stress experiments which are not given in Appendix B compared low-frequency filters of the Piezotron amplifier. The first filter, 545A, is a low pass filter of 150 kHz, and the second filter 545A16 is a low pass filter of 1 kHz. Both the first and second Piezotron filters were not adequate, because these filters did not diminsh the electronic noises. The filter system of the Farol electronics was used for all the experiments in Appendix B.

CHAPTER VI

SUMMARY AND CONCLUSION

6.1 Highlights

Since large shear rates are applied during the processing of polymers, industries are demanding mathematical models to describe the large deformation. Early investigators who used the WRG encountered some inadequacies in the machine design which permit the cone-plate gap to open. The most important enhancement to the unmodified WRG is the replacement of the bending cantilever beam by a stationary piezotron load cell. The second enhancement is the use of C-rings or weights to prevent the dove-tail slide to rock on pivot. The objective is to collect material functions from oscillatory shearing in the nonlinear region of polyisobutylene in cetane by using a modified R-16 WRG. Besides characterizing the fluid, stress growth and stress relaxation experiments give a "diagnostic" information of the machine's ability to respond to a sudden change of shear rate. The small- and large-amplitude oscillatory shearing experiments identify the transition from linear to nonlinear deformation. Similarly, experiments over a range of frequencies will identify the transition to the nonlinear region and identify the natural or resonance frequency on the WRG. From these experiments, strain amplitude and frequency response curves are constructed to characterize the fluid for formulating models by others.

6.2 Inferences

The stress growth experiments did not show a significant improvement in the response time for the modified WRG. Instead of using C-rings which do not have enough weight for the enhancement, a one kilogram weight on top of the torsion head would suffice as a substitute for a brace. For shear stress growths, there are small differences in the curves which may be attributed to the temperature effects on polyisobutylene.

The main results of this thesis are the frequency and strain response curves. Unfortunately, there is some scatter in the data due mostly to variation in room temperature. At a given shear strain the dynamic storage modulus increases with the increase in frequency or shear rate. For a given frequency the dynamic modulus decreases with the increase in shear strain. The loss storage modulus increases with the increase in frequency, but it is not a function of shear strain.

For nonlinear behavior the derivation in Chapters IV and V is that each odd component of the Fourier cosine series for shear stress is related to a distinct dynamic modulus and that each odd component of the Fourier cosine series is related to a distinct loss modulus. Since the odd components only show domance in the linear region for oscillatory shearing, the dynamic moduli and loss moduli are necessary for nonlinear mathematical models. As shown in Chapter IV, the other material functions are related to the dynamic and loss modulus; it follows that the other nonlinear material functions are

derivable from the dynamic moduli and loss moduli of the non-linear region.

CHAPTER VII

RECOMMENDATIONS

7.1 Temperature Control

There are some existing problems and needed repairs. First, the laboratory needs an individual room thermostat that is capable of heating or cooling the room. The tube electronics of the Farol power supply increases the room temperature which has an adverse effect on operations. When the room temperature reaches 35° C the electronics fail to operate and the experiment must be terminated. Secondly, the oven that surrounds the cone and plate has a broken resistance wire or heating element, because the circuit in the oven does not pass any electricity. Thirdly, the thermocouples that contact the cone or plate are frailed and they need to be replaced. And, last, the oven pinches on the frictionless air rotor so the oven needs to be adjusted.

For precise control at non-ambient temperatures there are many commercial controllers which use either an electric heater or gas thermostat.

Electric heating. For high-temperature in excess of 100°C, heater windings can be used in the cone and plate. Raha, Williams, and Lamb[44] design an independent heated cone and plate for polymer melts. A 250 watt element in the plate is the main heater and a 22 watt element in the cone is the secondary heater. The cone and plate reachs temperatures of 300°C in

about 30 minutes from a cold start. It has an accuracy of $\pm$ 1° C. For on-off controllers, the heated parts should be massive to smooth the fluctuations. The temperature controller should be near the heaters and the thermocouples measuring the test temperature should be close as possible to the test sample.

Gas Thermostat. For temperatures below ambient, air which has been bubbled through liquid nitrogen can be passed through the oven chamber surrounding the sample. Another method which gives better control involves evaporating liquid nitrogen with a small electric heater and then warming the cold gas to the required temperature. Van der Wal, et al.[45] have described an automatic control system based on this principle covering the range -180° C to +300° C with an accuracy of $\pm$ 1°C and long term stability of 0.05°C. For temperatures slightly above ambient such as 30°C some compressed filtered air which has been split from the air supply before the air bearing can be warmed by a small heater.

Regardless of the mode of heat transfer, a variable controller is preferred over an on-off controller. For accurate work, the resistance of a platinium resistance thermometer placed in the oven is compared with the standard resistance of a Wheatstone bridge circuit. The out of balance current is proportional to the error signal between the temperature of the oven and the temperature to be maintained. The current through the oven element is controlled by a semiconductor device known as a thyristor.[46] This conducts current only when both a posi-

tive voltage is applied and a positive trigger voltage is applied to a control grid. These trigger signals are applied at an interval after the start of each positive a.c. voltage cycle. By varying the delay before the trigger fires the thyristor, only a fraction of the current cycle is passed. Hence, the average current through the oven element is varied over a four to one range. This delay is controlled by an error signal. The correction applied to the oven current is proportional to the temperature error. The oscillation of the oven temperature due to the time lag between the change of current and the corresponding change in temperature is reduced to a minimum. Also, there is no loss of power in the control circuits as there would be with a simple rheostat.

7.2 Graphics Terminal

The College of Engineering has some graphic terminals that are portable. Some terminals that have already been interfaced to the IBM 1800 computer are also available with thermoprinters. It would be more convenient to use a graphic terminal instead of the IBM typewriter that is currently interfaced with the computer. For convenient use in the laboratory, it is necessary to run another line from the computer room to the laboratory. With the graphics terminal next to the WRG corrections and adjustments can be made before the hardcopy of the waveforms or the calculation of the Fourier components. The 12 input parameters that are given in section 3.5 can be entered via the graphics terminal. The request for a plot or

plots of shear stress, normal stress, or shear strain can be entered as well as starting a new run.

LIST OF REFERENCES

LIST OF REFERENCES

[1] Walters, K. Rheometry, Chapman and Hall, 1975.

[2] Williams, J. G. Stress Analysis in Polymers, Longman, 1973.

[3] Bauer, W. H. and Collins, E. H., Rheology: Theory and Applications, Vol.4 (edited by F. R. Eirich), pp. 423-59, Academic Press, 1967.

[4] Cheng, D.C.H. Brit. J. Appl. Phys. 17, pp. 253-63, 1966.

[5] Bird, R. B., Stewart, W. E. and Lightfoot, E.N., Transport Phenomena, Chap. 3, John Wiley, New York, 1960.

[6] Ibid, p.86

[7] Nally, M.C. Brit. J. of Appl. Phys., 16, p.1023, 1965.

[8] De Wacle, A. J. Oil Colloid Chem. Assoc., 6, p. 33, 1925.

[9] Bird, R. B., Stewart, W. E. and Lightfoot, E. N., op cit. Chap. 10.

[10] Bird, R. B., Steward, W.E. and Lightfoot, E.N., op. cit., p.318.

[11] Bird, R. B. and Turian, R. M., Chem. Engng. Sci., 17, pp. 331-334, 1962.

[12] Weissenberg, K. Int. Cong. Rheol., 1, p. 27, 1948.

[13] Ferry, J. D. Viscoelastic Properties of Polymers, 2nd ed. Wiley, 1970.

[14] Lodge, A.S., Elastic Liquid, Academic Press, 1964.

[15] Walters, op. cit., Chap. 6.

[16] MacDonald, I.F., Marsh, B. C. and Ashare, E. Chem Engng. Sci., 24, pp. 1615-25, 1969.

[17] Lee, K. H., Jones, L. G., Pandalai, K. and Brodkey, R. S., Trans. Soc. Rheology, 14:4, pp. 555-72, 1970.

[18] Higman, R. W. Rheol. Acta, 12, pp. 533-9, 1973.

[19] Meissner, J. J. Appl. Polym. Sci, 16, pp. 2877-99, 1972.

[20] MacDonald, I. F. Trans Soc. Rheol., 17, pp. 537-55, 1973.

[21] Crawley, R. L., Graessley, W. W., Trans Soc. Rheol., 21:2, pp. 19-49, 1977.

[22] Acierno, D., La Mantia, F. P., DeCindio, B. and Nicodemo, L., Trans. Soc. Rheol., 21, pp. 261-71, 1977.

[23] Walters, K., op. cite, p. 3.

[24] Spriggs, T. W. Huppler, J. D., and Bird, R. B. Trans. Soc. Rheol., 10:1, p. 191, 1966.

[25] Batchelor, J., Berry, J. P. and Horsfall, F. Rheol Acta, 8, pp. 221-5, 1969.

[26] Meissner, op. cite.

[27] Galvin, P. T. and Whorlow, R. W. J. Appl. Polym. Sci., 19, pp. 567-83, 1975.

[28] Chang, K. I., Yoo, S. S., and Hartnett, J. P., Trans. Soc., Rheol., 19:2, pp. 155-171, 1975.

[29] Kearsley, E. A. and Zapas, L. J., Trans Soc. Rheol., 20, pp. 623-37, 1976.

[30] Williams, M. C., and Bird, R. B., I & E.C. Fund., 3, 1, pp. 42-49, 1964.

[31] MacDonald, I. F., Marsh, B. D., and Ashare, E., Chem. Enging. Sci., 24, pp. 1615-1625, 1969.

[32] Walters, K. and Jones, T.E.R. Proc. 5th Int. Cong. on Rheol., 4, p. 337, 1970.

[33] Akers, L. C. and Williams, M. C., J. Chem. Phys., 51, p. 3834, 1969.

[34] Christiansen, E. B., and Leppard, W. R., Trans Soc. Rheol., 18, p. 65, 1974.

[35] Tanner, R. I., Trans. Soc. Rheol., 17:2, pp. 365-373, 1973.

[36] The Weissenberg Rheogoniometer Manual, Sangamo Controls Ltd., Bognor Regis.

[37] Ibid.

[38] Ibid.

[39] Van Rijn, C.F.H., Rheol. Acta., 6 pp. 295-6, 1967.

[40] Walters, op. cit., Appendix A.

[41] Smith, J.R., Smith, T.L. and Tschoegl, N.W. Rheol. Acta., 9, pp. 239-52, 1970.

[42] Churchill, R.V., Fourier Series and Boundary Value Problems. 2nd ed. McGraw Hill, New York, 1969.

[43] Carnahan, B., Luther, H.A., Willies, J.O. Applied Numerical Methods, John Wiley, New York, 1969.

[44] Raha, S., Williams, M.J. and Lamb, R.L. AICHE 20, pp. 474-84, 1974.

[45] Van der Wal, C.W., Nederveen, C.J. and Schwippert, G.A. Rheol. Acta. 8, pp. 130-3, 1969.

[46] Levitt, B. P.(ed), Findlay's Practical Physical Chemistry, 9th ed., Halsted Press, John Wiley, New York, 1972.

APPENDICES

APPENDIX A

APPENDIX A

COMPUTER PROGRAM LISTINGS

As mentioned in Chapter 3 this appendix comprises the listings for the WEISS and TESTY programs. For oscillatory shearing experiments the following input data is required for the WEISS program,

1.) Number of cycles for averaging (eg. 1-5)
2.) Number of the highest harmonic (eg. 1-6)
3.) JMAX for the Rhomberg integration (eg. 6-7)
4.) Cone angle in degrees (eg. 0.5522)
5.) Planten diameter in centimeters (eg. 7.5)
6.) Delay per point (eg. 9, 37, 109)
7.) Torsion bar constant in dynes - cm/thousandth (eg. 2.395 E 04)
8.) Strain amplitude dial indication (eg. 16.4)
9.) Frequency in cycles/second (eg. 0.0952)
10.) Range on torsion meter (eg. 2.5)
11.) Range on oscillatory meter (eg. 100)
12.) Transfer function for piezotran in volts/gm (eg. 0.02).

The program asks for the above information in this order, and the format for the entries is printed by the program before the input is required. The usual practice is to bring the IBM 1800 computer up from a cold start. The cold start is to press the computer ON button, install magnetic tape cartridge into the

tape driver, wait for 10 minutes for the green GO light, feed the two start cards through the card reader. The READY light on the computer should turn on. Now, the WEISS Fortran program can be fed through the card reader. Items 1 through 6 usually remain constant during the experiment, while items 7 through 12 may change between runs of an experiment. Also, it is not essential for the WRG to be running to answer items one through six. Item 7 through 12 can only be answered after entering the guess for the peak voltage which is typically between 0.4 and 0.6. The peak voltage activates the reading of the voltage signal by the digital voltmeter, so the WRG needs to be running at this time.

```
// FOR WEISS
*NONPROCESS PROGRAM
*ONE WORD INTEGERS
*IOCS (CARD,1443 PRINTER,TYPEWRITER)
*LIST ALL
      DIMENSION A(6),B(6),TORSH(257),OSCIL(257),PIEZO(257)
C  READ AND PRINT MAXIMUM NUMBER OF POINTS AND HARMONIC NUMBER
1     READ(2,2000) NAVEC,NHARM,JMAX,CONEA,PTDIA
2000  FORMAT(5X,I10,5X,I10,5X,I10,5X,F5.0,5X,F5.0)
      NMAX=2**(JMAX+1)+1
2     WRITE(1,2100)
2100  FORMAT(1X,50H DELAY=***** USE FORMAT I5 RIGHT JUSTIFIED COL. 1 ./,
     C' TORSION BAR CONSTANT...USE E11.4',/,' STRAIN AMPLITUDE DIAL..US
     EE FORMAT F5.0',/,' FREQUENCY IN C/S...USE FORMAT F5.0',/,/,' TORSI
     ION RANGE, OSCIL RANGE, PIEZO TRANS FUNC...USE F5.0/F5.0/F5.0')
      WRITE(1,2150)
2150  FORMAT(' WHAT IS PHASE VOLTAGE... USE F5.0')
      READ(6,2200) IDLAY,TORKB,SAMPD,FREQ,RANGT,RANGO,TRANF,PHASD
2200  FORMAT(I5,/,E11.4,/,F5.0,/,F5.0,/,F5.0,/,F5.0,/,F5.0,/,F5.0)
      IF(IDLAY) 100,500,500
500   WRITE(3,3000) NMAX,NHARM,JMAX,FREQ,NAVEX,IDLAY,TORKB,SAMPD
3000  FORMAT(63X,23H INTERVAL SPACING NO. =,I10,/,63X,22H MAXIMUM HARMON
     5IC NO.=,I10,/,63X,15H RHOMBERG JMAX=,I5,/,63X,11H FREQUENCY=,E14.7
     R,/,63X,21H CYCLE AVERAGING NO.=,I10,/,63X,14H DELAY/POINT =,I10,/,
     A63X,' TORSION BAR CONSTANT =',E11.4,/,63X,' STRAIN AMPLITUDE DIAL
     B=',F5.2)
      WRITE(3,3100) RANGT,RANGO,TRANF,CONEA,PTDIA
3100  FORMAT(63X,' TORSION HEAD RANGE ='F6.2,/,63X,' OSCILLATORY RANGE =
     G',F6.2,/,63X,' PIEZOTRON TRANSFER FUNCTION =',F6.2,/,63X,' CONE AN
     FGLE=',F10.5,/,63X,' PLATEN DIAMETER=',F10.5)
CALCULATE AND INITIALIZE CONSTANTS
      RHO=0.756                                                    GM/ML
      PIE=4.*ATAN(1.)
      NMAX1=NMAX-1
      SCALE=1./NAVEC
      FACTP=981.8./TRANF/PIE/PTDIA/PTDIA/3276.7/.40
      FACTO=RANGO/.83/22.34/CONEA/3276.7
      IF(RANGT-.26) 3,3,333
3     FACTT=3.82*RANGT*TORKB/.93/(PTDIA**3)/3276.7*.40
      GO TO 3333
333   FACTT=3.82*RANGT*TORKB/.90/(PTDIA**3)/3276.7*.40
3333  CONTINUE
C  INITIALIZE ARRAYS
      DO 4 J=1,NHARM
      A(J)=0.0
      B(J)=0.0
4     CONTINUE
      DO 5 N=1,NMAX
      TORSH(N)=0.0
```

```
      OSCIL(N)=0.0
      PIEZO(N)=0.0
5     CONTINUE
      WRITE(1,2250)
2250  FORMAT(1X,'WHAT IS THE PEAK VOLTAGE VOLTO...USE FORMAT F5.0')
      READ(6,2260) PEAKV
2260  FORMAT(F5.0)
      WRITE(3,2270) PEAKV
2270  FORMAT(63X,' PEAK VOLTAGE VOLTO=',F10.5)
      WRITE(3,2300)
2300  FORMAT(63X,7HWAITING,/)
7     CALL HFAIR(7,1,VOLTO)
      IF(-PEAKV+VOLTO) 7,7,8
8     CONTINUE
      WRITE(3,1300)
9     CALL HFAIR(7,1,VOLTO)
      IF(VOLTO-PHASD) 10,9,9
10    CONTINUE
      DO 15 M=1,NAVEC
      DO 12 N=1,NMAX1
      CALL HFAI(6,3,KTORS,KOSCI,KPIEZ)
      TORSH(N)=TORSH(N)-KTORS
      OSCIL(N)=OSCIL(N)-KOSCI
      PIEZO(N)=PIEZO(N)+KPIEZ
      CALL DELAY(IDLAY)
12    CONTINUE
15    CONTINUE
      TORSH(NMAX)=TORSH(1)
      OSCIL(NMAX)=OSCIL(1)
      PIEZO(NMAX)=PIEZO(1)
C  SCALE AND CONVERSION FACTOR
      DO 20 N=1,NMAX
      TORSH(N)=TORSH(N)*SCALE*FACTT
      OSCIL(N)=OSCIL(N)*SCALE*FACTO
      PIEZO(N)=PIEZO(N)*SCALE*FACTP
20    CONTINUE
      WRITE(3,1900)
1900  FORMAT(57X,63HAVERAGED VALUES FOR SIGNALS TO BE USED FOR FOURIER A
     ANALYSIS...  )
      WRITE(3,1500)
      WRITE(3,1400) (I,TORSH(I),OSCIL(I),PIEZO(I),I=1,NMAX)
      WRITE(1,1700)
      READ(6,1800) ICONT
      IF(1-ICONT) 1,25,2
25    CONTINUE
1700  FORMAT(1X,27HCHECK DATA FOR CONSISTANCY. ,/,34H TO CONTINUE, TYPE
     11 IN COLUMN ONE./)
1800  FORMAT(I1)
C  CALL ON FOURIER ANALYSIS
1000  FORMAT(1X,/,48X,I7,5I12,/,48X,6E12.5/48X,6E12.5,//)
```

```
1100  FORMAT(1X,' ERROR...NMAX NOT GREATER THAN OR EQUAL TO NHARM...ERRO
     OR    OR    ERROR...NHARM LESS THAN ZERO...ERROR')
      CALL FORIT(TORSH,NMAX,NHARM,AO,A,B,IER,JMAX,FREQ,PIE)
      IF(IER-1) 26,27,27
26    WRITE(3,1000) (I,I=1,6),(A(I),I=1,6),B(I),I=1,6)
      WRITE(1,1700)
      READ(6,1800) ICONT
      IF(1-ICONT) 1,57,58
57    CONTINUE
      CALL CALCM(TORSH,AO,A,B,PIE,FREQ,XSCAL,YSCAL,NMAX,NHARM)
58    CONTINUE
      PHASD=ATAN(-A(1)/B(1))
      THOMX=SQRT(A(1)*A(1)+B(1)*B(1))
      WRITE(1,1700)
      READ(6,1800) ICONT
      IF(1-ICONT) 1,65,2
65    CONTINUE
      GO TO 29
27    WRITE(3,1100)
29    CALL FORIT(OSCIL,NMAX,NHARM,AO,A,B,IER,JMAX,FREQ,PIE)
      IF(IER-1) 30,31,31
30    WRITE(3,1000) (I,I=1,6),(A(I),I=1,6),(B(I),I=1,6)
      WRITE(1,1700)
      READ(6,1800) ICONT
      IF(1-ICONT) 1,67,68
67    CONTINUE
      CALL CALCM(OSCIL,AO,A,B,PIE,FREQ,XSCAL,YSCAL,NMAX,NHARM)
68    CONTINUE
      PHASG=ATAN(-A(1)/B(1))
      GAMMO=SQRT(A(1)*A(1)+B(1)*B(1))
      AMPRO=THOMX/GAMMO/2./FREQ/PIE
      PHASD=PHASG-PHASD
      DYVIS=THOMX*SIN(PHASD)/GAMMO/2./PIE/FREQ
      STORM=THAMX*COS(PHASD)/GAMMO
      WRITE(1,1700)
      READ(6,1800) ICONT
      IF(1-ICONT) 1,75,2
75    CONTINUE
      GO TO 33
31    WRITE(3,1100)
33    CALL FORIT(PIEZO,NMAX,NHARM,AO,A,B,IER,JMAX,FREQ,PIE)
      IF(IER-1) 34,35,35
34    WRITE(3,1000) (I,I=1,6),(A(I),I=1,6),(B(I),I=1,6)
      WRITE(1,1700)
      READ(6,1800) ICONT
      IF(1-ICONT) 1,77,78
77    CONTINUE
      CALL CALCM(PIEZO,AO,A,B,PIE,FREQ,XSCAL,YSCAL,NMAX,NHARM)
78    CONTINUE
      WRITE(3,5000) GAMMO,AMPRO,PHASD,DYVIS,STORM,THOMX
```

```
5000  FORMAT(50X,'  STRAIN AMPLITUDE =',E12.5,/,50X,'  AMPLITUDE RATIO =
     D',E12.5,/,50X,'  SHEAR PHASE DIFFERINCE=',E12.5,RADIANS',/,50X,'
     TDYNAMIC VISCOSITY=',E12.5,'POISE',/,50X,'  STORAGE MODULUS=',E12.5
     H,'DYNES/CM2',/,50X,'  SHEAR STRESS AMPLITUDE=',E12.5,'DYNES/CM2')
CALCULATE THE MATERIAL FUNCTIONS...COMPLEX NORMAL STRESS COEFFICIENT
C      AND NARMAL STRESS DIDPLACEMENT FUNCTION
COMMIT...USE B ARRAY FOR EFFICIENCY ACCORDING WILLIAMS BIRD
C B(1)=H $ B(2)=K $ B(3)-QP $ B(4)=QM $ B(5)=S $ B(6)=T $ A(2)=A
      PHASD=ATAN(-A(2)/B(2))/2.
      A(2)=SQRT(A(2)*A(2)+B(2)*B(2))
      PHASD=PHASG-PHASD
      B(2)=RHO*2.*PIE*FREQ*PTDIA*PTDIA*DYVIS/4.
      B(2)=B(2)/(DYVIS*DYVIS+(STORM/2./PIE/FREQ)**2.)
      B(2)=RHO*PTDIA*PTDIA*STORM/4./(DYVIS*DYVIS+(STORM/2/PIE/FREQ)**2)
      B(3)=SQRT(SQRT(B(1)*B(1)/2.+B(2)*B(2))+B(2)/2.)*CONEA*PIE/180.
      B(4)=SQRT(SQRT(B(1)*B(1)/2.+B(2)*B(2))-B(2)/2.)*CONEA*PIE/180.
      B(5)=(((EXP(B(4))-EXP(-B(4)))/2.)*COS(B(3)))**2.
      B(5)=B(5)-(((EXP(B(4))-EXP(-B(4)))/2.)*SIN(B(3)))**2.
      B(6)=(EXP(2.*B(4))-EXP(-2.*B(4)))*SIN(B(3))*COS(B(3))/2.
      ZD=COS(CONEA*PIE/180.)
      ZD=-AO/((2*PIE*FREQ*GAMMO)**2)/SQRT(B(1)*B(1)+B(2)*B(2))/ZD/ZD
      ZD=ZD*((((EXP(B(4))-EXP(-B(4)))/2.)*COS(B(3)))**2.+(((EXP(B(4))-EX
     PP(-B(4)))/2.)*SIN(B(3)))**2.)
      ZP=A(2)/(2*PIE*FREQ)**2/(B(1)*B(1)+B(2)*B(2))/(COS(CONEA*PIE/180.)
     ***2.)
      ZPP=ZP*((B(2)*B(5)-B(1)*B(6))*SIN(2*PHASD)-(B(1)*B(5)+B(2)*B(6))*C
     OS(2.*PHASD))
      ZP=ZP*((B(2)*B(5)-B(1)*B(6))*COS(2*PHASD)-(B(1)*B(5)+B(2)*B(6))*SI
     PN(2.PHASD))
C--------PRINT OUT THE ANSWERS----------
      WRITE(3,6000) PHASD,A(2),AO,A,ZD,ZP,ZPP
6000  FORMAT(50X,' NORMAL PHASE DIFFERENCE='E12.5,'RADIANS',/,50X,' AMPL
     NTIUDE OF NORMAL STRESS',E12.5,'DYNES/CM2',/,50X,' AVERAGE DISPLACE
     MMENT OF NORMAL STRESS',E12.5,'DYNE/CM2',/,50X,' NORMAL STRESS DISP
     FLACIMENT FUNCTION',E12.5,'GM/CM',/,50X,' REAL PART OF COMPLEX NORM
     TAL STRESS COEFFICIENT',E12.5,'GM/CM',/,50X,' IMAGINARY PART OF NOR
     1MAL STRESS COEFFICIENT',E12.5,'GM/CM')
      GO TO 1
35    WRITE(3,1100)
100   CONTINUE
1300  FORMAT(63X,16HSIGNALS READ...   )
1400  FORMAT(63X,I5,5X,E12.5,5X,E12.5,5X,E12.5)
1500  FORMAT(63X,1HI,9X,8HTORSH(I),9X,8HOSCIL(I),9X,8HPIEZO(I)  )
      CALL EXIT
      END
```

```
// FOR FORIT
*NONPROCESS PROGRAM
*ONE WORD INTEGERS
*LIST ALL
      SUBROUTINE FORIT(FNT,NMAX,NHARM,AO,A,B,IER,JMAX,FREQ,PIE)
      DIMENSION A(6),B(6),FNT(257),FI(7,7)
CHANGE ORIGINAL ARRAY TO INTEGRAND.............
      DO 1 N=1,NMAX
      FNT(N)=FNT(N)*FREQ
1     CONTINUE
C      CHECK FOR PARAMETER ERRORS
      EPS=0.0005
      IER=0
      IF(NHARM) 2,3,3
2     IER=2
      RETURN
3     IF(NHARM-NMAX) 5,5,4
4     IER=1
      RETURN
COMPUTE AO - AVERAGE VALUE OVER SYMETRICAL INTERVAL
5     BELOW=-1.0/2./FREQ
      UPPER=-BELOW
      DO 9 J=1,JMAX
      DO 9 I=1,JMAX
      FI(I,J)=0.0
9     CONTINUE
         CALL ROMBG(BELOW,UPPER,FNT,EPS,JMAX,J,FI,NMAX,ANSWR)
      AO=ANSWR
      WRITE(3,6) J,AO
      WRITE(3,7) (J,J=1,JMAX)
      WRITE(3,8) (I,(FI(I,J),J=1,7),I=1,7)
      DO 10 J=1,JMAX
      DO 10 I=1,JMAX
      FI(I,J)=0.0
10    CONTINUE
COMPUTE A(N) AND B(N) FOR N=1,2,3,...NHARMONIC
      DO 11 N=1,NMAX
      TIME=(N-(NMAX+1)/2.)/(NMAX-1)/FREQ
11    FNT(N)=FNT(N)*COS(2.*PIE*FREQ*TIME)*2.
         CALL ROMBG(BELOW,UPPER,FNT,EPS,JMAX,J,FI,NMAX,ANSWR)
      A(1)=ANSWR
      WRITE(3,6) J,A(1)
      WRITE(3,7) (J,J=1,7)
      WRITE(3,8) (I,(FI(I,J),J=1,7),I=1,7)
      DO 16 M=2,NHARM
      DO 12 N=1,NMAX
      TIME=(N-(NMAX+1)/2.)/(NMAX-1)/FREQ
12    FNT(N)=FNT(N)*COS(2.*M*PIE*FREQ*TIME)/COS(2.*(M-1)*PIE*FREQ*TIME)
```

```
          CALL ROMBG(BELOW,UPPER,FNT,EPS,JMAX,J,FI,NMAX,ANSWR)
        A(M)=ANSWR
        WRITE(3,6) J,A(M)
        WRITE(3,7) (J,J=1,7)
        WRITE(3,8) (I,(FI(I,J),J=1,7),I=1,7)
        DO 15 J=1,JMAX
        DO 14 I=1,JMAX
14      FI(I,J)=0.0
15      CONTINUE
16      CONTINUE
        MHALF=(NMAX+1)/2
        SAVE=FNT(MHALF)
        DO 17 N=1,NMAX
        TIME=(N-(NMAX+1)/2.)/(NMAX-1)/FREQ
17      FNT(N)=FNT(N)*SIN(2.*PIE*FREQ*TIME)/COS(2.*NHARM*PIE*FREQ*TIME)
          CALL ROMBG(BELOW,UPPER,FNT,EPS,JMAX,J,FI,NMAX,ANSWR)
        B(1)=ANSWR
        WRITE(3,6) J,B(1)
        WRITE(3,7) (J,J=1,7)
        WRITE(3,8) (I,(FI(I,J),J=1,7),I=1,7)
        LHALF=(NMAX+1)/2-1
        NHALF=(NMAX+1)/2+1
        DO 20 M=2,NHARM
        DO 18 N=1,LHALF
        TIME=(N-(NMAX+1)/2.)/(NMAX-1)/FREQ
18      FNT(N)=FNT(N)*SIN(2.*M*PIE*FREQ*TIME)/SIN(2.*(M-1)*PIE*FREQ*TIME)
        DO 19 N=NHALF,NMAX
        TIME=(N-(NMAX+1)/2.)/(NMAX-1)/FREQ
19      FNT(N)=FNT(N)*SIN(2.*M*PIE*FREQ*TIME)/SIN(2.*(M-1)*PIE*FREQ*TIME)
          CALL ROMBG(BELOW,UPPER,FNT,EPS,JMAX,J,FI,NMAX,ANSWR)
        B(M)=ANSWP
        WRITE(3,6) J,B(M)
        WRITE(3,7) (J,J=1,7)
        WRITE(3,8) (I,(FI(I,J),J=1,7),I=1,7)
20      CONTINUE
C....RESTORE ORIGINAL ARRAY FNT ......
        DO 21 N=1,LHALF
        TIME=(N-(NMAX+1)/2.)/(NMAX-1)/FREQ
21      FNT(N)=FNT(N)/SIN(2.*NHARM*PIE*FREQ*TIME)/2./FREQ
        FNT(MHALF)=SAVE/2./FREQ
        DO 22 N=NHALF,NMAX
        TIME=(N-(NMAX+1)/2.)/(NMAX-1)/FREQ
22      FNT(N)=FNT(N)/SIN(2.*NHARM*PIE*FREQ*TIME)/2./FREQ
6       FORMAT(3OX,3H J=,I5,5X,1OH INTEGRAL=,E14.7)
7       FORMAT(3OX,3HJ K,7I12)
8       FORMAT(3OX,I3,1X,7F12.5)
        RETURN
        END
```

```
// FOR ROMBG
*NONPROCESS PROGRAM
*ONE WORD INTEGERS
*LIST ALL
      SUBROUTINE ROMBG(A,B,F,EPS,JMAX,J,FI,NMAX,ANSWR)
      DIMENSION FI(7,7),F(257)
C        PRESET CONSTANTS
      DO 7 J=1,JMAX
      N=2**J
      F2=0.0
      IBY=(NMAX+1)/2**J
      IBEGN=IBY+1
      M=NMAX-2
      DO 2 I=IBEGN,M,IBY
2     F2=F2+F(I)
      IBEGN=IBY/2+1
      F4=0.0
      M=NMAX-1
      DO 3 I=IBEGN,M,IBY
3     F4=F4+F(I)
      FI(J,1)=(B-A)*(F(1)+F(NMAX)+2.*F2+4.*F4)/6./N
      IF(J-1) 6,6,4
4     CONTINUE
      KM=J-1
      DO 5 K=1,KM
      JMK=J-K
      KPO=K+1
      JMKPO=J-K+1
5     FI(JMK,KPO)=(4.**K*FI(JMKPO,K)-FI(JMK,K))/(4.**K-1.)
      IF((ABS(FI(JMKPO,KM)-FI(JMK,KM))-EPS1) 8,8,6
6     CONTINUE
7     CONTINUE
8     ANSWR=FI(JMK,KPO)
      RETURN
      END
```

```
// FOR CALCM
*NONPROCESS PROGRAM
*ONE WORD INTEGERS
*LIST ALL
      SUBROUTINE CALCM(ARRAY,AO,A,B,PIE,FREQ,XSCAL,YSCAL,NMAX,NHARM)
      DIMENSION A(6),B(6),ARRAY(257)
C.....DRAWS ORIENT ABSCISSA......
      CALL HYPLT(0.,0.,0)
      CALL HYPLT(-3,75,0.,1)
      CALL HYPLT(3.75,0.,1)
      CALL HYPLT(0.,2.5,2)
      CALL HYPLT(0.,-2.5,1)
      CALL HYPLT(0.,0.,1)
60    CONTINUE
      WRITE(1,5050)
5050  FORMAT(' WHAT IS XSCALE AND YSCALE... USE F5.0/F5.0',/)
      READ(6,5060) XSCAL,YSCAL
5060  FORMAT(F5.0,/,F5.0)
      WRITE(3,5070) XSCAL,YSCAL
5070  FORMAT(60X,'XSCALE FOR PLOTTER+',F10.5,' YSCALE FOR PLOTTER=',F10.
      55)
      N=1
      TIMME=(N-(NMAX+1)/2.)/(NMAX-1)/FREQ
      ARAY=ARRAY(N)
      CALL HYPLT(0.,0.,2)
      CALL HYPLT(XSCAL,YSCAL,3)
      WRITE(1,91)
91    FORMAT(1X,'DO YOU WANT PLOT OF EXPERIMENTAL DATA,',/,' TYPE 1 IN C
      NNE',/)
      READ(6,92) ITRY
92    FORMAT(I1)
      IF(ITRY-1) 61,53,53
53    CONTINUE
      CALL HYPLT(TIME,ARAY,2)
        DO 54 N=2,NMAX
      TIME=(N-(NMAX+1)/2.)/(NMAX-1)/FREQ
      ARAY=ARRAY(N)
      CALL HYPLT(TIME,ARAY,1)
54      CONTINUE
      CALL HYPLT(0.,0.,2)
61    CONTINUE
      WRITE(1,500)
500   FORMAT(1X,'DO YOU WANT EVEN AND/OR ODD HARMONICS...',/,' USE FORMA
      TT I1, ODD IS 1,... EVEN ID 2,.... BOTH IS 3',/)
      READ(6,501) IPART
501   FORMAT(I1)
      N=1
      TIME=(N-(NMAX+1)/2.)/(NMAX-1)/FREQ
      CALL FUNCT(TIME,AO,A,B,PIE,FREQ,G,IPART,NHARM)
      ARAY=G
      CALL HYPLT(TIME,ARAY,2)
        DO 64 N=2,NMAX
      TIME=(N-(NAMX+1)/2.)/(NMAX-1)/FREQ
      CALL FUNCT(TIME,AO,A,B,PIE,FREQ,IPART,NHARM)
      ARAY=G
      CALL HYPLT(TIME,ARAY,1)
64      CONTINUE
      CALL HYPLT(0.,0.,2)
      WRITE(1,1900)
1900  FORMAT(1X,'DO YOU WANT TO TRY THIS ONE AGAIN... 1 YES, 0 NO',/)
      READ(6,2000) ITRY
2000  FORMAT(I1)
      IF(ITRY-1) 200,60,60
200   CONTINUE
      CALL HYPLT(0.,0.,-1)
      RETURN
      END
```

```
// FOR FUNCT
*NONPROCESS PROGRAM
*ONE WORD INTEGERS
*LIST ALL
      SUBROUTINE FUNCT(TIME,A0,A,B,PIE,FREQ,G,IPART,NHARM)
C  NEED THE FOURIER COMPONENTS
      DIMENSION
      ANSUM=0.0
      BNSUM=0.0
CALCULATION FOR FOURIER SERIES
      IF(IPART-2) 1,2,3
1     MSTAR=1
      IBY=2
      GO TO 4
2     MSTAR=2
      IBY=2
      GO TO 4
3     MSTAR=1
      IBY=1
4     CONTINUE
      DO 5 N=MSTAR,NHARM,IBY
        ANSUM=ANSUM+A(N)*COS(2.*N*PIE*FREQ*TIME)
        BNSUM=BNSUM+B(N)*SIN(2.*N*PIE*FREQ*TIME)
5     CONTINUE
      G=A0+ANSUM+BNSUM
      RETURN
      END
```

APPENDIX B

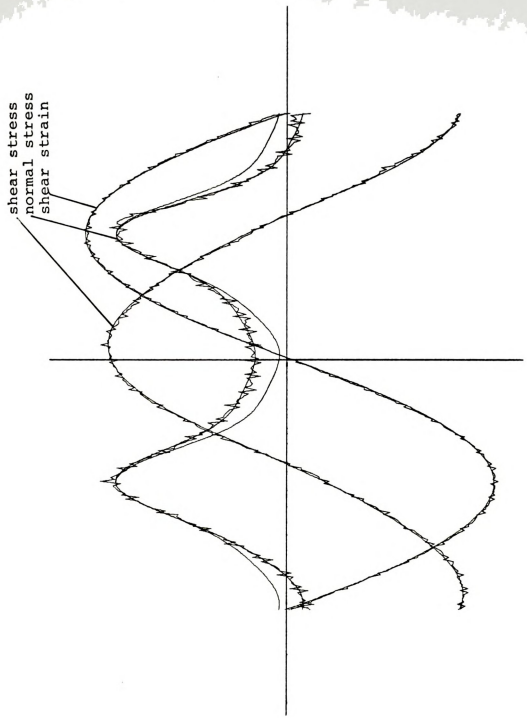

Figure 24. Calcomp Plot of the Large-Amplitude Oscillatory Shearing of Polyisobutylene in Cetane at the Frequency of 0.0952 c/s and Strain Amplitude of 3.3.

Table 2. Fourier Components and Material Functions

harmonic		1	2	3	4	5	6
stress	An	362.99	1.5835	6.0514	-1.1082	-1.4292	1.0232
	Bn	90.843	-4.4929	-6.5130	-1.3807	0.6366	0.4978
strain	An	-0.0534	0.0148	0.0044	0.0015	-0.0013	0.0008
	Bn	2.1708	-0.0225	0.0205	-0.0124	0.0070	-0.0053
normal	An	115.83	-401.33	18.440	101.08	-8.3871	-27.029
	Bn	-18.462	-9.1217	-7.2524	13.278	10.972	-18.245

shear stress Ao = 2.0177 dynes/sq cm
shear strain Ao = 0.0328
normal stress Ao = 367.03 dynes/sq cm

Strain Amplitude = 2.1714

Shear Stress

stress amplitude	= 374.18	dynes/sq cm
amplitude ratio	= 172.32	dynes/sq cm
phase shift	= 1.3501	radians
dynamic viscosity	= 281.10	poise
imaginary part	= 63.053	poise
dynamic rigidity	= 37.714	dynes/sq cm
loss modulus	= 232.66	dynes/sq cm

Normal Stress

normal stress displacement	=	367.03 dynes/sq cm
normal stress amplitude	=	401.43 dynes/sq cm
phase shift	=	0.7986 radians
normal stress displacement function	=	-0.0143 gm/cm
normal stress coefficient: real part of	=	0.0696 gm/cm
imaginary part of	=	0.1454 gm/cm

Computer Program Input

interval spacing number	= 257	torsion head range	= 2.5
rhomberg jmax	= 7	oscillatory range	= 25
maximum harmonic	= 6	peak voltage	= 0.6
cycle averaging number	= 1	cone angle	= 0.5522°
delay/point	= 109	frequency	= 0.0952 c/s

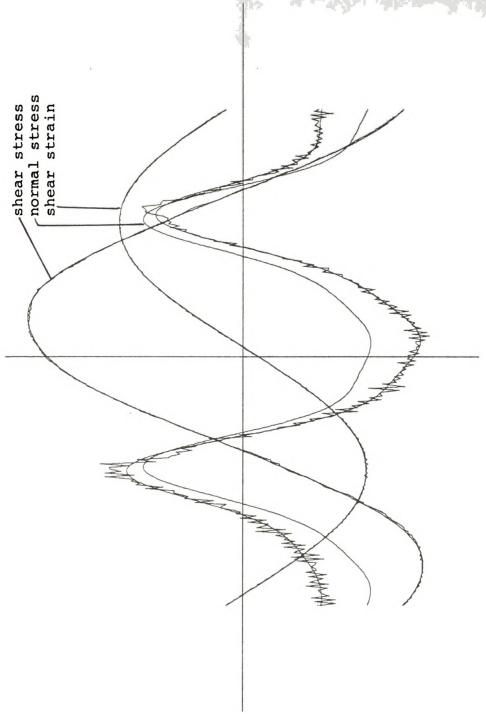

Figure 25. Calcomp Plot of the Large-Amplitude Oscillatory Shearing of Polyisobutylene in Cetane at the Frequency of 0.0952 c/s and Strain Amplitude of 1.31.

MODIFIED WRG

Table 3. Fourier Components and Material Functions

harmonic		1	2	3	4	5	6
stress	An	188.44	0.8677	-0.5596	0.1367	-0.2660	0.2248
	Bn	94.975	-0.8953	-1.3039	0.0229	-1.6931	-0.2310
strain	An	-0.1745	0.0065	-0.0016	0.0006	0.0004	-0.0003
	Bn	1.3006	0.0038	0.0034	0.0001	-0.0019	-0.0009
normal	An	-48.366	-105.08	1.1228	25.907	-1.1684	-2.7346
	Bn	-20.439	-31.539	3.5849	23.028	-3.9873	-11.003

shear stress Ao = 17.839 dynes/sq cm
shear strain Ao = -0.0001
normal stress Ao = -49.884 dynes/sq cm

Strain Amplitude = 1.3122

Shear Stress

stress amplitude = 211.02 dynes/sq cm
amplitude ratio = 160.81 dynes/sq cm
phase shift = 1.2373 radians
dynamic viscosity = 254.04 poise
imaginary part = 88.005 poise
dynamic rigidity = 52.641 dynes/sq cm
loss modulus = 151.95 dynes/sq cm

Normal Stress

normal stress displacement = -49.884 dynes/sq cm
normal stress amplitude = 109.71 dynes/sq cm
phase shift = 0.7730 radians
normal stress displacement function = gm/cm
normal stress coefficient: real part of = gm/cm
imaginary part of = gm/cm

Computer Program Input

interval spacing number = 257
rhomberg jmax = 7
maximum harmonic = 6
cycle averaging number = 10
delay/point = 109
torsion head range = 1.0
oscillatory range = 25.0
peak voltage = 0.42
cone angle = 0.5522°
frequency = 0.0952 c/s

MODIFIED WRG

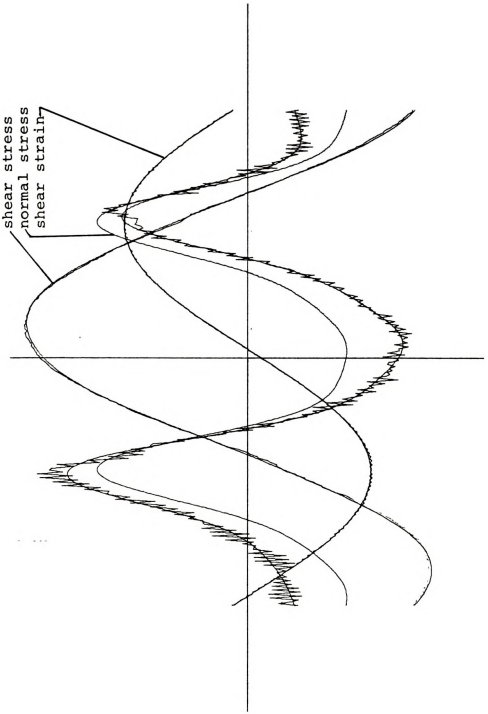

Figure 26. Calcomp Plot of the Large-Amplitude Oscillatory Shearing of Polyisobutylene in Cetane at the Frequency of 0.0952 c/s and Strain Amplitude of 1.31.

Table 4. Fourier Components and Material Functions

harmonic		1	2	3	4	5	6
stress	An	195.93	2.6662	0.8991	0.3121	-1.0033	-0.4566
	Bn	87.777	-0.7516	-0.0935	0.1268	-1.4421	0.2120
strain	An	-0.1520	0.0068	-0.0014	0.0011	-0.0004	-0.0005
	Bn	1.3031	0.0031	0.0041	-0.0004	-0.0020	-0.0005
normal	An	-52.388	-120.14	-0.0225	29.245	-2.228	-3.2796
	Bn	-32.496	-25.830	3.7987	23.061	-4.5396	-9.4770

shear stress Ao = 19.129 dynes/sq cm
shear strain Ao = 0.0003
normal stress Ao = -9.8511 dynes/sq cm

Strain Amplitude = 1.3119

Shear Stress

stress amplitude = 214.69 dynes/sq cm
amplitude ratio = 163.65 dynes/sq cm
phase shift = 1.2657 radians
dynamic viscosity = 260.96 poise
imaginary part = 70.042 poise
dynamic rigidity = 49.158 dynes/sq cm
loss modulus = 158.20 dynes/sq cm

Normal Stress

normal stress displacement = -9.8511 dynes/sq cm
normal stress amplitude = 122.89 dynes/sq cm
phase shift = 0.7957 radians
normal stress displacement function = gm/cm
normal stress coefficient: real part of = gm/cm
imaginary part of = gm/cm

Computer Program Input

interval spacing number = 257 torsion head range = 1.0
rhomberg jmax = 7 oscillatory range = 25.0
maximum harmonic = 6 peak voltage = 0.42
cycle averaging number = 10 cone angle = 0.5522°
delay/point = 109 frequency = 0.0952 c/s

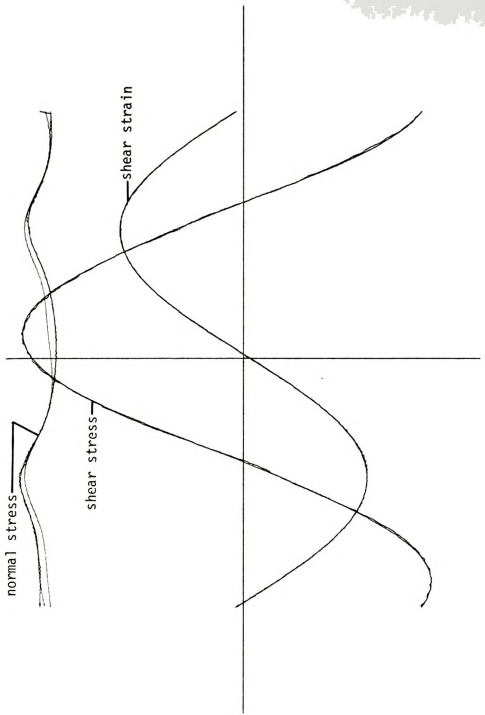

Figure 27. Calcomp Plot of the Large-Amplitude Oscillatory Shearing of Polyisobutylene in Cetane at the Frequencey of 0.0952 c/s and Strain Amplitude of 1.31.

MODIFIED WRG

Table 5. Fourier Components and Material Functions

harmonic		1	2	3	4	5	6
stress	An	204.26	0.98174	1.8865	0.0462	-1.0181	-0.3273
	Bn	69.819	-1.5688	-0.9018	-0.3374	-0.3436	0.6133
strain	An	-0.0777	0.0068	-0.0002	0.0007	-0.0007	-0.0006
	Bn	1.3080	0.0035	0.0034	0.0003	-0.0019	0.0001
normal		-52.419	-129.47	1.5563	36.224	-4.8126	-6.6001
		-48.800	2.1693	-10.752	25.410	-9.1877	-2.6846

shear stress Ao = 17.225 dynes/sq cm
shear strain Ao = 0.0001
normal stress Ao = 2131.7 dynes/sq cm

Strain Amplitude = 1.3103

Shear Stress

stress amplitude	= 215.86	dynes/sq cm
amplitude ratio	= 164.74	dynes/sq cm
phase shift	= 1.3008	radians
dynamic viscosity	= 265.43	poise
imaginary part	= 73.460	poise
dynamic rigidity	= 43.941	dynes/sq cm
loss modulus	= 158.77	dynes/sq cm

Normal Stress

normal stress displacement	= 2131.7	dynes/sq cm
normal stress amplitude	= 129.48	dynes/sq cm
phase shift	= -0.7177	radians
normal stress displacement function	=	gm/cm
normal stress coefficient: real part of	=	gm/cm
imaginary part of	=	gm/cm

Computer Program Input

interval spacing number	= 257	torsion head range	= 1.0
rhomberg jmax	= 7	oscillatory range	= 25.0
maximum harmonic	= 6	peak voltage	= 0.42
cycle averaging number	= 20	cone angle	= 0.5522°
delay/point	= 109	frequency	= 0.0952 c/s

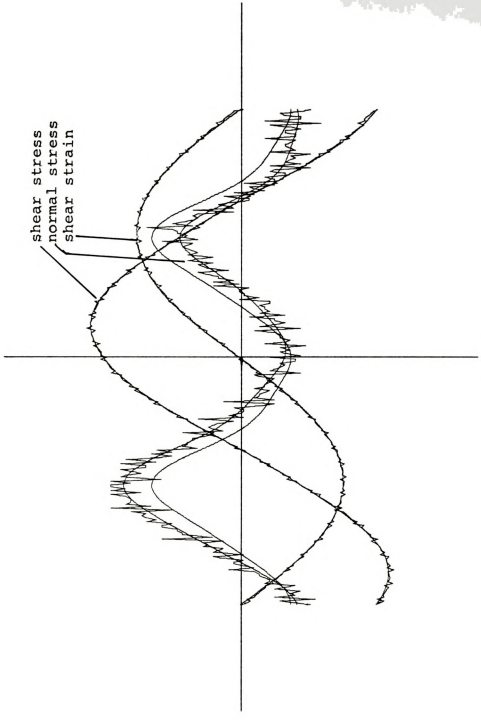

Figure 28. Calcomp Plot of the Small-Amplitude Oscillatory Shearing of Polyisobutylene in Cetane at the Frequency of 0.0952 c/s and Strain Amplitude of 0.5515.

MODIFIED WRG

Table 6. Fourier Components and Material Functions

harmonic		1	2	3	4	5	6
stress	An	71.816	0.2139	0.8271	-0.0380	-0.5480	0.0433
	Bn	29.917	-0.5894	0.6821	-0.1767	-0.1904	-0.2567
strain	An	0.0037	0.0028	-0.0004	0.0002	-0.0008	0.0003
	Bn	0.5515	-0.0052	0.0058	-0.0027	0.0006	-0.0020
normal	An	8.8982	-136.66	4.066	18.955	0.9066	-9.4814
	Bnm	-63.805	27.305	-1.7252	-8.054	2.7868	-3.7458

shear stress Ao = 0.9234 dynes/sq cm
shear strain Ao = 8.1466
normal stress Ao = 22.979 dynes/sq cm

Strain Amplitude = 0.5515

Shear Stress

stress amplitude = 77.798 dynes/sq cm
amplitude ratio = 141.07 dynes/sq cm
phase shift = 1.1692 radians
dynamic viscosity = 217.09 poise
imaginary part = 92.18 poise
dynamic rigidity = 55.131 dynes/sq cm
loss modulus = 192.84 dynes/sq cm

Normal Stress

normal stress displacement = 22.979 dynes/sq cm
normal stress amplitude = 139.33 dynes/sq cm
phase shift = -0.6936 radians
normal stress displacement function = -0.0139 gm/cm
normal stress coefficient: real part of = -0.0457 gm/cm
imaginary part of = -0.0156 gm/cm

Computer Program Input

interval spacing number = 257 torsion head range = 1.0
rhomberg jmax = 7 oscillatory range = 10.0
maximum harmonic = 6 peak voltage = 0.4
cycle averaging number = 1 cone angle = 0.5522°
delay/point = 109 frequency = 0.0952 c/s

MODIFIED WRG

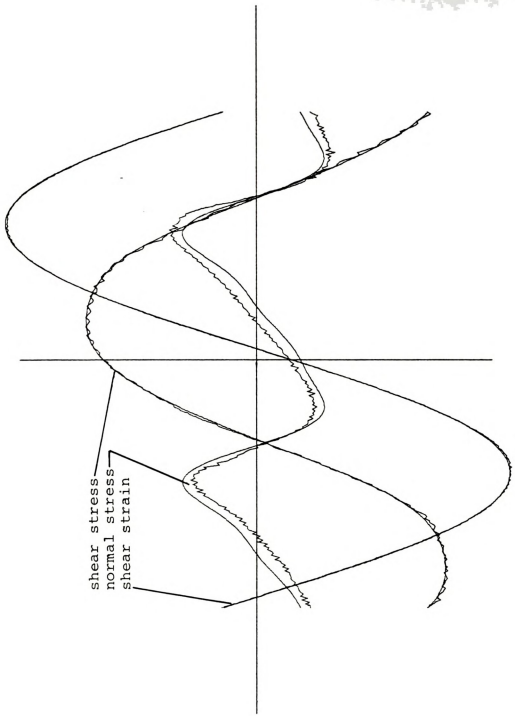

Figure 29. Calcomp Plot of the Small-Amplitude Oscillatory Shearing of Polyisobutylene in Cetane at the Frequency of 0.0952 c/s and Strain Amplitude of 0.53613.

MODIFIED WRG

Table 7. Fourier Components and Material Functions

harmonic		1	2	3	4	5	6
stress	An	85.692	-0.0056	-0.2720	-0.5486	0.6556	-0.2151
	Bn	50.322	-1.0898	-3.6896	2.5522	0.3557	0.1208
strain	An	-0.0744	0.0023	0.0000	0.0003	-0.0001	-0.0003
	Bn	0.5309	0.0017	0.0010	0.0004	-0.0006	0.0000
normal	An	25.510	-116.51	0.4003	42.566	-4.4282	-8.4051
	Bn	22.448	53.571	-4.9099	15.929	0.6154	-13.186

shear stress Ao = 5.0617 dynes/sq cm
shear strain Ao = -0.0036
normal stress Ao =- 10.793 dynes/sq cm

Strain Amplitude = 0.53613

Shear Stress

stress amplitude	= 99.375	dynes/sq cm
amplitude ratio	= 185.36	dynes/sq cm
phase shift	= 1.1791	radians
dynamic viscosity	= 286.4	poise
imaginary part	= 118.30	poise
dynamic rigidity	= 111.67	dynes/sq cm
loss modulus	= 171.32	dynes/sq cm

Normal Stress

normal stress displacement	= -10.793	dynes/sq cm
normal stress amplitude	= 128.23	dynes/sq cm
phase shift	= -0.4307	radians
normal stress displacement function	=	gm/cm
normal stress coefficient: real part of	=	gm/cm
imaginary part of	=	gm/cm

Computer Program Input

interval spacing number	= 257	torsion head range	= 1.0
rhomberg jmax	= 7	oscillatory range	= 25.0
maximum harmonic	= 6	peak voltage	= 0.5
cycle averaging number	= 10	cone angle	= 0.6522°
delay/point	= 108	frequency	= 0.0952 c/s

MODIFIED WRG

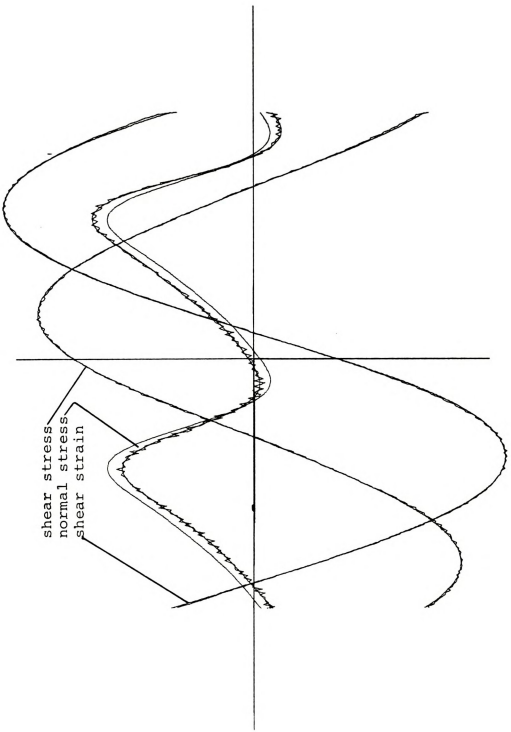

Figure 30. Calcomp Plot of the Small-Amplitude Oscillatory Shearing of Polyisobutylene in Cetane at the Frequency of 0.0952 c/s and Strain Amplitude of 0.5340.

MODIFIED WRG

Table 8. Fourier Components and Material Functions

harmonic		1	2	3	4	5	6
stress	An	91.132	0.3810	0.7035	-0.0528	0.1602	-0.2194
	Bn	62.900	-0.7124	1.1992	-0.3267	-0.1240	-0.2399
strain	An	-0.1776	0.0024	-0.0009	0.0003	0.0003	0.0000
	Bn	0.5036	-0.0032	0.0041	-0.0020	0.0015	-0.0015
normal	An	17.772	-157.96	8.3752	12.123	-1.2140	7.6909
	Bn	2.9049	-4.1664	-4.4100	40.225	-5.2268	-4.3855

shear stress Ao = 2.0103 dynes/sq cm
shear strain Ao = -0.0030
normal stress Ao = 123.38 dynes/sq cm

Strain Amplitude = 0.5340

Shear Stress

stress amplitude	= 110.73	dynes/sq cm
amplitude ratio	= 207.35	dynes/sq cm
phase shift	= 1.3057	radians
dynamic viscosity	= 334.54	poise
imaginary part	= 90.822	poise
dynamic rigidity	= 54.326	dynes/sq cm
loss modulus	= 200.11	dynes/sq cm

Normal Stress

normal stress displacement	= 123.38	dynes/sq cm
normal stress amplitude	= 158.01	dynes/sq cm
phase shift	= 1.1112	radians
normal stress displacement function	=	gm/cm
normal stress coefficient: real part of	=	gm/cm
imaginary part of	=	gm/cm

Computer Program Input

interval spacing number	= 257	torsion head range	= 1.0
rhomberg jmax	= 7	oscillatory range	= 25.0
maximum harmonic	= 6	peak voltage	= 0.50
cycle averaging number	= 10	cone angle	= 0.5522°
delay/point	= 108	frequency	= 0.0952 c/s

MODIFIED WRG

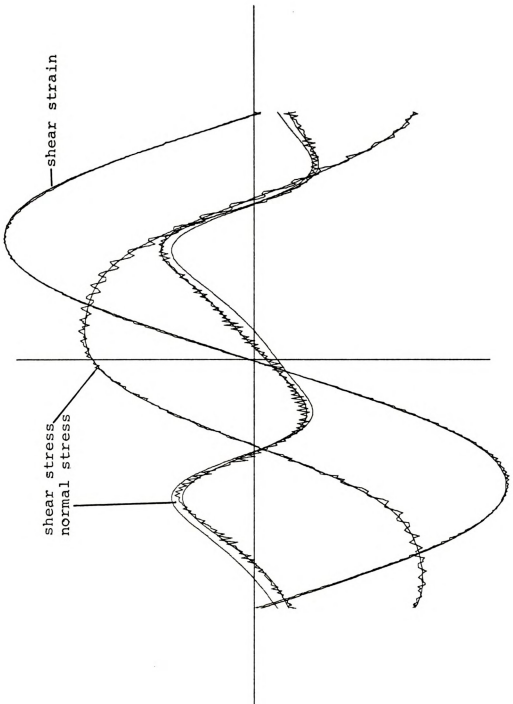

Figure 31. Calcomp Plot of the Small-Amplitude Oscillatory Shearing of Polyisobutylene in Cetane at the Frequency of 0.0952 c/s and Strain Amplitude of 0.5309

MODIFIED WRG

Table 9. Fourier Components and Material Functions

harmonic		1	2	3	4	5	6
stress	An	84.413	0.4778	0.1091	-0.3929	0.5825	-0.5014
	Bn	43.781	-0.1251	-5.7583	0.2431	0.0462	0.3822
strain	An	0.0107	0.0027	0.0005	0.0002	-0.0006	-0.0019
	Bn	0.5308	0.0048	-0.0017	0.0014	-0.0027	0.0019
normal	An	25.065	-98.127	-0.0835	37.733	-1.7162	-5.4318
	Bn	16.622	91.675	-0.3135	-10.018	4.8512	-3.4076

shear stress Ao = 0.1636 dynes/sq cm
shear strain Ao = -0.0037
normal stress Ao = 16.278 dynes/sq cm

Strain Amplitude = 0.5309

Shear Stress

stress amplitude = 95.091 dynes/sq cm
amplitude ratio = 179.11 dynes/sq cm
phase shift = 1.0722 radians
dynamic viscosity = 262.99 poise
imaginary part = 143.19 poise
dynamic rigidity = 85.649 dynes/sq cm
loss modulus = 157.30 dynes/sq cm

Normal Stress

normal stress displacement = 16.278 dynes/sq cm
normal stress amplitude = 134.29 dynes/sq cm
phase shift = -0.4298 radians
normal stress displacement function = gm/cm
normal stress coefficient: real part of = gm/cm
imaginary part of = gm/cm

Computer Program Input

interval spacing number = 257 torsion head range = 1.0
rhomberg jmax = 7 oscillatory range = 25.0
maximum harmonic = 6 peak voltage = 0.50
cycle averaging number = 10 cone angle = 1.533°
delay/point = 108 frequency = 0.0952 c/s

MODIFIED WRG

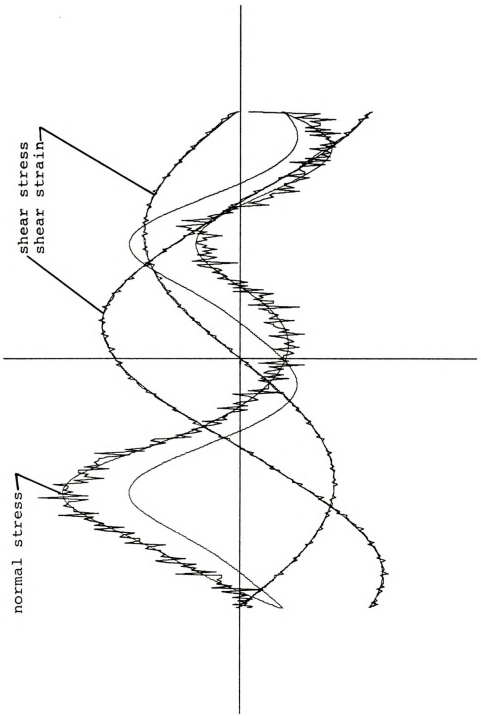

Figure 32. Calcomp Plot of the Small-Amplitude Oscillatory Shearing of Polyisobutylene in Cetane at the Frequencey of 0.0952 c/s and Strain Amplitude of 0.5097

MODIFIED WRG

Table 10. Fourier Components and Material Functions

harmonic		1	2	3	4	5	6
stress	An	66.746	0.1938	0.6951	-0.1101	-0.3502	-0.1118
	Bn	30.660	-0.7381	0.7541	-0.2300	-0.2856	-0.2260
strain	An	-0.0112	0.0029	-0.0004	0.0005	-0.0006	-0.0002
	Bn	0.5096	-0.0054	0.0059	-0.0026	0.0007	-0.0021
normal	An	-7.039	-157.64	5.0370	24.693	-2.679	-2.1033
	Bn	-143.52	63.296	-13.979	5.274	-8.724	2.864

shear stress Ao =-1.1761 dynes/sq cm
shear strain Ao = 0.0069
normal stress Ao = 44.082 dynes/sq cm

Strain Amplitude = 0.5097

Shear Stress

stress amplitude	= 73.451	dynes/sq cm
amplitude ratio	= 144.11	dynes/sq cm
phase shift	= 1.1622	radians
dynamic viscosity	= 221.07	poise
imaginary part	= 95.721	poise
dynamic rigidity	= 57.256	dynes/sq cm
loss modulus	= 132.24	dynes/sq cm

Normal Stress

normal stress displacement	= 44.082	dynes/sq cm
normal stress amplitude	= 169.88	dynes/sq cm
phase shift	= -0.5725	radians
normal stress displacement function	= -0.0312	gm/cm
normal stress coefficient: real part of	= -0.0022	gm/cm
imaginary part of	= -0.0441	gm/cm

Computer Program Input

interval spacing number	= 257	torsion head range	= 1.0
rhomberg jmax	= 7	oscillatory range	= 10.0
maximum harmonic	= 6	peak voltage	= 0.4
cycle averaging number	= 1	cone angle	= 0.5522°
delay/point	= 109	frequency	= 0.0952 c/s

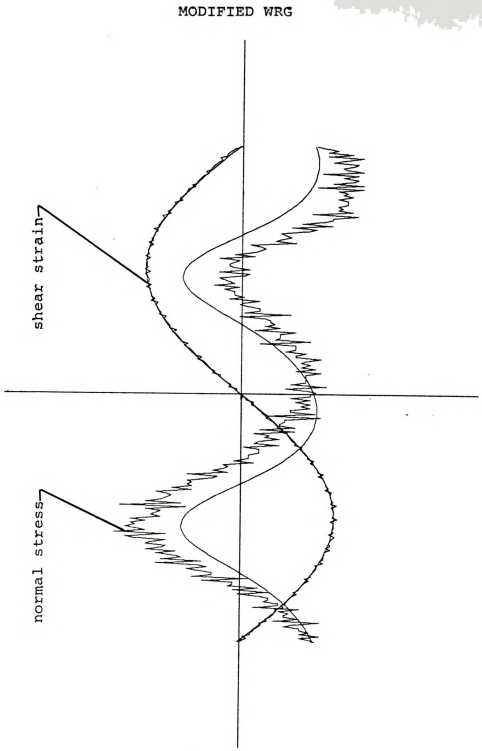

Figure 33. Calcomp Plot of the Small-Amplitude Oscillatory Shearing of Polyisobutylene in Cetane at the Frequency of 0.0952 c/s and Strain Amplitude of 0.5035

Table 11. Fourier Components and Material Functions

harmonic		1	2	3	4	5	6
stress	An						
	Bn						
strain	An	-0.0053	0.0023	0.0004	0.0002	-0.0009	0.0004
	Bn	0.5034	-0.0050	0.0047	-0.0024	0.0008	-0.0015
normal	An	21.315	-133.53	-1.8270	23.904	-2.0541	-3.5800
	Bn	-104.66	38.570	-5.0959	-4.8236	0.2457	0.6979

shear stress Ao = dynes/sq cm
shear strain Ao = 0.0072
normal stress Ao = -40.271 dynes/sq cm

Strain Amplitude = 0.5035

Shear Stress

stress amplitude = dynes/sq cm
amplitude ratio = dynes/sq cm
phase shift = radians
dynamic viscosity = poise
imaginary part = poise
dynamic rigidity = dynes/sq cm
loss modulus = dynes/sq cm

Normal Stress

normal stress displacement = 40.271 dynes/sq cm
normal stress amplitude = 138.99 dynes/sq cm
phase shift = -0.6342 radians
normal stress displacement function = 0.02725 gm/cm
normal stress coefficient: real part of = -0.0014 gm/cm
imaginary part of = -0.0455 gm/cm

Computer Program Input

interval spacing number = 257 torsion head range = 1.0
rhomberg jmax = 7 oscillatory range = 10.0
maximum harmonic = 6 peak voltage = 0.4
cycle averaging number = 1 cone angle = 0.5522°
delay/point = 109 frequency = 0.0952 c/s

MODIFIED WRG

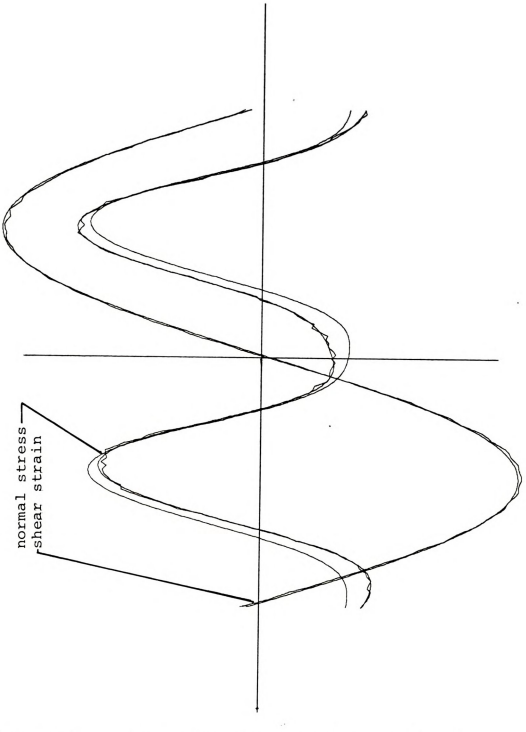

Figure 34. Calcomp Plot of the Oscillatory Shearing of Polyisobutylene in Cetane at the Frequency of 0.38 c/s and Strain Amplitude of 0.5488

MODIFIED WRG

Table 12. Fourier Components and Material Functions

harmonic		1	2	3	4	5	6
stress	An	52.184	35.040	43.115	2.7908	14.493	2.4823
	Bn	1136.6	75.346	52.487	17.300	-0.7683	5.1879
strain	An	-0.0274	0.00056	0.0014	0.0003	0.0008	0.0003
	Bn	0.5481	0.0061	0.0020	0.0001	-0.0001	0.0001
normal	An	42.898	-274.89	-10.521	31.629	0.5354	8.898
	Bn	36.525	-63.680	5.7919	19.427	4.7852	1.8845

shear stress Ao = 30.333 dynes/sq cm
shear strain Ao = 0.0012
normal stress Ao = 50.905 dynes/sq cm

Strain Amplitude = 0.5488

Shear Stress

stress amplitude = 1137.8 dynes/sq cm
amplitude ratio = 2073.2 dynes/sq cm
phase shift = 0.0958 radians
dynamic viscosity = 83.040 poise
imaginary part = 864.33 poise
dynamic rigidity = 2063.7 dynes/sq cm
loss modulus = 198.31 dynes/sq cm

Normal Stress

normal stress displacement = 50.905 dynes/sq cm
normal stress amplitude = 282.17 dynes/sq cm
phase shift = 1.3931 radians
normal stress displacement function = gm/cm
normal stress coefficient: real part of
imaginary part of = gm/cm

Computer Program Input

interval spacing number = 129 torsion head range = 25.0
rhomberg jmax = 6 oscillatory range = 25.0
maximum harmonic = 6 peak voltage = 0.5
cycle averaging number = 10 cone angle = 1.533°
delay/point = 36 frequency = 0.38 c/s

MODIFIED WRG

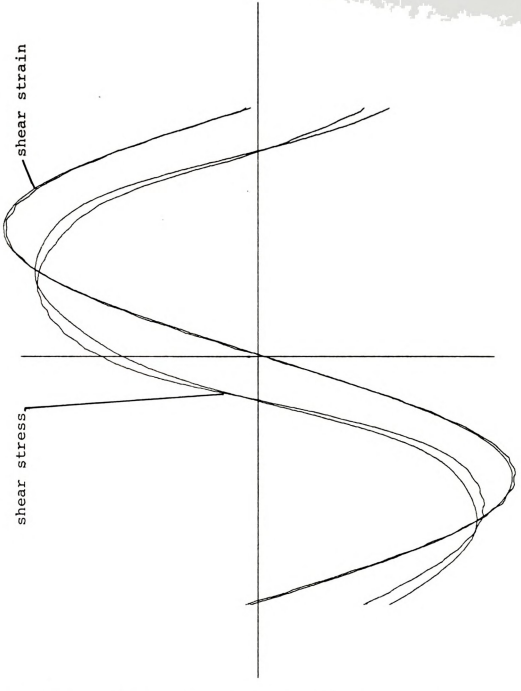

Figure 35. Calcomp Plot of the Oscillatory Shearing of Polyisobutylene in Cetane at the Frequency of 0.38 c/s and Strain Amplitude of 0.5390

Table 13. Fourier Components and Material Functions

harmonic		1	2	3	4	5	6
stress	An	307.13	47.720	46.307	12.627	-2.4911	2.5900
	Bn	538.46	20.420	-17.415	-2.0203	-13.691	-3.9300
strain	An	-0.0177	0.0052	0.0013	0.0001	0.0002	-0.0003
	Bn	0.5387	0.0048	-0.0011	0.0008	-0.0012	0.0010
normal	An						
	Bn						

shear stress Ao = 4.9025 dynes/sq cm
shear strain Ao = -0.0004
normal stress Ao = dynes/sq cm

Strain Amplitude = 0.5390

Shear Stress

stress amplitude = 619.89 dynes/sq cm
amplitude ratio = 1150.1 dynes/sq cm
phase shift = 0.5512 radians
dynamic viscosity = 252.28 poise
imaginary part = 410.35 poise
dynamic rigidity = 979.75 dynes/sq cm
loss modulus = 602.32 dynes/sq cm

Normal Stress

normal stress displacement = dynes/sq cm
normal stress amplitude = dynes/sq cm
phase shift = radians
normal stress displacement function = gm/cm
normal stress coefficient: real part of = gm/cm
imaginary part of = gm/cm

Computer Program Input

interval spacing number = 129 torsion head range = 25.0
rhomberg jmax = 6 oscillatory range = 25.0
maximum harmonic = 6 peak voltage = 0.5
cycle averaging number = 10 cone angle = 1.533°
delay/point = 36 frequency = 0.38 c/s

MODIFIED WRG

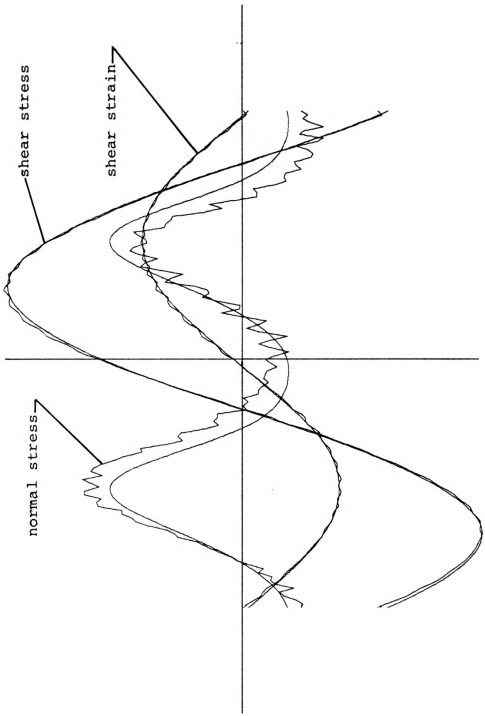

Figure 36. Calcomp Plot of the Oscillatory Shearing of Polyisobutylene in Cetane at the Frequency of 0.38 c/s and Strain Amplitude of 0.5200

MODIFIED WRG

Table 14. Fourier Components and Material Functions

harmonic		1	2	3	4	5	6
stress	An	301.59	5.8643	0.3053	0.6018	0.2710	0.1732
	Bn	397.81	5.7880	0.2840	2.7608	-2.8230	1.2150
strain	An	0.0387	0.0036	0.0015	0.0009	-0.0011	-0.0002
	Bn	0.5186	0.0090	-0.034	0.0030	-0.0027	0.0023
normal	An	42.000	-179.34	-11.019	34.310	5.638	-5.832
	Bn	-60.328	48.406	0.7473	-8.359	1.426	-2.087

shear stress Ao =-5.997 dynes/sq cm
shear strain Ao = 0.0066
normal stress Ao = 56.200 dynes/sq cm

Strain Amplitude = 0.5200

Shear Stress

stress amplitude	= 499.21	dynes/sq cm
amplitude ratio	= 960.02	dynes/sq cm
phase shift	= 0.5742	radians
dynamic viscosity	= 218.39	poise
imaginary part	= 337.60	poise
dynamic rigidity	= 806.05	dynes/sq cm
loss modulus	= 521.45	dynes/sq cm

Normal Stress

normal stress displacement	= 56.200	dynes/sq cm
normal stress amplitude	= 185.76	dynes/sq cm
phase shift	= -0.7281	radians
normal stress displacement function	=	gm/cm
normal stress coefficient: real part of	=	gm/cm
imaginary part of	=	gm/cm

Computer Program Input

interval spacing number	= 257	torsion head range	= 2.5
rhomberg jmax	= 7	oscillatory range	= 10.0
maximum harmonic	= 6	peak voltage	= 0.4
cycle averaging number	= 1	cone angle	= 0.5522°
delay/point	= 109	frequency	= 0.38 c/s

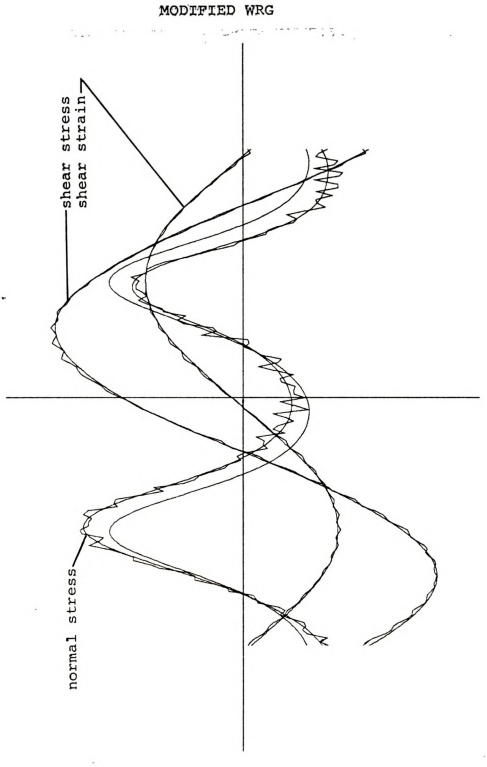

Figure 37. Calcomp Plot of the Oscillatory Shearing of Polyisobutylene Cetane at the Frequency of 0.38 c/s and Strain Amplitude of 0.5090

Table 15. Fourier Components and Material Functions

harmonic		1	2	3	4	5	6
stress	An	129.50	1.7977	0.4191	0.2459	0.1962	0.0555
	Bn	153.56	2.1543	0.1778	1.0867	-1.2885	0.5033
strain	An	0.04996	0.0025	0.0008	0.0007	-0.0006	0.0000
	Bn	0.5065	0.0085	-0.0029	0.0035	-0.0035	0.0022
normal	An	39.028	-196.71	-11.573	37.630	4.9411	-5.9970
	Bn	-62.249	59.193	3.4550	-16.585	2.4960	2.6140

shear stress Ao =-3.0753 dynes/sq cm
shear strain Ao = 0.0078
normal stress Ao = 30.951 dynes/sq cm

Strain Amplitude = 0.5090

Shear Stress

stress amplitude	= 200.87	dynes/sq cm
amplitude ratio	= 394.64	dynes/sq cm
phase shift	= 0.6023	radians
dynamic viscosity	= 93.641	poise
imaginary part	= 136.20	poise
dynamic rigidity	= 325.20	dynes/sq cm
loss modulus	= 223.58	dynes/sq cm

Normal Stress

normal stress displacement	= 30.95	dynes/sq cm
normal stress amplitude	= 205.42	dynes/sq cm
phase shift	= -0.7376	radians
normal stress displacement function	=	gm/cm
normal stress coefficient: real part of	=	gm/cm
imaginary part of	=	gm/cm

Computer Program Input

interval spacing number	= 257	torsion head range	= 2.5
rhomberg jmax	= 7	oscillatory range	= 10.0
maximum harmonic	= 6	peak voltage	= 0.4
cycle averaging number	= 1	cone angle	= 0.5522°
delay/point	= 37	frequency	= 0.38 c/s

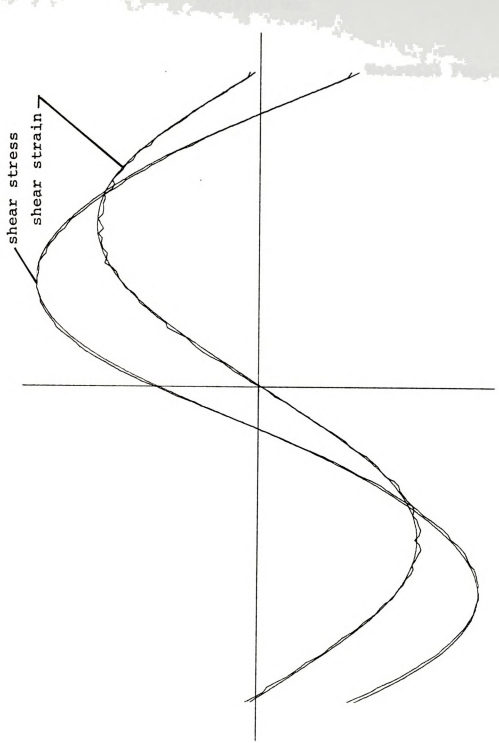

Figure 38. Calcomp Plot of the Large-Amplitude Oscillatory Shearing of Polyisobutylene in Cetane at the Frequency of 0.6 c/s and Strain Amplitude of 3.4123

Table 16. Fourier Components and Material Functions

harmonic		1	2	3	4	5	6
stress	An	507.83	17.971	12.789	2.6355	3.7482	-0.8826
	Bn	1076.86	13.226	30.436	2.8214	1.6487	2.8480
strain	An	-0.1094	0.0476	0.0122	-0.0041	0.0004	-0.0034
	Bn	3.4106	0.0393	-0.0086	0.0107	-0.0154	0.0113
normal	An	126.59	-338.44	4.0180	49.779	1.1075	-13.858
	Bn	-180.15	16.670	-16.688	-5.6510	-9.1564	-3.9132

shear stress Ao = 3.8435 dynes/sq cm
shear strain Ao = 0.0221
normal stress Ao = 1405.3 dynes/sq cm

Strain Amplitude = 3.4123

Shear Stress

stress amplitude	= 1190.6	dynes/sq cm
amplitude ratio	= 348.91	dynes/sq cm
phase shift	= 0.4727	radians
dynamic viscosity	= 42.140	poise
imaginary part	= 82.402	poise
dynamic rigidity	= 310.65	dynes/sq cm
loss modulus	= 171.80	dynes/sq cm

Normal Stress

normal stress displacement	= 1405.4	dynes/sq cm
normal stress amplitude	= 338.85	dynes/sq cm
phase shift	= -0.7287	radians
normal stress displacement function	=	gm/cm
normal stress coefficient: real part of	=	gm/cm
imaginary part of	=	gm/cm

Computer Program Input

interval spacing number	= 129	torsion head range	= 2.5
rhomberg jmax	= 6	oscillatory range	= 25.0
maximum harmonic	= 6	peak voltage	= 0.4
cycle averaging number	= 5	cone angle	= 0.5522°
delay/point	= 9	frequency	= 0.6 c/s

MODIFIED WRG

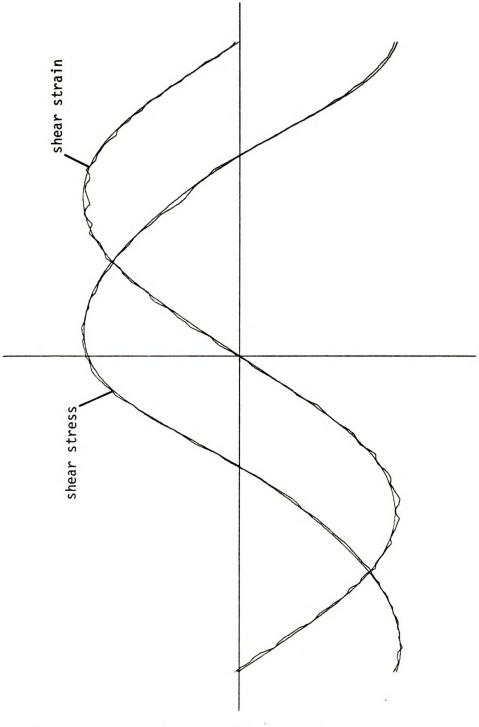

Figure 39. Calcomp Plot of the Large-Amplitude Oscillatory Shearing of Polyisobutylene in Cetane at the Frequency of 0.6 c/s and Strain Amplitude of 3.3088

Table 17. Fourier Components and Material Functions

harmonic		1	2	3	4	5	6
stress	An	1571.01	24.476	69.183	-3.8817	-8.7468	5.8667
	Bn	652.42	-14.578	-58.537	-39.804	-17.486	-3.8251
strain	An	-0.0331	0.0492	0.0093	-0.0077	0.0015	0.0036
	Bn	3.3086	0.0356	-0.0086	0.0057	-0.0193	0.0050
normal	An	140.32	-82.240	7.7130	-8.6480	0.5716	4.8585
	Bn	-22.332	-158.18	2.7542	19.682	1.6368	0.1037

shear stress Ao = -29.051 dynes/sq cm
shear strain Ao = 0.01034
normal stress Ao = 1149.31 dynes/sq cm

Strain Amplitude = 3.3088

Shear Stress

stress amplitude	= 1701.09	dynes/sq cm
amplitude ratio	= 514.11	dynes/sq cm
phase shift	= 1.1872	radians
dynamic viscosity	= 126.46	poise
imaginary part	= 51.038	poise
dynamic rigidity	= 192.41	dynes/sq cm
loss modulus	= 476.75	dynes/sq cm

Normal Stress

normal stress displacement	= 1149.30	dynes/sq cm
normal stress amplitude	= 178.35	dynes/sq cm
phase shift	= 0.2561	radians
normal stress displacement function	=	gm/cm
normal stress coefficient: real part of	=	gm/cm
imaginary part of	=	gm/cm

Computer Program Input

interval spacing number	= 129	torsion head range	= 10.0
rhomberg jmax	= 6	oscillatory range	= 25.0
maximum harmonic	= 6	peak voltage	= 0.6
cycle averaging number	= 5	cone angle	= 0.5522°
delay/point	= 9	frequency	= 0.6 c/s

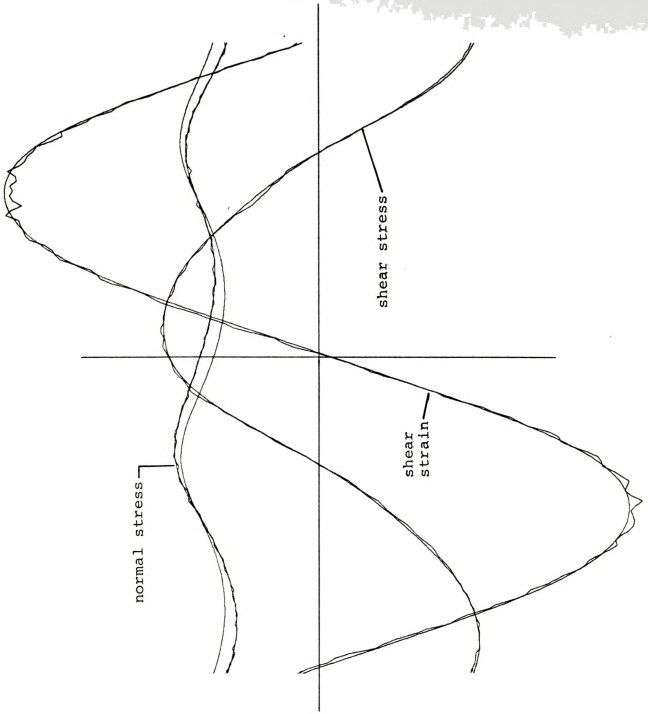

Figure 40. Calcomp Plot of the Large-Amplitude Oscillatory Shearing of Polyisobutylene in Cetane at the Frequency of 0.6 c/s and Strain Amplitude of 3.3048

MODIFIED WRG

Table 18. Fourier Components and Material Functions

harmonic		1	2	3	4	5	6
stress	An	1536.64	24.313	74.615	-3.0491	-8.0004	4.9087
	Bn	71.487	-12.509	-50.855	-3.5270	-20.359	-3.3800
strain	An	-0.1747	0.0448	0.01316	-0.0068	-0.0007	0.0037
	Bn	3.3001	0.0419	-0.0099	0.0018	-0.0249	0.0086
normal	An	135.74	-81.452	9.1036	-11.949	0.7236	2.7453
	Bn	4.7617	-216.14	5.0297	19.390	2.6911	-0.4144

shear stress Ao = -29.297 dynes/sq cm
shear strain Ao = 0.0128
normal stress Ao = 1198.16 dynes/sq cm

Strain Amplitude = 3.3048

Shear Stress

stress amplitude	= 1694.79	dynes/sq cm
amplitude ratio	= 512.82	dynes/sq cm
phase shift	= 1.1883	radians
dynamic viscosity	= 126.20	poise
imaginary part	= 50.771	poise
dynamic rigidity	= 191.43	dynes/sq cm
loss modulus	= 475.77	dynes/sq cm

Normal Stress

normal stress displacement	= 1198.15	dynes/sq cm
normal stress amplitude	= 230.98	dynes/sq cm
phase shift	= 0.2331	radians
normal stress displacement function	=	gm/cm
normal stress coefficient: real part of	=	gm/cm
imaginary part of	=	gm/cm

Computer Program Input

interval spacing number	= 129	torsion head range	= 10.0
rhomberg jmax	= 6	oscillatory range	= 25.0
maximum harmonic	= 6	peak voltage	= 0.6
cycle averaging number	= 5	cone angle	= 0.5522°
delay/point	= 9	frequency	= 0.6 c/s

MODIFIED WRG

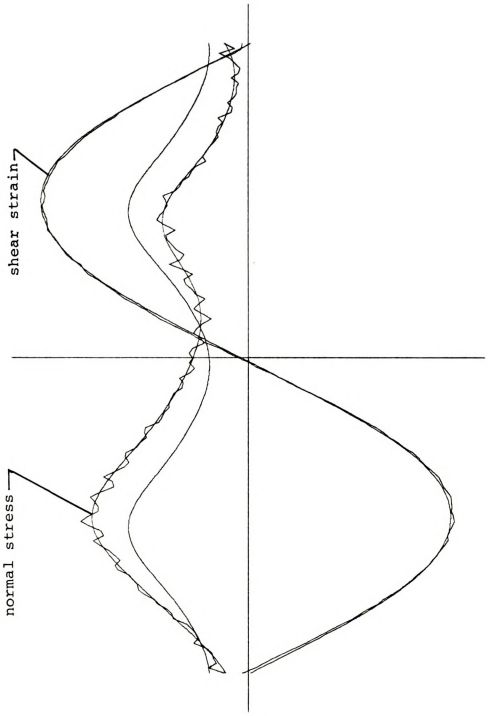

Figure 41. Calcomp Plot of the Large-Amplitude Oscillatory Shearing of Polyisobutylene in Cetane at the Frequency of 0.6 c/s and Strain Amplitude of 2.160

Table 19. Fourier Components and Material Functions

harmonic		1	2	3	4	5	6
stress	An	378.87	11.652	5.3933	1.3597	0.4375	0.6955
	Bn	815.27	10.321	13.675	3.0624	-0.6369	1.6052
strain	An	0.0429	0.0252	0.0051	0.0027	-0.0025	0.0025
	Bn	2.1675	0.0248	-0.0061	0.0086	-0.0077	0.0047
normal	An	78.975	-205.08	-2.311	17.973	9.5153	-4.5368
	Bn	-213.14	41.551	-13.143	-11.832	-0.8590	3.3143

shear stress Ao = 5.0905 dynes/sq cm
shear strain Ao = 0.0274
normal stress Ao = 398.86 dynes/sq cm

Strain Amplitude = 2.160

Shear Stress

stress amplitude	= 898.99	dynes/sq cm
amplitude ratio	= 416.20	dynes/sq cm
phase shift	= 0.4153	radians
dynamic viscosity	= 44.4	poise
imaginary part	= 101.01	poise
dynamic rigidity	= 379.44	dynes/sq cm
loss modulus	= 167.93	dynes/sq cm

Normal Stress

normal stress displacement	= 398.86	dynes/sq cm
normal stress amplitude	= 209.25	dynes/sq cm
phase shift	= -0.7051	radians
normal stress displacement function	=	gm/cm
normal stress coefficient: real part of	=	gm/cm
imaginary part of	=	gm/cm

Computer Program Input

interval spacing number	= 129	torsion head range	= 10.0
rhomberg jmax	= 6	oscillatory range	= 25.0
maximum harmonic	= 6	peak voltage	= 0.4
cycle averaging number	= 5	cone angle	= 0.5522°
delay/point	= 9	frequency	= 0.6 c/s

MODIFIED WRG

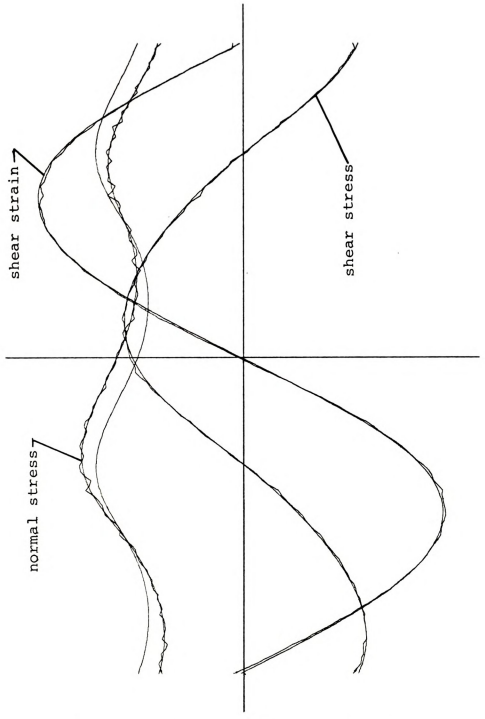

Figure 42. Calcomp Plot of the Large-Amplitude Oscillatory Shearing of Polyisobutylene in Cetane at the Frequency of 0.6 c/s and Strain Amplitude of 2.1363

MODIFIED WRG

Table 20. Fourier Components and Material Functions

harmonic		1	2	3	4	5	6
stress	An	1153.93	17.497	40.838	2.9242	-3.2570	4.9478
	Bn	555.78	-7.825	-19.004	1.2127	-4.7481	0.5273
strain	An	-0.0101	0.0224	0.0075	0.0013	-0.0005	0.0034
	Bn	2.1363	0.0198	-0.0050	0.0079	-0.0065	0.0062
normal	An	106.11	-69.034	2.4597	-1.2699	1.0045	-0.2438
	Bn	-27.803	-120.26	-1.9765	12.633	0.5818	-2.0195

shear stress Ao =-21.688 dynes/sq cm
shear strain Ao = 0.02514
normal stress Ao = 626.65 dynes/sq cm

Strain Amplitude = 2.1363

Shear Stress

stress amplitude	= 1280.8	dynes/sq cm
amplitude ratio	= 599.54	dynes/sq cm
phase shift	= 1.1267	radians
dynamic viscosity	= 143.61	poise
imaginary part	= 68.327	poise
dynamic rigidity	= 257.60	dynes/sq cm
loss modulus	= 541.39	dynes/sq cm

Normal Stress

normal stress displacement	= 626.651	dynes/sq cm
normal stress amplitude	= 138.67	dynes/sq cm
phase shift	= 0.2653	radians
normal stress displacement function	=	gm/cm
normal stress coefficient: real part of	=	gm/cm
imaginary part of	=	gm/cm

Computer Program Input

interval spacing number	= 129	torsion head range	= 10.0
rhomberg jmax	= 6	oscillatory range	= 25.0
maximum harmonic	= 6	peak voltage	= 0.6
cycle averaging number	= 5	cone angle	= 0.5522°
delay/point	= 9	frequency	= 0.6 c/s

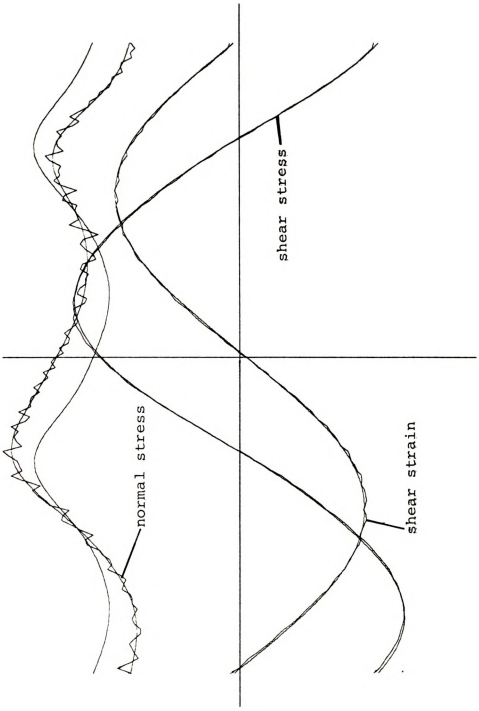

Figure 43. Calcomp Plot of the Large-Amplitude Oscillatory Shearing of Polysobutylene in Cetane at the Frequency of 0.6 c/s and Strain Amplitude of 1.3168

Table 21. Fourier Components and Material Functions

harmonic		1	2	3	4	5	6
stress	An	715.40	11.649	17.281	0.6266	-1.7119	-0.3267
	Bn	493.27	1.0388	3.3791	2.6989	-2.7457	1.9895
strain	An	-0.0677	0.0113	0.0006	-0.0016	-0.0002	-0.0012
	Bn	1.3150	0.0163	-0.0020	0.0046	-0.0043	0.0037
normal	An	77.058	-31.903	2.5572	-4.2238	-1.2758	3.7524
	Bn	-10.780	-67.866	-4.3538	12.301	-1.1712	-0.0144

shear stress Ao = 1.1833 dynes/sq cm
shear strain Ao =-0.0062
normal stress Ao = 341.65 dynes/sq cm

Strain Amplitude = 1.3168

Shear Stress

stress amplitude	= 868.98	dynes/sq cm
amplitude ratio	= 659.92	dynes/sq cm
phase shift	= 1.0186	radians
dynamic viscosity	= 149.03	poise
imaginary part	= 91.823	poise
dynamic rigidity	= 346.16	dynes/sq cm
loss modulus	= 660.77	dynes/sq cm

Normal Stress

normal stress displacement	= 341.65	dynes/sq cm
normal stress amplitude	= 74.991	dynes/sq cm
phase shift	= 0.2712	radians
normal stress displacement function	=	gm/cm
normal stress coefficient: real part of	=	gm/cm
imaginary part of	=	gm/cm

Computer Program Input

interval spacing number	= 129	torsion head range	= 2.5
rhomberg jmax	= 6	oscillatory range	= 25
maximum harmonic	= 6	peak voltage	= 0.4
cycle averaging number	= 5	cone angle	= 0.5522°
delay/point	= 9	frequency	= 0.600 c/s

Figure 44. Calcomp Plot of the Large-Amplitude Oscillatory Shearing of Polyisobutylene in Cetane at the Frequency of 0.6 c/s and Strain Amplitude of 1.2982

MODIFIED WRG

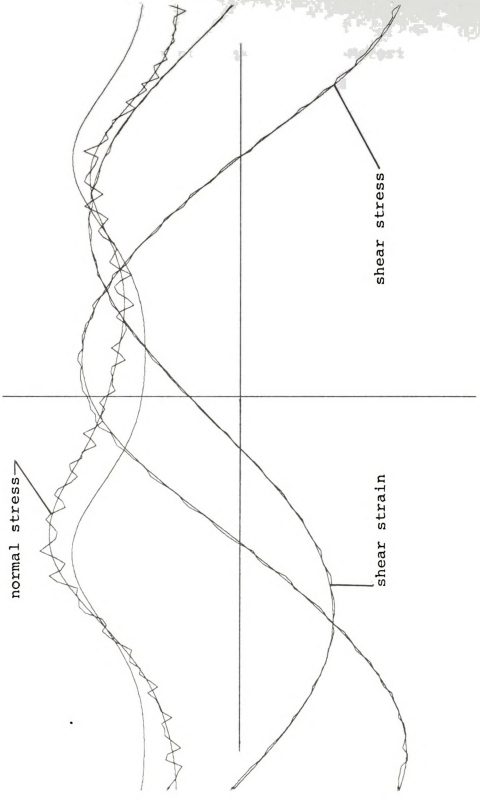

MODIFIED WRG

Table 22. Fourier Components and Material Functions

harmonic		1	2	3	4	5	6
stress	An	804.60	8.7434	16.160	2.5677	-1.8406	2.0686
	Bn	300.40	-5.1876	-8.082	-0.8924	-1.9413	-1.2144
strain	An	0.2244	0.0121	0.0039	0.0016	-0.0008	0.0015
	Bn	1.2787	0.0080	-0.0012	0.0032	-0.0043	0.00181
normal	An	74.449	-61.236	0.0109	4.5209	-0.7214	0.02536
	Bn	-24.458	-46.387	-5.6975	13.330	0.4320	-0.2122

shear stress Ao = 25.100 dynes/sq cm
shear strain Ao = 0.3038
normal stress Ao = 263.20 dynes/sq cm

Strain Amplitude = 1.2982

Shear Stress

stress amplitude	= 858.85	dynes/sq cm
amplitude ratio	= 661.57	dynes/sq cm
phase shift	= 1.0398	radians
dynamic viscosity	= 151.32	poise
imaginary part	= 570.47	poise
dynamic rigidity	= 335.02	dynes/sq cm
loss modulus	= 88.865	dynes/sq cm

Normal Stress

normal stress displacement	= 263.20	dynes/sq cm
normal stress amplitude	= 76.821	dynes/sq cm
phase shift	= 0.2876	radians
normal stress displacement function	=	gm/cm
normal stress coefficient: real part of	=	gm/cm
imaginary part of	=	gm/cm

Computer Program Input

interval spacing number	= 129	torsion head range	= 10.0
rhomberg jmax	= 6	oscillatory range	= 25.0
maximum harmonic	= 6	peak voltage	= 0.4
cycle averaging number	= 5	cone angle	= 0.5522°
delay/point	= 9	frequency	= 0.6 c/s

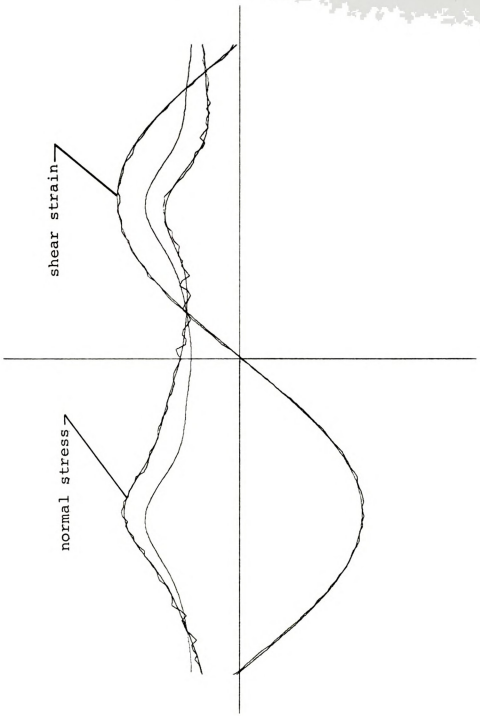

Figure 45. Calcomp Plot of the Large-Amplitude Oscillatory Shearing of Polyisobutylene in Cetane at the Frequency of 0.6 c/s and Strain Amplitude of 1.2973

MODIFIED WRG

Table 23. Fourier Components and Material Functions

harmonic		1	2	3	4	5	6
stress	An	190.17	5.013	-0.8333	0.3638	-0.6835	0.5678
	Bn	572.01	8.056	4.5456	2.4911	-0.4537	1.3098
strain	An	-0.0311	0.0117	0.0009	0.0003	-0.0020	-0.0002
	Bn	1.2969	0.0157	-0.0023	0.0047	-0.0041	0.0043
normal	An	62.847	-109.16	-7.8308	33.580	3.7231	-12.282
		-115.92	10.086	-3.0701	-8.4400	1.5108	0.0467

shear stress Ao = 5.9346 dynes/sq cm
shear strain Ao = 0.0019
normal stress Ao = 346.01 dynes/sq cm

Strain Amplitude = 1.2973

Shear Stress

stress amplitude	= 602.797	dynes/sq cm
amplitude ratio	= 464.66	dynes/sq cm
phase shift	= 0.3450	radians
dynamic viscosity	= 41.680	poise
imaginary part	= 115.99	poise
dynamic rigidity	= 437.30	dynes/sq cm
loss modulus	= 157.14	dynes/sq cm

Normal Stress

normal stress displacement	= 346.01	dynes/sq cm
normal stress amplitude	= 109.63	dynes/sq cm
phase shift	= -0.7153	radians
normal stress displacement function	=	gm/cm
normal stress coefficient: real part of	=	gm/cm
imaginary part of	=	gm/cm

Computer Program Input

interval spacing number	= 129	torsion head range	= 10.0
rhomberg jmax	= 6	oscillatory range	= 25.0
maximum harmonic	= 6	peak voltage	= 0.4
cycle averaging number	= 5	cone angle	= 0.5522°
delay/point	= 9	frequency	= 0.6 c/s

MODIFIED WRG

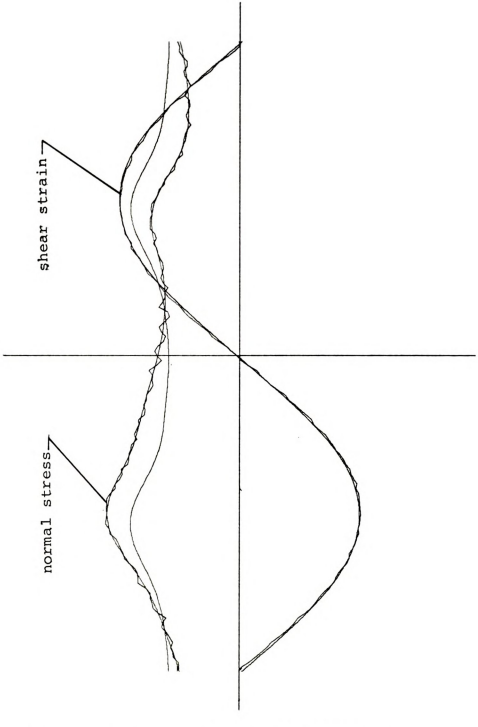

Figure 46. Calcomp Plot of the Large-Amplitude Oscillatory Shearing of Polyisobutylene in Cetane at the Frequency of 0.6 c/s and Strain Amplitude of 1.2678

MODIFIED WRG

Table 24. Fourier Components and Material Functions

harmonic		1	2	3	4	5	6
stress	An						
	Bn						
strain	An	0.0234	0.0099	0.0018	0.0005	-0.0004	-0.0005
	Bn	1.2676	0.0193	-0.0074	0.0066	-0.0039	0.0045
normal	An	63.342	-92.228	-8.9380	24.967	2.3603	-6.9247
	Bn	-125.78	19.720	0.2509	-12.281	-2.5140	3.0130

shear stress Ao = dynes/sq cm
shear strain Ao = -0.0011
normal stress Ao = 446.51 dynes/sq cm

Strain Amplitude = 1.2678

Shear Stress

stress amplitude	=	dynes/sq cm
amplitude ratio	=	dynes/sq cm
phase shift	=	radians
dynamic viscosity	=	poise
imaginary part	=	poise
dynamic rigidity	=	dynes/sq cm
loss modulus	=	dynes/sq cm

Normal Stress

normal stress displacement	= 446.51	dynes/sq cm
normal stress amplitude	= 94.313	dynes/sq cm
phase shift	= -0.6986	radians
normal stress displacement function	=	gm/cm
normal stress coefficient: real part of	=	gm/cm
imaginary part of	=	gm/cm

Computer Program Input

interval spacing number	= 129	torsion head range	= 2.5
rhomberg jmax	= 6	oscillatory range	= 25.0
maximum harmonic	= 6	peak voltage	= 0.4
cycle averaging number	= 5	cone angle	= 0.5522°
delay/point	= 9	frequency	= 0.6 c/s

Figure 47. Calcomp Plot of the Oscillatory Shearing of Polyisobutylene in Cetane at the Frequency of 0.6 c/s and Strain Amplitude of 0.5194

MODIFIED WRG

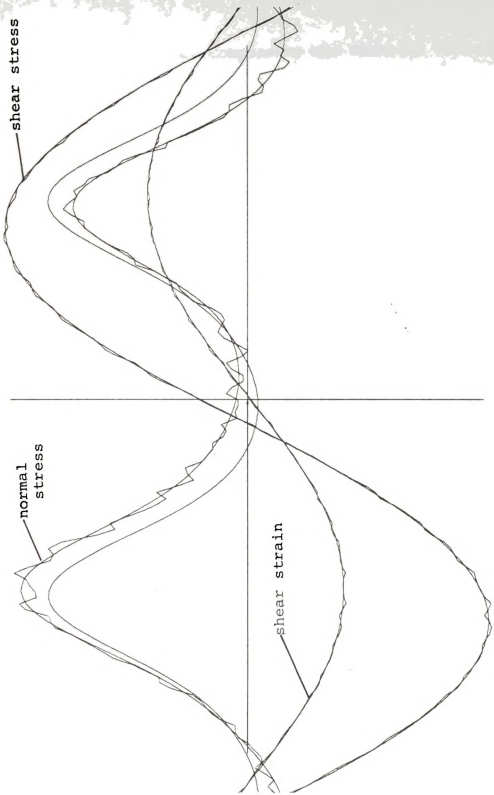

MODIFIED WRG

Table 25. Fourier Components and Material Functions

harmonic		1	2	3	4	5	6
stress	An	49.375	0.9597	-0.4332	-0.0591	-0.0247	0.1878
	Bn	251.45	1.3207	1.5757	0.5509	0.6856	0.2675
strain	An	-0.0269	0.0025	0.0009	-0.0002	-0.0004	0.0001
	Bn	0.5189	0.0029	0.0018	0.0014	-0.0004	0.0001
normal	An	49.031	-213.70	-6.166	45.695	3.2922	-7.764
	Bn	-63.090	2.532	-8.618	5.976	0.3984	-1.326

shear stress Ao = 0.2002 dynes/sq cm
shear strain Ao = 0.0095
normal stress Ao = 154.20 dynes/sq cm

Strain Amplitude = 0.5194

Shear Stress

stress amplitude	= 256.25	dynes/sq cm
amplitude ratio	= 493.17	dynes/sq cm
phase shift	= 0.2458	radians
dynamic viscosity	= 31.828	poise
imaginary part	= 126.89	poise
dynamic rigidity	= 478.37	dynes/sq cm
loss modulus	= 119.99	dynes/sq cm

Normal Stress

normal stress displacement	= 154.20	dynes/sq cm
normal stress amplitude	= 213.72	dynes/sq cm
phase shift	= -0.7277	radians
normal stress displacement function	=	gm/cm
normal stress coefficient: real part of	=	gm/cm
imaginary part of	=	gm/cm

Computer Program Input

interval spacing number	= 257	torsion head range	= 2.5
rhomberg jmax	= 7	oscillatory range	= 10.0
maximum harmonic	= 6	peak voltage	= 0.4
cycle averaging number	= 1	cone angle	= 0.5522°
delay/point	= 9	frequency	= 0.6 c/s

Figure 48a. Calcomp Plot of the Oscillatory Shearing of Polyisobutylene in Cetane at the Frequency of 0.6 c/s and Strain Amplitude of 0.5139 for Shear Stress Response

Figure 48b. Calcomp Plot of Oxcillatory Shearing of Polyisobutylene in Cetane at the Frequency of 0.6 c/s and Strain Amplitude of 0.5139 for Normal Stress Response

MODIFIED WRG

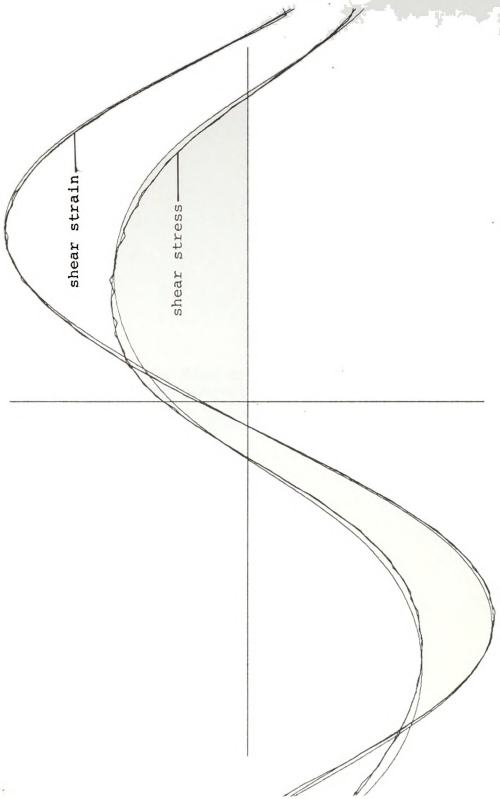

Figure 49. Calcomp Plot of Oscillatory Shearing of Polyisobutylene in Cetane at the Frequency of 0.6 c/s and Strain Amplitude of 0.5128

MODIFIED WRG

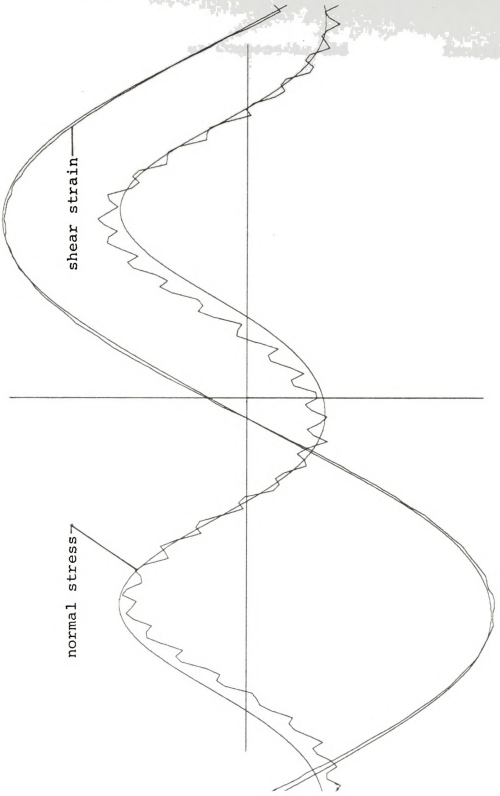

MODIFIED WRG

Table 26. Fourier Components and Material Functions

harmonic		1	2	3	4	5	6
stress	An	456.88	37.668	46.969	5.7976	1.4019	1.1561
	Bn	723.67	35.052	-8.677	7.0847	-5.1237	2.8878
strain	An	0.0945	0.0067	0.0013	0.0010	-0.0001	0.0001
	Bn	0.5051	0.0080	-0.0041	0.0034	-0.0031	0.0024
normal	An	-8.5027	-169.90	-8.3708	-6.9140	-2.0253	-0.4645
	Bn	72.207	317.00	23.056	18.450	-2.6840	1.4916

shear stress Ao = -108.91 dynes/sq cm
shear strain Ao = -0.0020
normal stress Ao = 91.539 dynes/sq cm

Strain Amplitude = 0.5139

Shear Stress

stress amplitude = 855.83 dynes/sq cm
amplitude ratio = 1665.5 dynes/sq cm
phase shift = 0.3783 radians
dynamic viscosity = 163.15 poise
imaginary part = 410.55 poise
dynamic rigidity = 1547.8 dynes/sq cm
loss modulus = 615.14 dynes/sq cm

Normal Stress

normal stress displacement = 91.539 dynes/sq cm
normal stress amplitude = 359.66 dynes/sq cm
phase shift = 0.06113 radians
normal stress displacement function = gm/cm
normal stress coefficient: real part of = gm/cm
imaginary part of = gm/cm

Computer Program Input

interval spacing number = 129 torsion head range = 100.0
rhomberg jmax = 6 oscillatory range = 25.0
maximum harmonic = 6 peak voltage = 0.5
cycle averaging number = 10 cone angle = 1.533°
delay/point = 9 frequency = 0.6 c/s

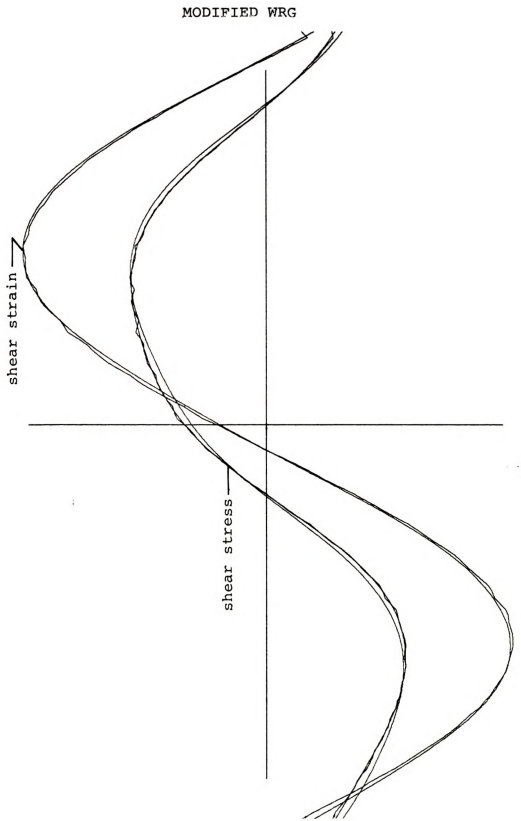
MODIFIED WRG
shear strain
shear stress

MODIFIED WRG

Table 27. Fourier Components and Material Functions

harmonic		1	2	3	4	5	6
stress	An	368.83	31.943	27.865	5.1873	0.2399	0.6240
	Bn	636.51	23.316	-38.805	1.4524	-5.3167	1.3730
strain	An	0.0974	0.0061	0.0012	0.0006	0.0004	0.0005
	Bn	0.5035	0.0079	-0.0040	0.0030	-0.0028	0.0020
normal	An	24.698	-107.86	-8.1107	-2.0691	-2.5524	-0.0677
	Bn	68.525	-344.54	-18.385	20.494	-2.9447	2.0509

shear stress Ao = -4.7462 dynes/sq cm
shear strain Ao = -0.0019
normal stress Ao = -131.75 dynes/sq cm

Strain Amplitude = 0.5128

Shear Stress

stress amplitude	= 735.65	dynes/sq cm
amplitude ratio	= 1434.6	dynes/sq cm
phase shift	= 0.3341	radians
dynamic viscosity	= 124.79	poise
imaginary part	= 359.50	poise
dynamic rigidity	= 1355.3	dynes/sq cm
loss modulus	= 470.45	dynes/sq cm

Normal Stress

normal stress displacement	= -131.75	dynes/sq cm
normal stress amplitude	= 361.03	dynes/sq cm
phase shift	= 0.0394	radians
normal stress function	=	gm/cm
normal stress displacement function	=	gm/cm
normal stress coefficient: real part of	=	gm/cm
imaginary part of	=	gm/cm

Computer Program Input

interval spacing number	= 129	torsion head range	= 100.0
rhomberg jmax	= 6	oscillatory range	= 25.0
maximum harmonic	= 6	peak voltage	= 0.5
cycle averaging number	= 10	cone angle	= 1.533°
delay/point	= 9	frequency	= 0.6 c/s